

ABSTRACT

Title of Document: LIGHT AVAILABLE TO THE SEAGRASS *ZOSTERA MARINA* WHEN EXPOSED TO CURRENTS AND WAVES

Katie L. McKone, Master of Science, 2009

Directed By: Dr. Evamaria W. Koch, Associate Professor
Marine, Estuarine, and Environmental Sciences

Aquatic organisms are regularly exposed to varying degrees of hydrodynamic forces such as currents and waves. Seagrasses, which are rooted in the sediment, have flexible leaves, allowing them to sway back and forth with waves and deflect with currents. Furthermore, seagrasses can acclimate to local hydrodynamic forces exerted upon them by changing their morphology, which may benefit the organism via reduced drag, but may also bring disadvantages such as increased self-shading. We examined the interaction between water flow and morphology of the seagrass *Zostera marina*, and how this interaction affects light availability to the plant. We also assessed carbon and nutrient content of *Z. marina*, as the uptake of these constituents has been linked to hydrodynamic conditions and sediment composition. Our results indicate that local hydrodynamics and sediment composition induce morphological variation in the seagrass *Z. marina*, and that this variation influences light availability to the seagrass canopy.

LIGHT AVAILABLE TO THE SEAGRASS *ZOSTERA MARINA* WHEN EXPOSED
TO CURRENTS AND WAVES

By

Katie L. McKone

Thesis submitted to the Faculty of the Graduate School of the
University of Maryland, College Park, in partial fulfillment
of the requirements for the degree of
Master of Science

2009

Advisory Committee:

Associate Professor Evamaria W. Koch, Chair

Professor Lawrence Sanford

Professor Richard Zimmerman

© Copyright by
Katie L. McKone
2009

Acknowledgements

I would like to thank my advisor, Dr. Evamaria Koch, for all her support throughout my graduate career. Her enthusiasm about my work, her willingness to discuss ideas, and her dedication to my education made my graduate experience full and successful. I am a better scientist because of her. I would also like to thank Dr. Richard Zimmerman for his dedication to my thesis, which allowed me to understand techniques and biological processes to their fullest. Dr. Larry Sanford provided important insight into the physical processes that were at the core of my thesis, and I appreciate his contributions.

Dale Booth, Terry Jordan, and Nicole Barth were the most enjoyable people to work in the field and laboratory with, and I am thankful for all their support, insight, and help throughout the years. I would also like to thank Chris Pickerell, Kim Petersen, and Steve Schott, who are the most amazing SCUBA divers and scientists that I have had the pleasure to work with, and my thesis would not have reached the quality it did without their help. In addition, Jack Seabrease was vital to the completion of my thesis, and I would like to thank him for the time and effort he put into designing and building many of the instruments I used throughout my time at Horn Point.

Last, but not least, I would like to thank my family for their love and support, as well as the Horn Point community, who I will miss terribly. I will end with Andy McDonald, whose encouragement and belief in me was amazing throughout my time in graduate school, especially the days leading up to my thesis defense.

Table of Contents

Acknowledgements.....	ii
Table of Contents.....	iii
List of Tables	v
List of Figures	vi
List of Illustrations.....	xii
Background and Introduction	1
Illustrations	3
Bibliography	4
Chapter 1: Going and growing with the flow: Linking seagrass morphology, sediment composition, and local hydrodynamic conditions.	5
Abstract.....	5
Introduction.....	6
Morphological Variation of Marine Macroalgae and Seagrasses.....	6
Sediment Composition.....	11
Objectives and Hypotheses	12
Methods.....	14
Site Location	14
Hydrodynamic Characteristics.....	15
Sediment Characteristics.....	15
Seagrass Morphology and Biomechanics	16
Flow Tank Experiment	17
Statistical Analysis.....	19
Results.....	19
Hydrodynamics.....	19
Sediment Characteristics.....	21
Seagrass Morphology and Biomechanics	21
Flow Tank Experiment	24
Discussion	25
Above Ground Morphological Variation.....	26
Biomechanical Variation	33
Below Ground Biomass Variation	34
Conclusions.....	36
Bibliography	39
Tables:.....	43
Figures.....	45
Illustrations	62
Chapter 2: Light availability in <i>Zostera marina</i> beds exposed to currents and waves: the importance of leaf morphology, shoot density, and self-shading.	65
Abstract.....	65
Introduction.....	66
Objectives and Hypotheses	69
Methods.....	71

Site Location	71
Hydrodynamics and Seagrass Leaf Motion	72
Light.....	73
Seagrass Morphology.....	73
Video Analysis.....	74
Horizontally Projected Leaf Area (l_p)	75
Calculations of Biomass and l_p	76
Bio-optical Properties of the Seagrasses.....	80
Flow Tank Experiment	80
Statistical Analysis.....	82
Results.....	83
Hydrodynamics	83
Light: Downwelling vs. Diffusive	84
Light vs. Turbidity	85
Seagrass Morphology.....	85
Video Analysis.....	86
Calculations of Biomass and l_p	87
Bio-optical Properties	90
Flow Tank Experiment	91
Discussion	91
Hydrodynamics and Light Availability	92
Hydrodynamics, Epiphytes, and Nutrient Uptake	97
Conclusions.....	100
Bibliography	102
Tables.....	106
Figures.....	110
Illustrations	130
Final Conclusions.....	134
Synthesis	134
Beyond Long Island Sound.....	138
Bibliography	140
Illustrations	142
Appendix 1: Spring versus summer morphology of the seagrass <i>Zostera marina</i> ...	146
Figures.....	149
Appendix 2: Linking carbon, chlorophyll, and water column nutrients (N & P) to <i>Zostera marina</i> productivity.	153
Bibliography	159
Figures.....	160
Complete Bibliography	167

List of Tables

Table 1.1. The degrees of freedom (DF), mean square (MS), F value (F) and p value (p) from the ANOVA performed on sediment organic content and morphology of <i>Z. marina</i> collected from the quiescent, high current, and high wave sites off Fisher's Island, NY. For leaf flexibility, the 50% analysis is the angle at which 50% of the leaves had broke, whereas the slope analysis is the slope of the linearized relationship between bending angle and percent broken at that angle. Italicized p-values represent significant differences at $p < 0.05$	43
Table 1.2. The degrees of freedom (DF), mean square (MS), F value (F) and p value (p) from the ANOVA performed on the morphology of <i>Z. marina</i> collected from the quiescent, high current, and high wave sites off Fisher's Island, NY for the flow tank experiment A) initially, and B) when planted in common garden conditions in flow tanks for 10 weeks, as well as sediment characteristics into which <i>Z. marina</i> shoots were transplanted. Italicized p-values represent significant differences at $p < 0.05$. .	44
Table 2.1. Summary of the average field conditions and <i>Z. marina</i> morphology \pm standard error from the quiescent, high current, and high wave sites off Fisher's Island, NY. Sites with different letters denote significant differences at $p < 0.05$. .	106
Table 2.2. The degrees of freedom (DF), mean square (MS), F value (F) and p value (p) from a regression analysis performed of K_d vs. wave height at the high wave site and K_d vs. current speed at the high current site off Fisher's Island, NY in June 2008. Italicized p-values represent significant differences at $p < 0.05$	107
Table 2.3. The degrees of freedom (DF), mean square (MS), F value (F) and p value (p) from the ANOVA performed on leaf characteristics of <i>Z. marina</i> collected from the quiescent, high current, and high wave sites off Fisher's Island, NY. Italicized p-values represent significant differences at $p < 0.05$	107
Table 2.4. The self-shading factor (SSF) (%) for each leaf orientation that is associated with the quiescent, high current, and high wave sites, and the self-shading factor weighted over a 12-hour light cycle [SSF(12)] and the epiphyte factor (EF) for the quiescent, high current, and high wave sites located off Fisher's Island, NY....	108
Table 2.5. Table of the degrees of freedom (DF), mean square (MS), F value (F) and p value (p) from the ANOVA performed on A) the yield of <i>Z. marina</i> leaves collected from the quiescent, high current, and high wave sites off Fisher's Island, NY and B) the yield of <i>Z. marina</i> leaves collected from the quiescent, high current, and high wave sites off Fisher's Island, NY and then planted in common garden conditions in outdoor flow tanks for 10 weeks. Italicized p-values represent significant differences at $p < 0.05$	109

List of Figures

Figure 1.1 A) Location of Fisher’s Island, NY within Long Island Sound, note the extremely long fetch in the SE direction, and B) location of three field sites around Fisher’s Island, NY: 1) quiescent site which is protected from currents and waves, 2) high current site as tidal currents are increased between the island and 3) high wave site with oceanic swell. 45

Figure 1.2. Significant wave height (m) at the quiescent (light grey triangles), high current (dark grey squares) and high wave (black triangles) sites measured over a two week period in August, 2007. The tidal signal present at the high wave site was found to be significantly related to water depth ($p < 0.0001$) such that when the tide was low, significant wave height decreased, and when the tide was high, significant wave height increased. 46

Figure 1.3. Average current speed (m s^{-1}) plotted over water depth for the quiescent (light grey diamonds), high wave (black triangles), and high current (dark grey, slack tide – circles, flood tide - squares) sites over a six hour period in June, 2008. Tidal phase was a neap tide. Canopy height was 29.5 cm, 4.8 to 27.8 cm, 103 cm, and 41.5 cm for the quiescent, high wave, and high current slack or high current flood tide..... 47

Figure 1.4. A) Average grain size distribution and B) average percent organic matter of sediment cores collected in July, 2007 from the quiescent, high current, and high wave sites off Fisher’s Island, NY. Error bars represent \pm S.E., $n = 7$ 48

Figure 1.5. Average length of the longest root of *Z. marina* collected from the quiescent, high current, and high wave sites off Fisher’s Island, NY in July, 2007. Error bars represent \pm S.E., $n = 7$ for high current and high wave sites, $n = 4$ for quiescent site. Quiescent > (High Current = High Wave). 49

Figure 1.6. Average number of roots per node of *Z. marina* collected from the quiescent, high current, and high wave sites in July, 2007. Error bars represent \pm S.E., $n = 7$ for high current and high wave sites, $n = 4$ for quiescent site. High Current > High Wave but High Current = Quiescent. 50

Figure 1.7. Average secondary (light grey) and tertiary (dark grey) leaf length (cm) of *Z. marina* collected from the quiescent, high current, and high wave sites in July, 2007. Error bars represent \pm S.E., $n = 7$ for high current and high wave sites, $n = 4$ for quiescent site. High Current >> (Quiescent = High Wave). 51

Figure 1.8. Average secondary (light grey) and tertiary (dark grey) leaf width (mm) of *Z. marina* collected from the quiescent, high current, and high wave sites in July, 2007. Error bars represent \pm S.E., $n = 7$ for high current and high wave sites, $n = 4$ for quiescent site. High Wave << Quiescent < High Current. 52

Figure 1.9. Average number of leaves of <i>Z. marina</i> shoots collected from the quiescent, high current, and high wave sites in July, 2007. Error bars represent +/- S.E., n = 7 for high current and high wave sites, n = 4 for quiescent site. Quiescent > (High Current = High Wave).	53
Figure 1.10. Average shoot density of <i>Z. marina</i> at the quiescent, high current, and high wave sites in July, 2007. Error bars represent +/- S.E., n = 7. High Wave >> (Quiescent = High Current).	54
Figure 1.11. Average force in Newtons (N) required to break the tertiary leaf of <i>Z. marina</i> collected from the quiescent, high current, and high wave site in July, 2007. Error bars are +/- SE, n = 7. High Current > (Quiescent = High Wave).	55
Figure 1.12. A) Cumulative distribution and B) the natural log of the cumulative distribution of the angle (degrees) required to break the tertiary leaf of <i>Z. marina</i> collected in July, 2008 from the quiescent (light grey diamonds), high current (dark grey squares), and high wave (black triangles) sites off Fisher's Island, NY. Error bars represent +/- S.E., n = 5. A: Quiescent = High Current = High Wave. B: Quiescent < (High Current = High Wave).	56
Figure 1.13. Average secondary (A) and tertiary (B) leaf lengths (cm) of <i>Z. marina</i> collected from the quiescent (white), high current (grey), and high wave (black) sites in April 2008 and grown in outdoor flow tanks under common garden conditions for 10 weeks. Error bars represent +/- S.E., n = 4.	57
Figure 1.14. Average secondary (A) and tertiary (B) leaf widths (mm) of <i>Z. marina</i> collected from the quiescent (white), high current (grey), and high wave (black) sites in April, 2008 and grown in outdoor flow tanks under common garden conditions for 10 weeks. Error bars represent +/- S.E., n = 4.	58
Figure 1.15. A) Average grain size distribution of sediment cores collected from flow tank trays initially, before <i>Z. marina</i> was transplanted, and at the end of the 10 week flow tank experiment. B) Average percent organic matter of sediment collected via cores from flow tank trays initially, before <i>Z. marina</i> was transplanted, and at the end of the 10 week flow tank experiment. Error bars represent +/- S.E., n = 4 for final conditions and 6 for initial conditions.	59
Figure 1.16. Average length of the longest root of <i>Z. marina</i> collected from the quiescent (white), high current (grey), and high wave (black) sites in April, 2008 (Initial) and grown in outdoor flow tanks for 10 weeks. Error bars represent +/- S.E., n = 4.	60
Figure 1.17. Average number of roots per node of <i>Z. marina</i> collected from the quiescent (white), high current (grey), and high wave (black) sites in April, 2008 (Initial) and grown in outdoor flow tanks for 10 weeks. Error bars represent +/- S.E., n = 4.	61

Figure 2.1. A) Location of Fisher's Island, NY within Long Island Sound; note the extremely long fetch in the SE direction, and B) location of the three field sites around Fisher's Island, NY: 1) quiescent site which is protected from currents and waves, 2) high current site as tidal currents are increased between the island and 3) high wave site with oceanic swell..... 110

Figure 2.2. Significant wave height (m) at quiescent (light grey diamonds), high current (dark grey squares), and high wave (black triangles) sites off Fisher's Island, NY measured over a five day period in July, 2007. Arrows indicate when videos of seagrass in motion were taken. The tidal signal present at the high wave site was found to be significantly related to water depth ($p < 0.0001$) such that when the tide was low, significant wave height decreased, and when the tide was high, significant wave height increased. 111

Figure 2.3. Average current profile (cm s^{-1}) throughout the water column at the high current site during slack (white circles), beginning (light grey squares), increasing (dark grey triangles), and maximum (black x) flood tide over a six-hour period in June, 2008 during a neap tide. Pictures were taken at each of these tidal phases to supplement the video analysis and to determine bending angle over an entire tidal cycle. 112

Figure 2.4. Average cosine for downwelling light ($\overline{\mu_d}$) calculated at the surface, 0.5, 1.0, 1.5 and 2.0 m (if available) below the surface at the quiescent (light grey diamonds), high current (dark grey squares), and high wave (black triangles) sites off Fisher's Island, NY. Numbers at the bottom of the profile are averages over depth. 113

Figure 2.5. K_d (m^{-1}) over time at the quiescent site off Fisher's Island, NY measured in July 2008 between 13:30 and 16:00. 114

Figure 2.6. At the high wave site off Fisher's Island, NY: A) Significant wave height (m) and K_d (m^{-1}) measured between 10:30 and 12:30 in July 2008. B) Linear relationship between significant wave height and K_d was not significant ($p = 0.5132$). 115

Figure 2.7. At the high current site off Fisher's Island, NY: A) Current speed (cm s^{-1}) and K_d (m^{-1}) measured between 11:30 and 15:00 in July 2008. B) Positive, linear relationship between current speed and K_d ($p = 0.0006$) such that as current speed increases by 10 cm s^{-1} , K_d increases by 0.02. 116

Figure 2.8. Average $\delta^{13}\text{C}$ (‰) (bars) and carbon content (‰) (black diamonds) of *Z. marina* leaves collected from the quiescent, high current and high wave sites off Fisher's Island, NY. Error bars represent \pm S.E., $n = 4$ 117

Figure 2.9. Average $\delta^{15}\text{N}$ (‰) (bars) and nitrogen content (%) (black diamonds) of <i>Z. marina</i> leaves collected from the quiescent, high current and high wave sites off of Fisher's Island, NY. Error bars represent \pm S.E., $n = 4$	118
Figure 2.10. Schematic view of the average shape of a <i>Z. marina</i> leaf video taped at the quiescent site off Fisher's Island, NY where β_n = leaf bending angle and L_n = leaf length at β_n . Leaves stayed in this position at all times.	119
Figure 2.11. Schematic view of the average shapes of a <i>Z. marina</i> leaf video taped and photographed over a half tidal cycle at the high current site off Fisher's Island, NY. Tidal currents ranged from 3 to 41 cm s^{-1} during different phases of the tide. The percent of time a leaf spent bent at a certain angle for current velocities of 6, 16, 25, and 38 cm s^{-1} are shown below each shape.....	120
Figure 2.12. Schematic view of the average shapes a <i>Z. marina</i> leaf occupies during a passage of a wave at the high wave site off Fisher's Island, NY where significant wave height ranged from 0.15 to 0.37 m. The percent of time a leaf spent at a certain position for each of the 7 key phases of the plants motion are shown below each shape.	121
Figure 2.13. Vertical biomass (%) distribution for <i>Z. marina</i> at A) the quiescent site, B) the high current site for each of the 4 dominate shapes that the canopy occupied during different current velocities, and C) the high wave site for each of the 7 shapes that the seagrass canopy occupied under different wave phases. Note that the vertical biomass distribution in A does not change over time; biomass distribution fluctuated every few hours between curves in B and in a matter of seconds or fractions of a second in C.....	122
Figure 2.14. Horizontally projected leaf area [$l_p(z)$] (m^2 leaf m^{-2} seabed) for <i>Z. marina</i> at A) the quiescent site, B) the high current site for each of the 4 dominate shapes that the canopy occupied during different current velocities, and C) the high wave site for each of the 7 shapes that the seagrass canopy occupied under different wave phases.	123
Figure 2.15. B) Vertically integrated horizontally projected leaf area [$l_p(12)$] for <i>Z. marina</i> leaves from the quiescent, high current, and high wave sites located off Fisher's Island, NY.	124
Figure 2.16. Vertically integrated horizontally projected leaf area [$l_p(12)$] adjusted for self-shading (gray) and self-shading plus epiphyte growth (black) for <i>Z. marina</i> leaves from the quiescent, high current, and high wave sites located off Fisher's Island, NY.	125
Figure 2.17. Range of vertically integrated horizontally projected leaf area [$l_p(12)$] (m^2 leaf m^{-2} seabed) adjusted for self-shading and epiphytic growth for <i>Z. marina</i> at the quiescent, high current, and high wave sites off Fisher's Island, NY. The	

horizontal line represents the average $I_p(12)$. The top of the vertical line is the maximum $I_p(12)$ and the bottom of the vertical line is the minimum $I_p(12)$. The horizontal dashed line is an extension of the minimum $I_p(12)$ possible for the quiescent site, which is greater than and equal to the high current and high wave maximums, respectively. 126

Figure 2.18. Average photosynthetic leaf absorbance of tertiary *Z. marina* leaves collected from the quiescent (light grey), high current (dark grey), and high wave (black) sites off Fisher's Island, NY in July, 2008. 127

Figure 2.19. Average photosynthetic yield ($\mu\text{mols electrons m}^{-2} \text{ s}^{-1}$) of tertiary *Z. marina* leaves from the quiescent (light grey diamonds), high current (dark grey squares), and high wave (black triangles) sites off Fisher's Island, NY measured in June, 2008. Error bars represent \pm S.E., $n = 5$ 128

Figure 2.20. Average photosynthetic yield ($\mu\text{mols electrons m}^{-2} \text{ s}^{-1}$) of tertiary *Z. marina* leaves collected from quiescent (diamonds), high current (squares), and high wave (triangles) sites off Fisher's Island, NY and transplanted into outdoor flow tanks with similar currents ($9 \pm 2 \text{ cm s}^{-1}$) and sediment (fine sand, 0.52% organic content). Shown measurements were made at weeks 3 (grey) and 5 (black). Error bars represent \pm S.E., $n = 4$ 129

Figure A1.1. Average leaf length of the secondary (grey) and tertiary (black) leaves of *Z. marina* collected from the quiescent, high current, and high wave sites off Fisher's Island, NY in May, 2007. Error bars represent \pm S.E., $n = 5$ 149

Figure A1.2. Average leaf width of the secondary (grey) and tertiary (black) leaves of *Z. marina* collected from the quiescent, high current, and high wave sites off Fisher's Island, NY in May, 2007. Error bars represent \pm S.E., $n = 5$ 150

Figure A1.3. Average root length of *Z. marina* collected from the quiescent, high current, and high wave sites off Fisher's Island, NY in May, 2007. Error bars represent \pm S.E., $n = 5$ 151

Figure A1.4. Average number of roots of *Z. marina* collected from the quiescent, high current, and high wave sites off Fisher's Island, NY in May, 2007. Error bars represent \pm S.E., $n = 5$ 152

Figure A2.1. Average carbon (%) content of *Z. marina* leaves collected from the quiescent, high current, and high wave sites off Fisher's Island, NY in August, 2007. Error bars represent \pm S.E., $n = 5$ 160

Figure A2.2. Average carbon (%) content of *Z. marina* collected at the quiescent, high current, and high wave sites off Fisher's Island, NY in April, 2008 for the purpose of the flow tank experiment A) initially and B) after 10 weeks of growing under common garden conditions. Error bars represent \pm S.E., $n = 4$ 161

Figure A2.3. Average water column A) ammonia (μM), nitrate-nitrite (μM), and B) orthophosphate (μM) concentrations collected at the surface from the quiescent, high current, and high wave sites off Fisher's Island, NY in April, 2008. Error bars represent \pm S.E., $n = 4$ 162

Figure A2.4. Average water column A) ammonia (μM) and B) nitrate-nitrite (μM) concentrations that *Z. marina* shoots experienced in each tank at weeks 3, 5, 7 and 9 of the flow tank experiment. Error bars represent \pm S.E., $n = 1 - 4$ 163

Figure A2.5. Average water column orthophosphate (μM) concentrations that *Z. marina* shoots experienced in each tank at weeks 3, 5, 7 and 9 of the flow tank experiment. Error bars represent \pm S.E., $n = 1 - 4$ 164

Figure A2.6. Average chlorophyll a concentration ($\mu\text{g cm}^{-2}$) of the tertiary leaf of *Z. marina* collected from the quiescent, high current, and high wave sites in August, 2007. Error bars represent \pm S.E., $n = 4$ 165

Figure A2.7. Average chlorophyll a concentration ($\mu\text{g cm}^{-2}$) of the tertiary leaf of *Z. marina* collected from the quiescent, high current, and high wave sites in April, 2008 and then planted in common garden conditions. Analysis of chlorophyll a was done initially and at weeks 2, 5 and 10. Error bars represent \pm S.E., $n = 4$ 166

List of Illustrations

Illustration B.1. Schematic of how waves and currents, and the sediment found under those hydrodynamic conditions, affect seagrass leaf morphology, leaf motion and orientation, light availability, and thus, the productivity of seagrass beds. 3

Illustration 1.1. Illustration of modified dynamometer used to measure the strength of the tertiary leaf of *Z. marina* collected from the quiescent, high current, and high wave sites. The base of the tertiary leaf was secured with the clip, while the tip of the leaf was held in place. The end of the dynamometer was pulled, moving the black rubber piece along the length of the fishing line. When the leaf broke, the distance that the rubber piece had moved was recorded, and used to calculate force from a linear regression achieved from a calibration. 62

Illustration 1.2. Diagram of the apparatus used to measure the breaking angle of the tertiary leaf of *Z. marina* collected from the quiescent, high current, and high wave site. Base of tertiary leaf was secured in the center of the circular base. The tip was then rotated around the circle with equal tension until the leaf broke. The angle at which the leaf broke was recorded to the nearest 5°. 63

Illustration 1.3. Schematic of flow tank set-up used for the common garden experiment. Current was generated with a trolling motor, which circulated water around the flow tank. Water flow was directed through a flow straightener and collimator before flowing over *Z. marina* shoots. There were 6 of these flow tanks, making a total of 12 trays with transplanted seagrass, which contained 6 *Z. marina* shoots each. 64

Illustration 2.1. Schematic of how a *Z. marina* shoot was treated in order to calculate horizontally projected leaf area (l_p). The maximum canopy height (H_c) was divided into 100 sections (z); only 3 are represented here ($z_1, z_2, \dots z_n$). For each section (z), the amount of photosynthetic tissue that occupied that section of the water column (based on leaf length, width, and shoot density) was multiplied by the sine of the bending angle (β). l_p is denoted by the horizontal dashed line. As the leaf length is bent at a greater angle (β_2), the leaf occupies less of H_c , but l_p increases. This schematic does not take into account self-shading or epiphyte colonization, but visually demonstrates how a shoot, and the entire canopy, is manipulated in the calculations. 130

Illustration 2.2. Schematic of how the average distance between *Z. marina* shoots, bending angle, and leaf area were used to determine the shaded and non-shaded area of the leaf tissue, which was used in the EF calculation. In this example, $\beta = 45^\circ$ was used. 131

Illustration 2.3. Schematic of flow tank set-up used for the common garden experiment. Current was generated with a trolling motor, which circulated water around the flow tank. Water flow was directed through a flow straightener and

collimator before flowing over *Z. marina* shoots. There were 6 of these flow tanks, making a total of 12 trays with transplanted seagrass, which contained 6 *Z. marina* shoots each. 132

Illustration 2.4. Schematic view of how bending angle alters the amount of seagrass tissue occupying each canopy section (z), how much self-shading occurs, and how this affects horizontally projected leaf area [$l_p(z)$]. When a seagrass leaf is bent at a small angle and is in a more upright position, more z contain seagrass tissue, yet there is less tissue per z . Therefore, l_p per z is small but more z have l_p . Conversely, when a seagrass leaf is bent at a larger angle and is in a more horizontal position, fewer z contain seagrass tissue, yet there is more tissue per z . Therefore, l_p per z is large but fewer z have l_p . This schematic also demonstrates the self-shading factor (SSF), which is the percent of the leaf tissue that is potentially shaded by a neighboring leaf, which is bent over at some angle, as denoted by the dashed line. Bending leaves decrease the light incident on the tissue layer below the top layer of tissue, and the SSF increases with increasing bending angle. 133

Illustration FC.1. Original schematic of how water flow and sediment affect seagrass morphology and light availability with the complexities presented in this thesis added. These complexities include self-shading, epiphyte colonization, hydrodynamically induced turbidity, leaf movement, and carbon availability, all of which contribute to the productivity of seagrass beds and are directly related to the local hydrodynamic climate. 142

Illustration FC.2. Conceptual diagram of the advantages and disadvantages of occupying an environment dominated by low water flow, as was observed for *Z. marina* at our quiescent site. Solid lines represent variables that were quantified, whereas dashed lines represent hypotheses. Self-shading was low, and therefore light availability was high, yet epiphytic colonization was present at a moderate level, which slightly reduced light availability to the seagrass leaves. Additionally, we hypothesized that carbon and nitrogen availability were low due to a thick diffusive boundary layer and low organic matter turnover rates in the sediment, respectively. *Z. marina* roots at this site were long as a result of the nutrient poor sediment. 143

Illustration FC.3. Conceptual diagram of the advantages and disadvantages of occupying an environment dominated by strong currents, as was observed at our high current site. Solid lines represent variables that were quantified, whereas dashed lines represent hypotheses. Self-shading was high, and therefore light availability was low. Additionally, currents seemed to reduce the amount of epiphyte colonization, yet epiphytes were still present in a low abundance and therefore slightly reduced light availability to the seagrass leaves. However, we hypothesized that carbon and nitrogen availability were high due to a thin leaf diffusive boundary layer and high organic matter turnover rates in the sediment, respectively. This increase in nutrient availability in the sediment may account for the longer leaves present at this site. . 144

Illustration FC.4. Conceptual diagram of the advantages and disadvantages of occupying an environment dominated by waves, as was observed at our high wave site. Solid lines represent variables that were quantified, whereas dashed lines represent hypotheses. Self-shading was high, and therefore light availability to seagrass leaves was low, yet was not as low as the high current site, presumably because *Z. marina* was benefiting from the opening and closing of the canopy, which provides moments of high light availability (when the canopy is open). Additionally, wave action eliminated epiphyte colonization. We hypothesized that carbon and nitrogen availability were high due to a thin leaf diffusive boundary layer and high organic matter turnover rates in the sediment, respectively. However, at the high wave site sediment was a mixture of gravel and fine sand, which is less permeable than the sediment at the high wave site. On the other hand, *Z. marina* from the high wave site was the least carbon limited, which may account for the high shoot density present at this site..... 145

Background and Introduction

Water flow plays an important role in all phases of the life of aquatic organisms by directly affecting plants and animals and the environment they inhabit. In shallow coastal areas that are colonized by a variety of organisms including benthic plants such as macroalgae and seagrasses, tidal currents and wind-generated waves dominate water flow. Seagrasses are believed to have originated from terrestrial angiosperms (flowering plants) when they transitioned back to the aquatic environment (Den Hartog 1970), as selection favored those plants that had flexible morphologies over those plants with rigid, woody characteristics. Having a flow-compatible morphology is of the utmost importance for long-term survival in an aquatic environment and the success of seagrasses in this arena can be mainly attributed to reduced drag exerted on flexible leaves when compared to stiff trunks and branches of woody plants (Bouma et al. 2005).

Despite exerting a force (drag) on their leaves, water flow also plays an important role in sustaining life for seagrasses as they deflect and sway with currents and waves. Water flow fertilizes flowers (Ackerman 1986), disperses seeds that affect the growth and development of new seagrass populations (Fonseca and Kenworthy 1987), and delivers nutrients (Thomas et al. 2000, Thomas and Cornelisen 2003, Cornelisen and Thomas 2004, Morris et al. 2008) and carbon (Koch 1994) to the plant surface thereby affecting productivity. Water flow also affects the composition of the sediment seagrasses colonize (Koch 1999). As current velocity and wave energy increase, sediments tend to become coarser and contain less organic

content (Koch 1999), thereby creating a compounding effect when studying hydrodynamic processes in seagrass beds.

The biological feedbacks of water flow are dynamic and their impacts may change over scales of seconds (wave-induced) to days and weeks (tidally induced) (Koch et al. 2009). Here, we incorporate biological consequences and feedbacks of water flow induced processes into existing models of light reaching seagrass canopies. Specifically, leaf morphology, shoot density, and sediment composition are a function of local hydrodynamic conditions, which also affect how seagrasses grow, move and orient themselves throughout the water column (Illustration B.1). In order to further understand the role of water flow in light availability to seagrass leaves, leaf morphology, shoot density, and leaf orientation under quiescent, as well as current and wave-dominated conditions, were quantified *in situ* and applied to a light availability model developed by Zimmerman (2003).

Illustrations

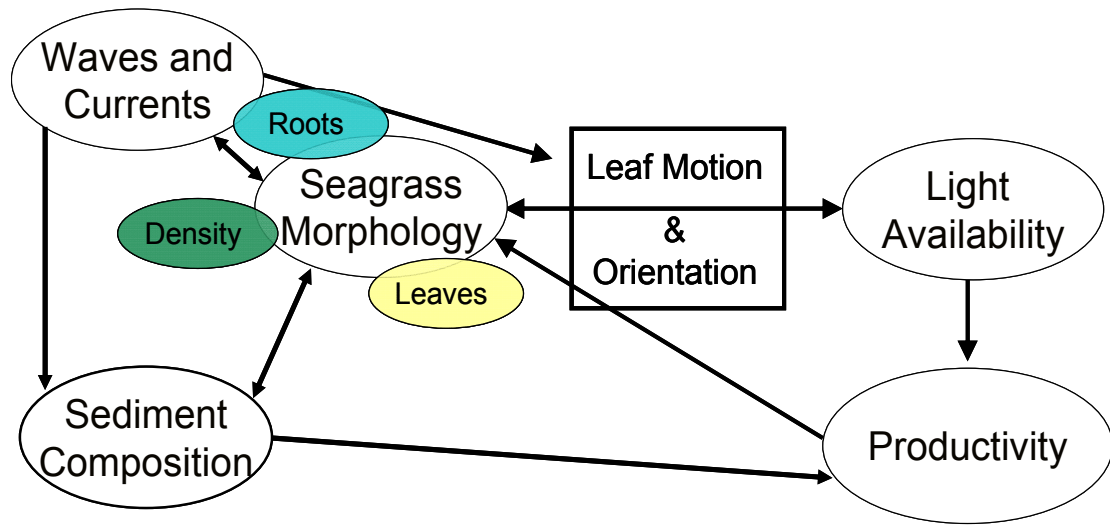


Illustration B.1. Schematic of how waves and currents, and the sediment found under those hydrodynamic conditions, affect seagrass leaf morphology, leaf motion and orientation, light availability, and thus, the productivity of seagrass beds.

Bibliography

- Ackerman, J.D. 1986. Mechanistic implications for pollination in the marine angiosperm *Zostera marina*. *Aquatic Botany* 24: 343 – 353.
- Bouma, T.J., M.B De Vries, E. Low, G. Peralta, I.C. Tanczos, J. van de Koppel, and P.M.J. Herman. 2005. Trade-offs related to ecosystem engineering: A case study on stiffness of emerging macrophytes. *Ecology* 86: 2187 – 2199.
- Cornelisen, C.D., and F.I.M. Thomas. 2004. Ammonium and nitrate uptake by leaves of the seagrass *Thalassia testudinum*: impact of hydrodynamic regime and epiphyte cover on uptake rate. *Journal of Marine Systems* 49: 177 – 194.
- Den Hartog, C. 1970. *The Seagrasses of the World*. North-Holland Publishers, Amsterdam.
- Fonseca, M.S., and W.J. Kenworthy. 1987. Effects of current on photosynthesis and distribution of seagrasses. *Aquatic Botany* 27: 59 – 78.
- Koch, E.W. 1994. Hydrodynamics, diffusion-boundary layers and photosynthesis of the seagrasses *Thalassia testudinum* and *Cymodocea nodosa*. *Marine Biology* 118: 767 – 776.
- Koch, E.W. 1999. Preliminary evidence on the interdependent effect of currents and porewater geochemistry on *Thalassia testudinum* Banks ex König seedlings. *Aquatic Botany* 63: 95 – 102.
- Koch, E.W., E.B. Barbier, B.R. Silliman, D.J. Reed, G.M.E. Perillo, S.D. Hacker, E.F. Granek, J.H. Primavera, N. Muthiga, S. Polasky, B.S. Halpern, C.J. Kennedy, C. V. Kappel, and E. Wolanski. 2009. Non-linearity in ecosystem services: temporal and spatial variability in coastal protection. *Frontiers in Ecology and the Environment* 7: 29 – 37.
- Morris, E.P., G. Peralta, F.G. Brun, L. van Duren, T.J. Bouma, and J.L. Perez-Llorens. 2008. Interaction between hydrodynamics and seagrass canopy structure: Spatially explicit effects on ammonium uptake rates. *Limnology and Oceanography* 53: 1531 – 1539.
- Thomas, F.I.M., C.D. Cornelisen, and J.M. Zande. 2000. Effects of water velocity and canopy morphology on ammonium uptake by seagrass communities. *Ecology* 81: 2704 – 2713.
- Thomas, F.I.M., and C.D. Cornelisen. 2003. Ammonium uptake by seagrass communities: effects of oscillatory versus unidirectional flow. *Marine Ecology Progress Series* 247: 51 – 57.
- Zimmerman, R.C. 2003. A biooptical model of irradiance distribution and photosynthesis in seagrass canopies. *Limnology and Oceanography* 48: 568 – 585.

Chapter 1: Going and growing with the flow: Linking seagrass morphology, sediment composition, and local hydrodynamic conditions.

Abstract

Previous studies that examined the effect of water flow on seagrass morphology present contradicting results: leaves have been reported to become both longer and shorter or wider and narrower with increasing water flow. In an attempt to clarify these contradictions, sediment characteristics, a parameter affected by water flow, seagrass morphology, and biomechanics were quantified in order to understand how waves, currents, or the lack there of, and the sediment present under these hydrodynamic conditions, affects seagrass morphology. Our results suggest that both water flow and sedimentary processes affect below- and above-ground morphology of *Z. marina*. Differences in root length were related to sediment composition while differences in root number were related to water flow. The long and wide leaves of *Z. marina* exposed to currents may be a result of increased porewater nutrient turnover rates due to water flow induced particle entrainment. The drag exerted on such long and wide leaves would theoretically be large, but being strong and flexible allows these plants to deflect with the current thereby reducing drag. Conversely, when *Z. marina* is exposed to oceanic swell, a high shoot density and increased flexibility may reduce within canopy flow and drag, while an intermediate leaf length may be necessary to avoid entanglement as leaves sway back and forth. Therefore, drag minimization in *Z. marina* exposed to currents and waves appears to be the result of both “going” (i.e. bending and swaying) and “growing” (i.e. changing morphology) with the flow.

Introduction

Marine organisms have acclimated (phenotypically plastic) and adapted (genetically fixed) to the aquatic environment they inhabit. A particular species can acclimate to varying hydrodynamic forces exerted upon them by changing their morphology (streamlining), thus increasing their potential of survival under extreme conditions. Such hydrodynamically-induced changes have been observed in feeding appendages of calanoid copepods (Koehl 1994), fin location, body depth, and caudal peduncle length of pumpkinseed *Lepomis gibbosus* populations (Vila-Gispert et al. 2007) and in frond width and degree of undulation in macroalgae (Gerard and Mann 1979, Gerard 1982, Koehl and Alberte 1988, Molloy and Bolton 1996, Kawamata 2001, Denny and Roberson 2002, Roberson and Coyer 2004). The effect of water flow on seagrass morphology has also been observed (Dennison and Alberte 1982, Fonseca and Kenworthy 1987, Sidik et al. 1999, Peralta et al. 2000, Schanz and Asmus 2003, Peralta et al. 2005, Jordan 2008) but the data are mostly anecdotal and reach conflicting conclusions.

Morphological Variation of Marine Macroalgae and Seagrasses

The effect of water flow on kelp has received more attention than seagrasses. Therefore, the kelp literature allows us to better understand how water flow may affect marine plant morphology. In this process it is necessary to keep in mind the differences between kelp and seagrasses, which are the focus of this study: kelp, as almost all macroalgae, attach to hard substrates via holdfasts while seagrasses colonize soft substrates via roots that serve to anchor the plants and also take up nutrients. As a result, while water flow directly affects both kelp and seagrasses

through physical forcing, water flow also indirectly affects seagrasses via sediment composition.

Water flow clearly affects kelp morphology. Kelp found in high water flow areas are characterized by thick, long, and narrow fronds, whereas those found in low water flow areas are characterized by broad, thin, textured or undulate fronds (Gerard and Mann 1979, Gerard 1982, Koehl and Alberte 1988, Molloy and Bolton 1996, Kawamata 2001, Denny and Roberson 2002, Roberson and Coyer 2004). The capacity to acclimate to hydrodynamic forces allows these algae to prosper in a broad range of environments. The high water flow morphology reduces the drag exerted on the fronds thereby decreasing the likelihood of dislodgement. Conversely, the low water flow morphology allows for increased uptake of nutrients and CO₂ via decreased frond diffusive boundary layer (DBL) thickness (Gerard and Mann 1979, Gerard 1982, Koehl and Alberte 1988, Molloy and Bolton 1996, Kawamata 2001, Denny and Gaylord, 2002, Denny and Roberson 2002, Roberson and Coyer 2004), which is a barrier to the flux of molecules from the water column to the plant surface (Koch 1994). Furthermore, fronds of *Turbinaria ornate* located in protected backreef areas have pneumatocysts that provide positive buoyancy, while those located in wave-exposed areas lack pneumatocysts and are negatively buoyant (Stewart 2006). Positively buoyant fronds are advantageous in a low water flow environment where crowding and shading are common (Stewart 2006).

Morphological variations as a function of water flow are also observed in the anchoring mechanism of kelp. Kelp from low water flow environments have smaller holdfasts than kelp from high water flow environments (Roberson and Coyer 2004).

By adjusting holdfast size, algae ensure a minimization of energy expenditure in low water flow environments where a strong holdfast is unnecessary, while providing a strong holdfast in high water flow environments where dislodgement is more likely (Roberson and Coyer 2004).

As seen above, it is well understood that kelp become more streamlined (longer and thinner) with increasing current velocity (Gerard and Mann 1979, Gerard 1982, Koehl and Alberte 1988, Molloy and Bolton 1996, Kawamata 2001, Denny and Gaylord 2002, Denny and Roberson 2002, Roberson and Coyer 2004, Stewart 2006). Since seagrasses and kelp have similar hydrodynamic stresses to overcome, it would seem that seagrasses, as do kelp, would also get longer and narrower with increasing water flow. However, sometimes this seems to be the case, while other times it does not.

The seagrass genus *Phyllospadix*, which inhabits rocky substrates, experience strong wave and current action and are characterized by long and narrow leaves that have a high shoot density. *P. scouleri* and *P. torreyi* located along the Pacific coast of Baja California (Mexico) were reported to have maximum leaf lengths from 30 to 60 cm and 50 to 70 cm, respectively (Ramirez-Garcia et al. 1998, Ramirez-Garcia et al. 2002), and densities of 8,472 shoots m⁻² for *P. scouleri* and 6,759 shoots m⁻² for *P. torreyi* (Ramirez-Garcia et al. 1998). Additionally, *Phyllospadix* was found to have greater hypodermal fiber and root hair development, thickened rhizomes, and smaller lacunae when compared to other species found in protected coastal environments with sandy bottoms (Cooper and McRoy 1988). The authors noted that seagrasses

exposed to strong currents might develop thicker cell walls and cuticles as a mechanism to protect their tissues from mechanical damage.

Redirecting our attention to the Wadden Sea, the opening of a channel in a barrier island provided a unique opportunity to evaluate the effect of water flow on seagrass morphology. *Zostera noltii* experienced large physical impacts and was eventually lost. New shoots appeared in the previously quiescent and later wave-dominated area with clear morphometric changes: shorter and narrower leaves with longer internodes than shoots located in the nearby sheltered meadow (Peralta et al. 2005). These observations are in accordance with those of Schanz and Asmus (2003), who showed a significant decrease in leaf length and shoot number of *Z. noltii* with increasing current velocity when current speed was manipulated *in situ* with a field flume. Notably, sediment grain size was dominated by very coarse sand that was poorly sorted at the exposed site and coarse sand that was well to poorly sorted at the sheltered site (Schanz and Asmus 2003). When current velocity was manipulated *in situ*, the sediment nutrient concentrations at the sheltered site decreased when subjected to faster current speeds (Schanz and Asmus 2003).

In contrast to the above studies that focused on *Zostera noltii*, *Z. marina* exposed to current velocities of 2, 16, and 34 cm s⁻¹ under controlled flume conditions showed increasing leaf length with increasing current velocity (Fonseca and Kenworthy 1987). Furthermore, Jordan (2008) showed increasing shoot length and decreasing shoot width with increasing current velocity when *Z. marina* was exposed to current velocities of 0, 1, and 20 cm s⁻¹ in outdoor flumes. Interestingly, this trend

was only observed when sediment was sandy, a sediment characteristic usually found under high water flow conditions.

Yet another unresolved question in this arena is whether morphological differences found in seagrasses of varying water flow regimes are an adaptation or an acclimation. In some cases (Sidik et al. 1999, Peralta et al. 2000) two morphotypes of the same species co-exist, suggesting that morphological differences are genetically fixed. In other cases, morphological changes have been related to changes in local hydrodynamic regimes, suggesting a phenotypic change as a means of acclimation to water flow (Schanz and Asmus 2003, Peralta et al. 2005).

An aspect of morphology not considered in the above studies is the strength and flexibility of seagrass leaves. As currents and waves exert a force upon the seagrass leaves, the seagrass leaves respond accordingly. If the plants are to be successful in an area dominated by waves or currents, their structure must be compatible; that is, strong enough or flexible enough to 'go with the flow' without breaking or dislodgement. It was noted by Patterson et al. (2001) that the biomechanical properties such as breaking strength, stiffness, and toughness of reproductive shoots of *Zostera marina* follow a Weibull, not normal, distribution; which is characterized by an extended tail toward higher values. This type of distribution demonstrates that although a population may have a certain average for a biomechanical property, there are certain individuals within a population that are able to withstand the extremes, ensuring survival of the entire population (Patterson et al. 2001).

Sediment Composition

Although above ground morphology (leaf length and width) has been observed to change in response to hydrodynamic conditions, below ground morphology (root length and number) has been observed to change in response to both hydrodynamic conditions and sediment composition (Short 1983 and 1987, Fonseca and Kenworthy 1987, Peralta et al. 2000, Di Carlo 2007, Jordan 2008). Sediment grain size and porewater nutrient content are strongly influenced by local hydrodynamic conditions: sediments in high water flow environments are coarser and lower in organic content and nutrients than in low water flow environments (Christiansen et al. 1981, Koch 1999, Wargo and Styles 2007).

It has been well documented that sediment composition affects seagrass morphology (Short 1983 and 1987, Fonseca and Kenworthy 1987, Peralta et al. 2000, Cunha and Duarte 2007, Di Carlo 2007). Belowground biomass (roots and rhizome) of the seagrass *Cymodocea nodosa* was greater than aboveground biomass (leaves) in sandy sediments while the ratio was close to 1 in muddy sediments (Cunha and Duarte 2007). Additionally, Jordan (2008) found that *Zostera marina* roots in sandy (0.1% organic content) sediments were longer than those in muddier sediments (1% organic content), and that roots only become longer as a function of water flow in muddy sediments. Perhaps roots in sandy substrates are already long enough to provide extensive anchoring capacity under increasing current velocities. Therefore, sediments need to be considered a co-variable in hydrodynamic experiments involving seagrasses.

Objectives and Hypotheses

The goal of this study was to understand the relationships between water flow, seagrass morphology (leaf width and length, root length and number, and shoot density) and biomechanics (leaf strength and flexibility) with sediment type as a co-variable of water flow. The flowering marine plant *Zostera marina* was selected for this study due to its broad range of distribution (temperate waters of North America and Asia, the genus *Zostera* is found in temperate waters worldwide), its ecological and economical importance (Den Hartog 1970, Orth et al. 2006), its wide range of morphological variations observed *in situ*, and the wide range of hydrodynamic conditions under which it grows. We tested the following hypotheses:

Hypothesis 1: Zostera marina found in high water flow (strong current or large wave) environments will have longer, narrower leaves, longer roots and lower shoot density such that leaf area per m² seafloor is reduced yet the total amount of root material is increased, whereas *Z. marina* found in low water flow (weak current or small wave) environments will have shorter, wider leaves, shorter roots and higher shoot density such that leaf area per m² seafloor is increased yet the total amount of root material is reduced.

Rationale for Hypothesis 1: In order to successfully colonize an area, seagrass morphology needs to be compatible with local hydrodynamic conditions such that the morphology of *Zostera marina* exposed to currents and waves should reduce the amount of drag a leaf experiences via a streamlined morphology, and the amount of below ground biomass should increase to aid in anchorage.

Hypothesis 2: Sediment composition can counteract flow-induced morphological changes in the seagrass *Zostera marina*.

Rationale for Hypothesis 2: Based on preliminary results, sediment composition needs to be considered as a co-variable of flow-induced morphological changes; in most cases, sediment composition reflects local hydrodynamic conditions.

Hypothesis 3: *Zostera marina* found in high water flow (strong current or large wave) environments will be stronger (force (N) necessary to break leaf when pulled) and more flexible (angle necessary to break leaf when bent) than *Z. marina* found in low water flow (weak current or small wave) environments.

Rationale for Hypothesis 3: As described by Patterson et al. (2001), in high water flow environments a population is expected to have individuals that are stronger and more flexible than the bulk of the population, driving the overall average of the strength and flexibility of *Zostera marina* exposed to strong currents and waves higher than *Z. marina* exposed to low water flow environments.

Hypothesis 4: *Zostera marina* grown under the same hydrodynamic conditions (“common garden”) will develop the same morphological characteristics. Therefore, differences among *Z. marina* from different flow regimes are an acclimation to water flow.

Rationale for Hypothesis 4: Previous studies suggest that some seagrasses may acclimate to water flow while others may be adapted to local hydrodynamic conditions; this concept has not yet been tested for *Zostera marina*.

Methods

In order to address the hypotheses and questions presented above, a combination of field and laboratory work was conducted in 2007 and 2008.

Site Location

Field sites were located in Long Island Sound off Fisher's Island (Figure 1.1 A), which provided a broad range of hydrodynamic conditions for *Zostera marina* populations growing there. Three sites were studied: 1) a quiescent site that experienced minimal waves and currents, which was located on the north side of the island within a protected cove, 2) a high current site located on the northwest side of the island between Fisher's Island and South Dumpling Island, such that as the tide comes in and out, water is forced between these two land masses, thereby increasing current speed, and 3) a high wave site located on the southwest side of the island that was continually exposed to oceanic swell (Figure 1.1 B). At each of the three sites, 4 to 7 patches (quiescent and high wave sites), or when patches were not present (high current site), 4 to 7 areas within a bed separated by at least 3 m were used as replicates. All replicate patches at the same site and between sites were located at approximately the same depth (mean water level = 2.0 m +/- 0.2 m, tidal range = 0.8 m). Sampling events took place in July and August, 2007 and June and July, 2008.

During that time, salinity ranged between 30 and 35 and water temperature ranged between 15 and 23 °C.

Hydrodynamic Characteristics

At each of our three sites, we recorded current velocity (AquaDopp Current Profiler, Nortek AS) and wave height and length (MacroWave pressure gauge, Coastal USA) simultaneously. The current profiler and wave gauge were deployed in an unvegetated area adjacent to the replicate locations. The current profiler recorded at 2 Hz and averaged current velocity measurements for 5 minutes every 15 minutes for 6 hours over the depth of the water column starting 5 cm above the instrument (15 cm above the bottom) and every 10 cm thereafter. The wave gauges recorded pressure at 5Hz, and averaged data for 13.5 minutes every 15 minutes for two weeks (Aug. 14th – 27th, 2007).

The pressure data were Fast-Fourier transformed to obtain significant wave height (Hs) and wave period (P) in addition to average water depth (z) (Denman 1975). Wave period was used to calculate wavelength (L) from the equation:

$$L = \frac{gP^2}{2\pi}, \text{ which assumes the waves are deep water waves (Open University 1999).}$$

L, P, Hs and z were then used to calculate the maximum near-bottom orbital velocity (U_b) (Infantes et al. 2009), giving further insight as to how the waves were affecting the bottom and the seagrass beds inhabiting the benthos.

Sediment Characteristics

The top 10 cm of sediment was sampled from each replicate patch (n=7 per site) using push cores (diameter =10 cm). Coarser grain sizes (gravel) were located at

the surface, while less coarse grain sizes (very coarse sand to silt and clay) were located beneath the coarse surface layer. The sediment cores were homogenized before being analyzed for grain size (sieving) and organic content (combustion) according to Erflemeijer and Koch (2003).

Seagrass Morphology and Biomechanics

From each replicate patch (n=4 for the quiescent site, n=7 for the high current and high wave sites) at each field site, 10 *Zostera marina* shoots were collected for morphological measurements such as leaf length, width, and number, as well as root length and number. Leaf length was measured from the top of the sheath to the tip of the leaf, whereas width was measured half way between the sheath and tip. The number of roots per node were counted for at least 3 nodes per shoot, and at each node, the longest and shortest intact root was measured for length. Seagrass shoot density was also quantified (n=7) using the quadrat method (25 X 25 cm) according to Duarte and Kirkman (2003).

The tensile strength of *Zostera marina* leaf tissue was measured by determining how much force was required to break the tertiary leaf of 5 to 10 shoots from each replicate patch (n=7) using a modified Dynamometer (Illustration 1.1) (Bell and Denny 1994). The tertiary leaf was detached from the shoot directly above the sheath. The base of the leaf was then clipped onto the dynamometer, while the tip of the leaf was held stationary. The dynamometer, with the tertiary leaf attached, was pulled gently until breakage occurred; the distance the spring stretched to achieve breakage was recorded to the nearest millimeter. This recorded distance was used to calculate force (N) from a linear regression created by stretching the springs with a

known mass, and therefore force ($F = \text{mass} * \text{acceleration due to gravity}$). The tertiary leaves were selected because they are among the longest such that they are likely to be continually affected by currents and waves, whereas the primary and sometimes secondary leaves are not exposed to the full force of currents and waves as they are protected by older leaves. The quaternary leaves (outermost) were not used as they are usually senescent and naturally shed by the plant. By using the tertiary leaf a standard of comparison was set, allowing us to understand how healthy, water flow exposed leaves respond to drag.

The flexibility of the leaves was also quantified which was defined as the angle required in order for breakage of the tertiary leaf of a *Zostera marina* shoot to occur when rotated around an axis. An apparatus (Illustration 1.2) was built that allowed the base of the tertiary leaf to be held in place at the center of a circle, while the tip of the leaf was pulled along the arc of the circle with consistent tension. Along the arc, angles were marked every 5 degrees, such that when the leaf broke, the breaking angle could be recorded. This was done for 10 plants from 5 replicate patches located at each of our three sites.

Flow Tank Experiment

In order to address if water flow induced changes in *Zostera marina* are an acclimation or an adaptation, a “common garden” experiment was conducted. *Z. marina* shoots from the 3 study sites in Long Island Sound were collected on April 1st, 2008 and grown for 2.5 months in 6 outdoor flow tanks (3.0 m L X 0.7 m W X 0.6 m D) located at Horn Point Laboratory, Cambridge, MD. Water salinity between 28 and 30 was obtained by mixing Choptank River water and sea salts (Crystal Sea

Marine Mix), and the temperature throughout the experiment ranged from 8.8 °C in April to 35.1 °C in June.

Each of the 6 flow tanks were split down the middle with a divider (Illustration 1.3) such that water circulated in a race track fashion at a current speed of $9 \text{ cm s}^{-1} \pm 2 \text{ cm s}^{-1}$, which was achieved with a 2 pound thrust Sevylor trolling motor. Two trays were placed on each side of the divider, such that there were 4 trays per flow tank (Illustration 1.3) achieving a total of 24 trays. All trays contained sediment dominated by fine sand that had an organic content of 0.52% collected from Chincoteague Bay; a location where *Z. marina* is naturally occurring, and therefore the sediment is suitable for seagrass growth. The first tray on each side was filled with only sediment in order to homogenize the water flow before it reached the second tray where *Z. marina* was planted at a density of 6 shoots tray⁻¹ (Illustration 1.3). Each of the three sites was randomly assigned 4 replicate trays; the 6 *Z. marina* shoots from each tray were considered sub-replicates while the tray itself was considered a true replicate.

Leaf morphology was initially measured on 10 separate shoots from each site to establish a baseline. Two shoots, which were sub-replicates and therefore averaged, were collected from each replicate tray at weeks 2, 5 and 10 (June 8th, 2008) for morphology measurements. To ensure that the shoots did not become nutrient limited, a water change was done every two weeks for the duration of the experiment. Two-thirds of the water was replaced with Choptank River water mixed with sea salts to bring the salinity between 28 and 30.

Statistical Analysis

For all data sets, a test for normality was run on the errors (residuals) of the statistical model. If the errors were not normally distributed, the data were ln-transformed, which achieved normality for all skewed data, and therefore the assumptions of Analysis of Variance (ANOVA) were fulfilled. One-way ANOVA was performed on field collected data (significant difference defined as $p < 0.05$) with a Tukey's Test for comparison of treatment means. Two-way ANOVA was performed on data collected from the flow tank experiment as the variable of time was introduced. If no significant interaction was present, the effects of time and site were analyzed separately using one-way ANOVA and a Tukey's Test for comparison of treatment means. Lastly, a regression analysis was performed on wave height data in relation to water depth to understand how wave height was changing in relation to the tidal cycle.

Results

Hydrodynamics

The high wave site experienced larger waves than the quiescent and high current sites, whereas the high current site experienced faster currents than the quiescent and high wave sites. Over a 10 day period in August 2007, significant wave height at the high wave site was, on average, 2.4 times larger than significant wave height from the quiescent and high current sites. At the high wave site, significant wave height ranged between 0.18 and 0.88 m with an average wave height of 0.36 m, whereas at the same time significant wave heights at the quiescent and

high current sites ranged from 0.10 to 0.41 m and 0.09 to 0.36 m with an average wave height of 0.15 m at both sites (Figure 1.2).

Wave period at the high wave site was 8.3 seconds, while it was 3.1 and 2.7 seconds at the quiescent and high current sites, respectively. Using the equations developed by Infantes et al. 2009, the maximum near-bottom orbital velocity (U_b) at the high wave site was 1.2 m s^{-1} , whereas U_b at the quiescent and high current site was 0.07 and 0.11 m s^{-1} , respectively; a full magnitude slower. Lastly, the tidal signal that is present in the significant wave height graph at the high wave site (Figure 1.2) was significantly related to water depth (regression analysis, $p < 0.0001$), such that when the tide was low, the wave height was reduced, and when the tide was high, the wave height increased. Therefore, the waves were shoaling at low tide, which reduced the energy associated with the wave.

The high current site had the highest tidal influence. At slack water in June 2008, current speed was relatively slow, averaging 0.051 m s^{-1} over the depth of the water column, which was similar to the current speed of the quiescent and high wave sites, which averaged 0.055 and 0.057 m s^{-1} , respectively. When the tide was ebbing or flooding, maximum current speed at the high current site was 2.3 and 2.5 times faster than maximum current speed at the quiescent or high wave sites, respectively. At the high current site, current speed averaged 0.184 m s^{-1} over the height of the water column, and the average maximum current speed of 0.287 m s^{-1} was located 150 cm above the bottom, which ranged between 0.228 and 0.383 m s^{-1} . Even when current speed was at its maximum, nearbed current remained slow and averaged around 0.060 m s^{-1} between 10 and 30 cm above the seabed (Figure 1.3). Notably,

current speeds up to 0.420 m s^{-1} were measured at this site during a deployment in July 2008 (data not shown). Current speed at the quiescent and high wave site during maximum flood or ebb tide averaged 0.079 m s^{-1} and 0.087 m s^{-1} , respectively, over the height of the water column, and had a maximum current speed of 0.169 m s^{-1} , which occurred 1.1 m above the bottom, and 0.154 m s^{-1} , which occurred 1.0 m above the bottom, respectively.

Sediment Characteristics

Sediment characteristics varied between sites. The quiescent site was dominated by medium ($250 \text{ }\mu\text{m}$) and fine ($125 \text{ }\mu\text{m}$) sand, the high wave site was dominated by fine sand covered by gravel (2 mm) (i.e. bimodal grain size distribution), and the high current site was dominated by medium sand ($250 \text{ }\mu\text{m}$) covered by gravel (2 mm) but had a broader distribution of grain sizes between 1.00 mm and $< 63 \text{ }\mu\text{m}$ than the other two sites (i.e. less well sorted) (Figure 1.4 A). Despite varying grain sizes, the sites did not vary significantly in regards to percent sediment organic matter content ($p=0.1618$, Table 1.1); the organic matter averaged 1.45, 2.00, and 1.42 % at the quiescent, high current, and high wave sites, respectively, and replicates ranged between 0.723 and 2.937 % (Figure 1.4 B). Sediment permeability was not quantified.

Seagrass Morphology and Biomechanics

Below the sediment surface, *Zostera marina* from the quiescent site had significantly longer roots ($p=0.0003$, Table 1.1) than plants from the high current and high wave sites (Figure 1.5), whereas *Z. marina* from the high current site had significantly more roots per node ($p=0.0446$, Table 1.1) than plants from the high

wave site, but not from the quiescent site (Figure 1.6). Differences in root length and number of roots per node affect the total amount of root material present at each node. *Z. marina* from the quiescent, high current and high wave sites had 830, 652, and 556 mm of total root length per node, respectively, assuming that all roots were as long as the longest root measured.

Above ground characteristics such as leaf length and width varied between sites. *Zostera marina* leaves from the high current site were significantly longer ($p < 0.0001$, Table 1.1) than leaves from the quiescent and high wave sites (Figure 1.7). Secondary leaves of *Z. marina* from the high wave site were significantly narrower than leaves from the high current and quiescent sites ($p < 0.0001$, Table 1.1), whereas all sites were significantly different from one another in regards to leaf width of the tertiary leaves ($p < 0.0001$, Table 1.1, Figure 1.8), with *Z. marina* from the high current site having the widest leaves and *Z. marina* from the high wave site having the narrowest leaves. *Z. marina* located at the quiescent site had significantly more leaves ($p = 0.0073$, Table 1.1) than the high current and high wave sites (Figure 1.9), as *Z. marina* from the quiescent site often had 5 or 6 leaves, whereas plants from the high current and high wave site most often had 4 or 5 leaves. Furthermore, *Z. marina* from the high wave site, despite being narrow and short, had a significantly higher shoot density ($p < 0.0001$, Table 1.1) when compared to the quiescent and high current site (Figure 1.10) such that *Z. marina* from the high wave site was 3 times more dense than the other two sites. Shoot length, width, and density determine the photosynthetic leaf area per m^2 of seabed [leaf area index (LAI)] that a *Z. marina* bed possesses. Morphological variation between sites resulted in different LAI such that

the quiescent site had 1.10 m² leaf m⁻² seabed, the high current site had 3.95 m² leaf m⁻² seabed, and the high wave site had 2.46 m² leaf m⁻² seabed.

Zostera marina leaves from the high current site were significantly stronger ($p < 0.0001$, Table 1.1) than leaves from the quiescent and high wave sites as it required 35 and 42 % more force (N) to break the tertiary leaf of the high current site when compared to leaves from the quiescent and high wave sites, respectively (Figure 1.11). When pulled, leaf breakage often occurred close to the tip, but there were exceptions to this trend as sometimes the leaf broke in the middle or near the base, demonstrating that the tips were most often the weakest point along the tertiary leaf of *Z. marina*.

The cumulative frequency distribution for the angle necessary to break the tertiary leaf demonstrates that 50% of the leaves from the quiescent site broke by an angle of 33°, while angles of 36 and 39° were required to break 50% of the tertiary leaves from the high current and high wave sites, respectively (Figure 1.12 A). This difference in the angle necessary to break 50% of the leaves was not significant ($p = 0.0682$, Table 1.1). However, when the cumulative frequency distribution is linearized with a natural log, the slopes from the high current and high wave sites were significantly steeper than the slope from the quiescent site ($p = 0.0037$, Table 1.1). The differences in slope demonstrate that a higher percent of *Z. marina* leaves broke at smaller angles at the quiescent site, which drove the slope shallower, while a higher percent of *Z. marina* leaves broke at larger angles at the high current and high wave sites, which drove the slope steeper (Figure 1.12 B).

Flow Tank Experiment

After 10 weeks under common garden conditions, transplanted *Zostera marina* shoots were healthy and growing (i.e. leaf elongation) but were not producing new shoots. No interaction between site and time was found for leaf length and width, but significant differences for site and time, independent of each other, were found, showing that over time leaf length and width were changing, and that there were differences in these changes between sites. Initially, *Z. marina* shoots from the three field sites were not significantly different in leaf length (secondary leaf $p=0.3410$, tertiary leaf $p=0.1707$, Table 1.2 A), but after 10 weeks of growth under common garden conditions *Z. marina* leaves from the high current site were significantly longer than leaves from the quiescent and high wave sites (secondary leaf $p=0.0027$, tertiary leaf $p=0.0045$, Table 1.2 B) (Figure 1.13 A & B). In regards to leaf width, *Z. marina* leaves from the high current site were significantly wider (secondary leaf $p<0.0001$, tertiary leaf $p<0.0001$, Table 1.2 A & B) than leaves from the quiescent and high wave sites initially and continued to stay significantly wider than leaves from the other two sites throughout the duration of the experiment. The only exception was during week 5 in which there was no significant difference in measured secondary leaf width between the quiescent and high current sites (Figure 1.14 A & B). Therefore, leaf length and width of *Z. marina* from each site did not converge, but instead diverged, over time.

The sediment grain size used in the flow tank trays initially, and at the end of 10 weeks, was dominated by medium (250 μm) and fine (125 μm) sand (Figure 1.15 A), which was similar to the quiescent site in Long Island Sound. Percent organic

matter in the flow tank trays was 0.52 %, which did not significantly differ between sites ($p=0.7291$, Table 1.2 B) or time ($p=0.2688$, Table 1.2 B), and was at least half of that found at the *Zostera marina* sites in Long Island Sound (Figure 1.15 B).

For root length there was a significant interaction between site and time ($p=0.0213$, Table 1.2 B). *Zostera marina* from the quiescent site had similar root lengths throughout the duration of the experiment, while roots of *Z. marina* from the high current and high wave sites became longer over time. Initially, root lengths of *Z. marina* from the high current and high wave sites were significantly shorter than roots from the quiescent site ($p=0.0014$, Table 1.2 A), but by week 5 roots from all three sites were not significantly different from one another. At week 10 all sites had increased their root length when compared to week 5, but root lengths from each site were not significantly different from one another (Figure 1.16).

The number of roots per node was found to significantly change over time ($p=0.0040$, Table 1.2 B), but there were no significant differences between sites initially ($p=0.3275$, Table 1.2 A) or over the duration of the experiment ($p=0.7083$, Table 1.2 B). During the 10 week flow tank experiment, *Zostera marina* from all three sites significantly decreased the number of roots located at each node (Figure 1.17). Therefore, unlike leaf length and width, root length and number of *Z. marina* from each site converged over time.

Discussion

Our results indicate that water flow indeed affects seagrass morphology, as previously suggested by Dennison and Alberte (1982), Fonseca and Kenworthy

(1987), Sidik et al. (1999), Peralta et al. (2000), Schanz and Asmus (2003), Peralta et al. (2005), and Jordan et al. (2008). However, a direct mechanism by which this happens has not been demonstrated. Water flow could affect morphology directly such that morphology changes in response to the mechanical stress that water flow imposes upon seagrass, but may also affect seagrass morphology indirectly by affecting nutrient uptake, carbon availability, or light availability. Our results also indicate that currents may induce different morphological variation than waves, flexibility and canopy morphology may be more important than shoot morphology in reducing drag exerted on seagrass leaves, and sediment characteristics and nutrient availability, which are affected by water flow, may also play a major role in seagrass morphology. Perhaps these complexities explain the contradicting results found in the literature.

Above Ground Morphological Variation

Zostera marina exposed to quiescent waters, currents, or waves were found to have different morphological properties in regards to leaf length and width, shoot density, and biomechanical attributes (strength and flexibility). Hence, it is necessary to specify the hydrodynamic conditions being evaluated as dominated by currents or waves, as these varying types of water flow seem to induce varying morphological changes, and can also impose different restrictions on nutrient and light availability. Therefore, morphological properties cannot merely be discussed as being induced by ‘water flow’, in general.

Seagrass flexibility appears to be more important than seagrass morphology in minimizing drag exerted on the leaves. It seems unreasonable to conclude that

morphological variation experienced by *Zostera marina* in Long Island Sound is a means to reduce drag that is inflicted upon leaves by local hydrodynamics. Although it has been suggested that seagrass leaves become more streamlined (narrow and long) under strong hydrodynamic regimes (Fonseca and Kenworthy 1987, Jordan 2008) we found that leaves of *Z. marina* exposed to currents were significantly longer and wider than leaves from the quiescent and high wave sites. If morphological variation observed at the high current site were a mechanism to reduce drag, it would be expected that leaves would become narrower (not wider as observed *in situ*) in order to decrease leaf area exposed to water flow. Additionally, it has been found that morphological variations that macroalgae possess in relation to water flow do not always effectively reduce drag (Milligan and DeWreede 2004, Haring and Carpenter 2007), and that bending over, which is a result of being flexible, is a more effective means of reducing drag. Seagrasses are inherently flexible, and this flexibility may effectively reduce drag exerted upon seagrasses exposed to currents and waves by allowing the plants to reorient themselves, thereby becoming more streamlined, or to simply go with the flow, thereby minimizing hydrodynamic forces by never being fully extended (Koehl 1996, Denny and Gaylord 2002).

Alternatively, one could attribute increased leaf length and width of *Zostera marina* from the high current site to other factors beyond those of local hydrodynamic conditions. Percent sediment organic matter at the high current site, although not significantly different, was slightly higher, potentially giving plants from this location a nutrient advantage. However, it seems unlikely that an increase of 0.5% in sediment organic matter that *Z. marina* from the high current site experienced would

promote growth of leaves over 3 times longer than leaves from the quiescent and high wave sites.

Although the pool of nutrients was not significantly different, the flux of nutrients may have been different between sites. Therefore, differences in sediment characteristics, which affect nutrient flux, could potentially provide an explanation as to why *Z. marina* from the high current site was so much longer and wider than *Z. marina* from the quiescent and high wave sites. Huettel et al. (1996) described a scenario in which suspended particles are advected into permeable sediments that are characterized by topographical variations (or mounds) via pressure gradients, and that as flow velocity increases, the differential pressure also increases, causing advection of particles to increase with increasing flow velocity. Once these particles are advected into the sediment, they can be processed via microbial communities, thereby increasing nutrient availability within the sediment (Huettel et al. 1996, Huettel et al. 2003). Furthermore, porewater rich in nutrients (especially ammonia) is brought closer to the sediment surface directly underneath the topographical variation, further enhancing nutrients in the surface layer (Huettel et al. 1996, Huettel et al. 2003).

Koch and Huettel (2000) observed this same phenomenon in seagrass beds, as a seagrass shoot could effectively act as a “mound” where a pressure gradient could be established. As organic particles are advected into permeable sediment around a seagrass shoot and degraded via microbial processes, nutrients become available to the seagrass roots. Sediment from the high current site was probably more permeable when compared to sediment from the quiescent and high wave sites, as it had the highest percent of grain sizes $> 500 \mu\text{m}$ and permeability and grain size have been

shown to be related ($r^2 = 0.66$, Wilson et al. 2008). Huettel and Rusch (2000) demonstrated that advection of algae into sediment increased with increasing grain size and permeability, and that coarser sand resulted in more overall transport of material. Additionally, the turnover rate of this process has been shown to be quite high (Huettel et al. 2003), thereby potentially providing a constant replenishment of nutrients to the seagrass shoot, which may explain why sediment from the high current site had slightly higher percent organic matter than sediment from the quiescent and high wave sites. Hence, we hypothesize that *Z. marina* leaves from the high current site may be benefiting from increased particle advection and higher nutrient turnover due to potentially more permeable sediment as a result of grain size distribution (Wilson et al. 2008) and fast current velocities. This potential difference in biogeochemical processes may explain why *Z. marina* leaves from the high current site were wider and over 3 times longer than leaves from the quiescent and high wave sites, as nutrient uptake from the sediment via roots has been shown to be more important for nutrient acquisition for *Z. marina* than uptake from the water column via leaves (Zimmerman et al. 1987), especially when the concentration of nutrients is higher in the sediment than the water column (Hasegawa et al. 2005). Furthermore, it has been demonstrated that the interaction between water flow and nutrient concentration is complex, such that aquatic plants have reduced size with increasing water flow when nutrient concentrations are low, yet have increased size with increasing water flow when nutrient concentrations are high (Puijalon et al. 2007), exemplifying that the combination of high current speed and potentially high porewater nutrient turnover rates may be responsible for the long and wide leaves of

Z. marina observed at the high current site. Further studies are needed to evaluate this hypothesis.

The morphology observed for *Zostera marina* exposed to waves may be a result of the short time scales that seagrass leaves spend in varying positions and the dynamic movement that this environment inflicts upon the seagrass bed. Leaves of *Z. marina* exposed to waves were narrower than leaves from the quiescent and high current sites. Other studies have shown that *Zostera* leaves become shorter (Dennison and Alberte 1982, Peralta et al 2005) and narrower (Peralta et al. 2005) when exposed to waves when compared to shoots located in sheltered areas. However, we did not observe a significant change in leaf length of *Z. marina* exposed to waves, only leaf width, when compared to plants from the quiescent site.

Our results may differ from previous studies due to the type of waves that *Zostera marina* from the high wave site was exposed to. The high wave site was continually affected by oceanic swell, which is characterized by large wave heights, long wave periods, and causes dynamic leaf movement. It may be that wind generated surface waves in estuaries, which have smaller significant wave heights and shorter periods, cause less leaf movement and mechanical stress, and therefore the seagrass bed responses differently via leaf width and length. We hypothesize that when seagrasses are exposed to waves as large as those of oceanic swell, an intermediate leaf length may be optimal. Since waves cause seagrass leaves to sway back and forth, a short leaf may increase the likelihood of dislodgement if the leaf is pulled to its full extent, whereas a long leaf may increase the likelihood of

entanglement, causing leaf breakage and reduced productivity (sensu Koehl and Wainwright 1977).

Seagrass shoot density appears to be determined by light availability, nutrient availability (Marbà and Duarte 2003, Bouma et al. 2005, Peralta et al. 2005), and hydrodynamic conditions (Schanz and Asmus 2003, Peralta et al. 2005). Previous studies that have linked hydrodynamic conditions and seagrass shoot density have come to conflicting conclusions. Some have found that *Zostera* shoots exposed to waves were less dense (Schanz and Asmus 2003, Peralta et al. 2005) whereas others have observed that *Zostera* shoots exposed to waves were more dense (Dennison and Alberte 1982) when compared to beds in sheltered areas. We found that *Z. marina* exposed to waves had a significantly higher shoot density than plants from the quiescent and high current sites.

The presence of a seagrass canopy has been shown to effectively alter current velocity (Fonseca et al. 1982, Gambi et al. 1990, Ackerman and Okubo 1993, Koch and Gust 1999, Nepf and Koch 1999, Hasegawa et al. 2008, Hendriks et al. 2008, Morris et al. 2008, Widdows et al. 2008), and may be a mechanism that explains shoot density differences between our field sites. When a current comes into contact with a seagrass canopy, the leaves bend with the current (as was seen at both the high current and high wave sites in this study), and the current is redirected above the canopy thereby reducing current speed within the canopy while accelerating currents over the bed (Fonseca et al. 1982, Gambi et al. 1990, Ackerman and Okubo 1993, Koch and Gust 1999, Nepf and Koch 1999, Hasegawa et al. 2008, Hendriks et al. 2008, Morris et al. 2008, Widdows et al. 2008). Furthermore, density of a seagrass

canopy can affect the degree to which this reduction in current velocity occurs, with increasing density resulting in decreasing within-canopy flow (Gambi et al. 1990, Hasegawa et al. 2008, Morris et al. 2008, Widdows et al. 2008). Hence, an increase in aboveground biomass, which was achieved by a high shoot density at the high wave site and long and wide leaves at the high current site, may act as a barrier to the local hydrodynamic conditions. Therefore, an increase in aboveground biomass may be an effective means of reducing drag via reducing the within-canopy flow.

Although we hypothesized that biogeochemical processes may have contributed to the long and wide leaves of *Zostera marina* from the high current site, it could conversely be attributed to the possibility that these traits (long and wide leaves) may be genetically fixed, and that a seagrass population with these genetic traits is more successful in an area dominated by fast currents. Leaf length and width of *Z. marina* from the high current site grown under common garden conditions appears to be an adaptation, not acclimation, to an environment dominated by fast current speeds, and are in agreement with the results of Sidik et al. (1999) and Peralta et al. (2000) who found two morphotypes of the same species to co-exist. However, when a new shoot emerges from its sheath, the new shoot is affected by its local environment and responds accordingly; therefore, whether or not morphological variations are an adaptation or an acclimation can only be conclusively determined from the morphology of a newly produced shoot; not shoots collected from their original field sites where they already experienced other hydrodynamic conditions. Since *Z. marina* in our flow tank experiment never produced new shoots, no

conclusive statements about whether the observed morphological variations are an adaptation or acclimation can be made.

Biomechanical Variation

Although it was mentioned earlier that seagrass leaves are inherently flexible (thereby reducing drag), differences in leaf strength and flexibility between sites were observed, demonstrating the phenotypic plasticity of seagrasses and their ability to adjust to local hydrodynamic conditions. Leaves of *Zostera marina* acclimated to water flow by being stronger at the high current site, where currents pull leaves, and more flexible at both the high current and high wave sites, as waves and currents cause seagrass leaves to sway.

Strength and flexibility of vegetative *Zostera marina* shoots from Long Island Sound did have normal distributions, suggesting that it is necessary for all vegetative shoots, not just a few individuals, to be strong or flexible. The only exception to a normal distribution was observed for flexibility measurements of *Z. marina* from the high current site, which were skewed toward higher angles. This is unlike Patterson et al. (2001) who found that biomechanical properties of reproductive shoots of *Z. marina* such as breaking strength, stiffness, and toughness were not normally distributed, but instead followed a Weibull distribution. The high current flexibility data were skewed only slightly skewed and the distribution of the data would not be considered a true Weibull distribution. Patterson et al. (2001) hypothesized that there are a few strong reproductive shoots within a population that are more able to resist extreme events, and that it is these individuals that decrease the risk of local extinction. This hypothesis was not supported from our strength and flexibility data

for vegetative *Z. marina*, suggesting that a Weibull distribution for reproductive shoots for *Z. marina* may also be a reproductive strategy, such as release of seeds under different hydrodynamic conditions. In contrast, the normal distribution of strength and flexibility of vegetative shoots may demonstrate the importance of having a morphology that is compatible with day-to-day local hydrodynamic conditions that a seagrass bed experiences, and that seagrasses have the ability to achieve these morphologies via altering the strength and flexibility of their leaves, thereby increasing the likelihood of survival.

Below Ground Biomass Variation

This study demonstrates the importance of considering sediment as a co-variable when studying hydrodynamics and seagrass growth. If below ground biomass was a response to local water flow, one would expect plants exposed to waves and currents to have longer roots and more roots per node in order to aid in anchorage. However, as we hypothesized, sediment composition can counteract flow-induced morphological changes in the seagrass *Z. marina*. Sediment composition from the quiescent site was well sorted and dominated by sand; a sediment type that is characterized by low nutrient availability. Therefore, we hypothesize that *Z. marina* from the quiescent site produced longer roots in search of nutrients. These longer roots may also contribute to the shorter leaves observed at the quiescent site, as the plant may be allocating more of its resources to below ground biomass (sensu Di Carlo et al. 2007). Sediment composition at the high current and high wave sites was poorly sorted. Grain sizes equal to or greater than 500 μm were present at a higher percentage at the high current and high wave sites when compared

to the quiescent site, indicating that sediment at the high current and high wave sites was potentially more permeable than sediment from the quiescent site (Wilson et al. 2008). It has been demonstrated that permeable sediments promote particle advection in the presence of currents (sensu Huettel et al. 1996) and waves (sensu Precht and Huettel 2003), which may keep nutrient availability and recycling high. Therefore, it may be that *Z. marina* located at these sites did not have to produce long roots in search of nutrients, potentially allowing the plant to allocate its resources toward longer leaves, as was observed at the high current site, or the production of new shoots, as was observed at the high wave site (Di Carlo et al. 2007).

The results from the flow tank experiment demonstrate that sediment composition, and the associated nutrient concentration, affects root length, whereas water flow affects root number. When *Zostera marina* from the quiescent, high current, and high wave sites were grown under common garden conditions, root length, which started out different between sites, converged over time. Therefore, differences in sediment grain size distribution accounted for differences in root length, not hydrodynamic conditions. On the other hand, root number was never different between sites over the course of the 10-week flow tank experiment, but decreased over time. Although no initial significant differences were found between sites for the number of roots per node of *Z. marina* collected in April for the purpose of the flow tank experiment, it was found that roots of *Z. marina* from the high current site collected in July had significantly more roots per node. Unlike root length, root number may be responding to local hydrodynamic conditions, and hence

a reduced water flow, which would reduce the amount of drag experienced by *Z. marina* leaves, resulted in fewer roots per node.

Conclusions

This study illustrates the complexity of the effect of water flow on seagrasses and suggests that a distinction between water flow type (i.e. currents or waves) is vital for a more concrete understanding of how hydrodynamic conditions affect seagrass morphology. Additionally, more controlled experiments that examine how waves and currents in isolation of each other affect seagrass morphology are necessary to understand direct mechanism by which seagrasses respond to water flow. *In situ*, seagrasses exposed to fast currents were wide, long, and strong, while seagrasses exposed to large and long waves were of an intermediate length, narrow, and dense. These very different morphological characteristics ensure survival in dynamic conditions, but cannot be discussed in light of ‘water flow’, in general.

Our results suggest that variation among leaf length and width were not necessarily a mechanism to reduce drag. We hypothesized that an intermediate leaf length of *Zostera marina* exposed to waves was necessary to reduce the likelihood of entanglement as leaves exposed to waves sway back and forth (sensu Koehl and Wainwright 1977). Therefore, the inherent flexibility of seagrass leaves and their ability to deflect with the currents or sway in the waves may be the main mechanism by which drag is reduced. In contrast, leaf strength may be an important acclimation when seagrass leaves are exposed to strong currents by allowing them to deflect without breaking. Whether these morphological variations are adaptations or

acclimations to local hydrodynamic conditions is still merely speculative, although our results suggest that some traits (strength, flexibility, root length and number) may be highly plastic, while other traits (leaf length and width) may be genetically fixed. However, the long and wide leaves observed at the high current site could also be a result of biogeochemical processes. Therefore, sediment characteristics also need to be considered when evaluating the effect of water flow on seagrasses.

The relatively coarse, poorly sorted sediments and fast current speeds at the high current site may be promoting the entrainment of particulate matter into the sediment, which is broken down by microbial processes making nutrients available to *Zostera marina* roots (sensu Huettel et al. 1996). We hypothesize that porewater nutrient turnover was relatively high at the high current site as a result of this process, thereby continually replenishing porewater nutrients leading to long and wide leaves. Wave-induced particle intrusion into the sediments (sensu Precht and Huettel 2003) may also contribute to the high biomass at the high wave site but to a lesser extent as the sediment is finer and, therefore, less permeable. Conversely, the well sorted sand found at the quiescent site and slow current speeds and small waves did not facilitate particulate matter entrainment, resulting in lower porewater nutrient availability that led to longer *Z. marina* roots.

In summary, differences between the type of water flow (waves vs. currents), sediment composition, and the interaction among these parameters, as well as how these parameters affect nutrient or light availability, are most likely the source of disagreement within the literature as to how and why seagrasses acclimate (or have adapted) morphologically to their local water flow environment. More focused

research that first examines each parameter individually in carefully designed and controlled experiments, and then seeks to quantify how these parameters interact to affect seagrass morphology, is needed. This type of research is of the utmost importance during a time when eutrophication is forcing seagrass habitats into shallower waters where wave and current action are pronounced. Additionally, the frequency and intensity of storms is predicted to increase, such that viable seagrass habitat is likely to become more hydrodynamically active in the future.

Bibliography

- Ackerman, J.D., and A. Okubo. 1993. Reduced mixing in a marine macrophyte canopy. *Functional Ecology* 7: 305 – 309.
- Bell, E.C. and M.W. Denny. (1994) Quantifying "wave exposure": a simple device for recording maximum velocity and results of its use at several field sites. *Journal of Experimental Biology and Ecology*. 181: 9 – 29.
- Brown, E., A. Colling, D. Park, J. Phillips, D. Rothery, and J. Wright. 1999. Wave, Tides, and Shallow-Water Processes, 2nd Edition. Butterworth-Heinemann in association with The Open University, Oxford. Pp 11 – 49.
- Christiansen, C., H. Christoffersen, and S.E. Knud. 1981. Hydrography, sediments, and sedimentation in a low-energy embayment, Knebel Vig, Denmark. *Geografiska Annaler Series A, Physical Geography* 63: 95 – 103.
- Cooper, L.W., and C.P. McRoy. 1988. Anatomical adaptations to rocky substrates and surf exposure by the seagrass genus *Phyllospadix*. *Aquatic Botany* 32: 365 – 381.
- Cunha, A.H., and C.M. Duarte. 2007. Biomass and leaf dynamics of *Cymodocea nodosa* in the Ria Formosa lagoon, South Portugal. *Botanica Marina* 50: 1 – 7.
- Den Hartog, C. 1970. The Seagrasses of the World. North-Holland Publishers, Amsterdam.
- Denman, K.L. 1975. Spectral analysis: A summary of the theory and techniques. Fisheries and Marine Service, Technical Report N. 539.
- Dennison, W.C. and R.S. Alberte. 1982. Photosynthetic responses of *Zostera marina* L. (Eelgrass) to *in situ* manipulations of light intensity. *Oecologia (Berl)* 55: 137 – 144.
- Denny, M., and B. Gaylord. 2002. The mechanics of wave-swept algae. *The Journal of Experimental Biology* 205: 1355 – 1362.
- Denny, M., and L. Roberson. 2002. Blade motion and nutrient flux to the kelp *Eisenia arborea*. *Biological Bulletin* 203: 1 – 13.
- Di Carlo, G., F. Badalamenti, A. Terlizzi. 2007. Recruitment of *Posidonia oceanica* on rubble mounds: Substratum effects on biomass partitioning and leaf morphology. *Aquatic Botany* 87: 97 – 103.
- Duarte, C.M. and H. Kirkman. 2003. Methods for the measurement of seagrass abundance and depth distribution. In: Short, F.T. and R.G. Coles (eds.), *Global Seagrass Research Methods*, Elsevier Science, Amsterdam. Pp 141 – 153.
- Erflemeijer, P.L.A. and Koch, E.W. 2003. Measurements of Physical Parameters in Seagrass Habitats. In: Short, F.T. and R.G. Coles (eds.), *Global Seagrass Research Methods*, Elsevier Science, Amsterdam. Pp 345 – 367.
- Fonseca, M.S., J.S. Fisher, J.C. Zieman, and G.W. Thayer. 1982. Influence of the seagrass, *Zostera marina* L., on current flow. *Coastal and Shelf Science* 15: 351 – 364.
- Fonseca, M.S., and W.J. Kenworthy. 1987. Effects of current on photosynthesis and distribution of seagrasses. *Aquatic Botany* 27: 59 – 78.

- Gambi, M.C., A.R.M. Nowell, and P.A. Jumars. 1990. Flume observations on flow dynamics in *Zostera marina* (eelgrass) beds. *Marine Ecology Progress Series* 61: 159 – 169.
- Gerard, V.A. 1982. *In situ* water motion and nutrient uptake by the giant kelp *Macrocystis pyrifera*. *Marine Biology* 69: 51 – 54.
- Gerard, V.A., and K.H. Mann. 1979. Growth and production of *Laminaria longicruris* (Phaeophyta) populations exposed to different intensities of water movement. *Journal of Phycology* 15: 33 – 41.
- Harring, R.N. and R.C. Carpenter. 2007. Habitat-induced morphological variation influences photosynthesis and drag on the marine macroalga *Pachydictyon coriaceum*. *Marine Biology* 151: 243 – 255.
- Hasegawa, N., H. Iizumi, M. Mukai. 2005. Nitrogen dynamics of the surfgrass *Phyllospadix iwatensis*. *Marine Ecology Progress Series* 293: 59 – 68.
- Hasegawa N., M. Hori, H. Mukai. 2008. Seasonal changes in eelgrass functions: Current velocity reduction, prevention of sediment resuspension, and quiescent of sediment-water column nutrient flux in relation to eelgrass dynamics. *Hydrobiologia* 596: 387 – 399.
- Hendriks, I.E., T. Sintes, T.J. Bouma, C.M. Duarte. 2008. Experimental assessment and modeling evaluation of the effects of the seagrass *Posidonia oceanica* on flow and particle trapping. *Marine Ecology Progress Series* 356: 163 – 173.
- Huettel, M., W. Ziebis, and S. Forster. 1996. Flow-induced uptake of particulate matter in permeable sediments. *Limnology and Oceanography* 41: 309 – 322.
- Huettel, M. and A. Rusch. 2000. Transport and degradation of phytoplankton in permeable sediment. *Limnology and Oceanography* 45: 534 – 549.
- Huettel, M., H. Roy, E. Precht, and S. Ehrenhauss. 2003. Hydrodynamical impact on biogeochemical processes in aquatic sediments. *Hydrobiologia* 494: 231 – 236.
- Infantes, E., J. Terrados, A. Orfila, B. Canellas, and A. Alvarez-Ellacuria. 2009. Wave energy and the upper depth limit distribution of *Posidonia oceanica*. *Botanica Marina* 52: In Press.
- Jordan, T. 2008. Acclimation of two marine macrophytes (*Saccharina latissima* and *Zostera marina*) to water flow. Masters of Science Thesis. University of Maryland, Center for Environmental Sciences, Horn Point Laboratory. Cambridge, MD.
- Kawamata, S. 2001. Adaptive mechanical tolerance and dislodgement velocity of the kelp *Laminaria japonica* in wave-induced water motion. *Marine Ecology Progress Series* 211: 89 – 104.
- Koch, E.W. 1994. Hydrodynamics, diffusion-boundary layers and photosynthesis of the seagrasses *Thalassia testudinum* and *Cymodocea nodosa*. *Marine Biology* 118: 767 – 776.
- Koch, E.W. 1999. Preliminary evidence on the interdependent effect of currents and porewater geochemistry on *Thalassia testudinum* Banks ex Konig seedlings. *Aquatic Botany* 63: 95 – 102.
- Koch, E.W., and G. Gust. 1999. Water flow in tide- and wave-dominated beds of the seagrass *Thalassia testudinum*. *Marine Ecology Progress Series* 184: 63 – 72.

- Koch, E.W., and M. Huettel. 2000. The impact of single seagrass hoots on solute fluxes between the water column and permeable sediments. *Biologia Marina Mediterranea* 7: 235 – 239.
- Koehl, M.A.R. 1994. Biomechanics of microscopic appendages: Functional shifts caused by changes in speed. *Journal of Biomechanics* 37: 789 – 795.
- Koehl, M.A.R. 1996. When does morphology matter? *Annual Review of Ecology Systems* 27: 501 – 542.
- Koehl, M.A.R., and S.A. Wainwright. 1977. Adaptations of a giant kelp. *Limnology and Oceanography* 22: 1067 – 1071.
- Koehl, M.A.R., and R.S. Alberte. 1988. Flow, flapping, and photosynthesis of *Nereocystis luetkeana*: a functional comparison of undulate and flat blade morphologies. *Marine Biology* 99: 435 – 444.
- Milligan K.L.D., and R.E. DeWreede. 2004. Morphological variations do not effectively reduce drag forces at high wave-exposure for the macroalgal species, *Hedophyllum sessile* (Laminariales, Phaeophyta). *Phycologia* 43: 236 – 244.
- Molloy, F.J., and J.J. Bolton. 1996. The effects of wave exposure and depth on the morphology of inshore populations of the Namibian Kelp, *Laminaria schinzii* Foslie. *Botanica Marina* 39: 525 – 531.
- Morris, E.P., G. Peralta, F.G. Brun, L. van Duren, T.J. Bouma, and J.L. Perez-Llorens. 2008. Interaction between hydrodynamics and seagrass canopy structure: Spatially explicit effects on ammonium uptake rates. *Limnology and Oceanography* 53: 1531 – 1539.
- Nepf, H.M. and E.W. Koch. 1999. Vertical secondary flows in submersed plant-like arrays. *Limnology and Oceanography* 44: 1072 – 1080.
- Orth, R.J., et al. 2006. A global crisis for seagrass ecosystems. *BioScience* 56: 987 – 996.
- Patterson, M.P., M.C. Harwell, L.M. Orth, and R.J. Orth. 2001. Biomechanical properties of the reproductive shoots of eelgrass. *Aquatic Botany* 69: 27 – 40.
- Peralta, G., J.L. Perez-Llorens, I. Hernandez, F. Brun, J.J. Vergara A. Bartual, J.A. Galvez, J., and C.M. Garcia. 2000. Morphological and physiological differences between two morphotypes of *Zostera noltii* Hornem. From the south-western Iberian Peninsula. *Helgoland Marine Research* 54: 80 – 86.
- Peralta, G., F.G. Brun, I. Hernandez, J.J. Vergara, and J.L. Perez-Llorens. 2005. Morphometric variations as acclimation mechanisms in *Zostera noltii* beds. *Estuarine, Coastal and Shelf Science* 64: 347 – 356.
- Precht, E., and M. Huettel. 2003. Advective pore-water exchange drive by surface gravity waves and its ecological implications. *Limnology and Oceanography* 48: 1674 – 1684.
- Puijalon, S., J.-P. Lena, and G. Bornette. 2007. Interactive effects of nutrient and mechanical stresses on plant morphology. *Annals of Botany* 100: 1297 – 1305.
- Ramirez-Garcia P., A. Lot, C.M. Duarte, J. Terrados, and N.S.R. Agawin. 1998. Bathymetric distribution, biomass and growth dynamics of intertidal *Phyllospadix scouleri* and *Phyllospadix torreyi* in Baja California (Mexico). *Marine Ecology Progress Series* 173: 13 – 23.

- Ramirez-Garcia, P., J. Terrados, F. Ramos, A. Lot, D. Ocana, and C.M. Duarte. 2002. Distribution and nutrient limitation of surfgrass *Phyllospadix scouleri* and *Phyllospadix torreyi*, along the Pacific coast of Baja California (Mexico). *Aquatic Botany* 74: 121 – 131.
- Roberson, L.M., and J.A. Coyer. 2004. Variation in blade morphology of the kelp *Eisenia arborea*: incipient speciation due to local water motion? *Marine Ecology Progress Series* 282: 115 – 128.
- Schanz, A., and H. Asmus. 2003. Impact of hydrodynamics on development and morphology of intertidal seagrasses in the Wadden Sea. *Marine Ecology Progress Series* 261: 123 – 134.
- Short, F.T. 1983. The seagrass, *Zostera marina* L: Plant morphology and bed structure in relation to sediment ammonium in Izembek Lagoon, Alaska. *Aquatic Botany* 16: 149 – 161.
- Short, F.T. 1987. Effects of sediment nutrients on seagrasses: Literature review and mesocosm experiment. *Aquatic Botany* 27: 41 – 57.
- Sidik, J.B., M.Z. Harah, M.A. Pauzi, and S. Madhavan. 1999. *Halodule* species from Malaysia – distribution and morphological variation. *Aquatic Botany* 65: 33 – 45.
- Stewart, H.L. 2006. Morphological variation and phenotypic plasticity of buoyancy in the macroalga *Turbinaria ornate* across a barrier reef. *Marine Biology* 149: 721 – 730.
- Vila-Gispert, A., M.G. Fox, L. Zamora, and R. Moreno-Amich. 2007. Morphological variation in pumpkinseed *Lepomis gibbosus* introduction into Iberian lakes and reservoirs; adaptation to habitat type and diet? *Journal of Fish Biology* 71: 163 – 181.
- Wargo, C.A., and R. Styles. 2007. Along channel flow and sediment dynamics at North Inlet, South Carolina. *Estuarine, Coastal, and Shelf Science* 71: 669 – 682.
- Widdows, J., N.D. Pope, M.D. Brinsley, H. Asmus, and R.M. Asmus. 2008. Effects of seagrass beds (*Zostera noltii* and *Z. marina*) on near-bed hydrodynamics and sediment resuspension. *Marine Ecology Progress Series* 358: 125 – 136.
- Wilson, A.M., M. Huettel, S. Klein. 2008. Grain size and depositional environment as predictors of permeability in coastal marine sands. *Estuarine, Coastal and Shelf Science* 80: 193 – 199.
- Zimmerman, R.C., R.D. Smith, R.S. Alberte. 1987. Is growth of eelgrass nitrogen limited? A numerical simulation of the effects of light and nitrogen on the growth dynamics of *Zostera marina*. *Marine Ecology Progress Series* 41: 167 – 176.

Tables:

Table 1.1. The degrees of freedom (DF), mean square (MS), F value (F) and p value (p) from the ANOVA performed on sediment organic content and morphology of *Z. marina* collected from the quiescent, high current, and high wave sites off Fisher's Island, NY. For leaf flexibility, the 50% analysis is the angle at which 50% of the leaves had broke, whereas the slope analysis is the slope of the linearized relationship between bending angle and percent broken at that angle. Italicized p-values represent significant differences at $p < 0.05$.

Variable	DF	MS	F	p
Sediment Organic Content	2	0.72	2.03	0.1618
Root Length	2	1503.65	14.51	<i>0.0003</i>
Roots per Node	2	3.25	3.91	<i>0.0446</i>
Leaf Length - Secondary	2	7124.33	88.81	<i><0.0001</i>
Leaf Length - Tertiary	2	11291.05	254.4	<i><0.0001</i>
Leaf Width - Secondary	2	8.95	34.14	<i><0.0001</i>
Leaf Width - Tertiary	2	8.54	47.99	<i><0.0001</i>
# Leaves	2	1.4	6.95	<i>0.0073</i>
Shoot Density (ln transformation)	2	3.44	28.66	<i><0.0001</i>
Leaf Strength (ln transformation)	2	0.46	30.49	<i><0.0001</i>
Leaf Flexibility - 50%	2	47.77	3.38	0.0682
Leaf Flexibility - slope	2	271.45	9.23	<i>0.0037</i>

Table 1.2. The degrees of freedom (DF), mean square (MS), F value (F) and p value (p) from the ANOVA performed on the morphology of *Z. marina* collected from the quiescent, high current, and high wave sites off Fisher's Island, NY for the flow tank experiment A) initially, and B) when planted in common garden conditions in flow tanks for 10 weeks, as well as sediment characteristics into which *Z. marina* shoots were transplanted. Italicized p-values represent significant differences at $p < 0.05$.

A)

Variable	DF	MS	F	p
Leaf Length - Secondary	2	3.94	1.14	0.3410
Leaf Length - Tertiary	2	7.08	1.94	0.1707
Leaf Width - Secondary	2	2.16	23.32	<0.0001
Leaf Width - Tertiary	2	2.25	20.13	<0.0001
Root Length	2	3267.55	9.48	0.0014
Roots per Node (ln transformation)	2	8.90	1.27	0.3275

B)

	Time				Site			
Variable	DF	MS	F	p	DF	MS	F	p
Sediment Organic Matter	1	0.021	1.31	0.2688	3	0.008	0.44	0.7291
Roots per Node	2	21.45	6.83	0.004	2	1.1	0.35	0.7083
Leaf Length - Secondary	2	766.94	25.56	<0.0001	2	225.79	7.52	0.0025
Leaf Length - Tertiary	2	876.65	37.03	<0.0001	2	246.22	10.4	0.0004
Leaf Width - Secondary	2	2.31	11.91	0.0002	2	4.62	23.87	<0.0001
Leaf Width - Tertiary	2	2.39	15.82	<0.0001	2	5.36	35.46	<0.0001
	Site*Time							
Root Length: Significant interaction between site & time	4	1064.78	3.44	0.0213				

Figures

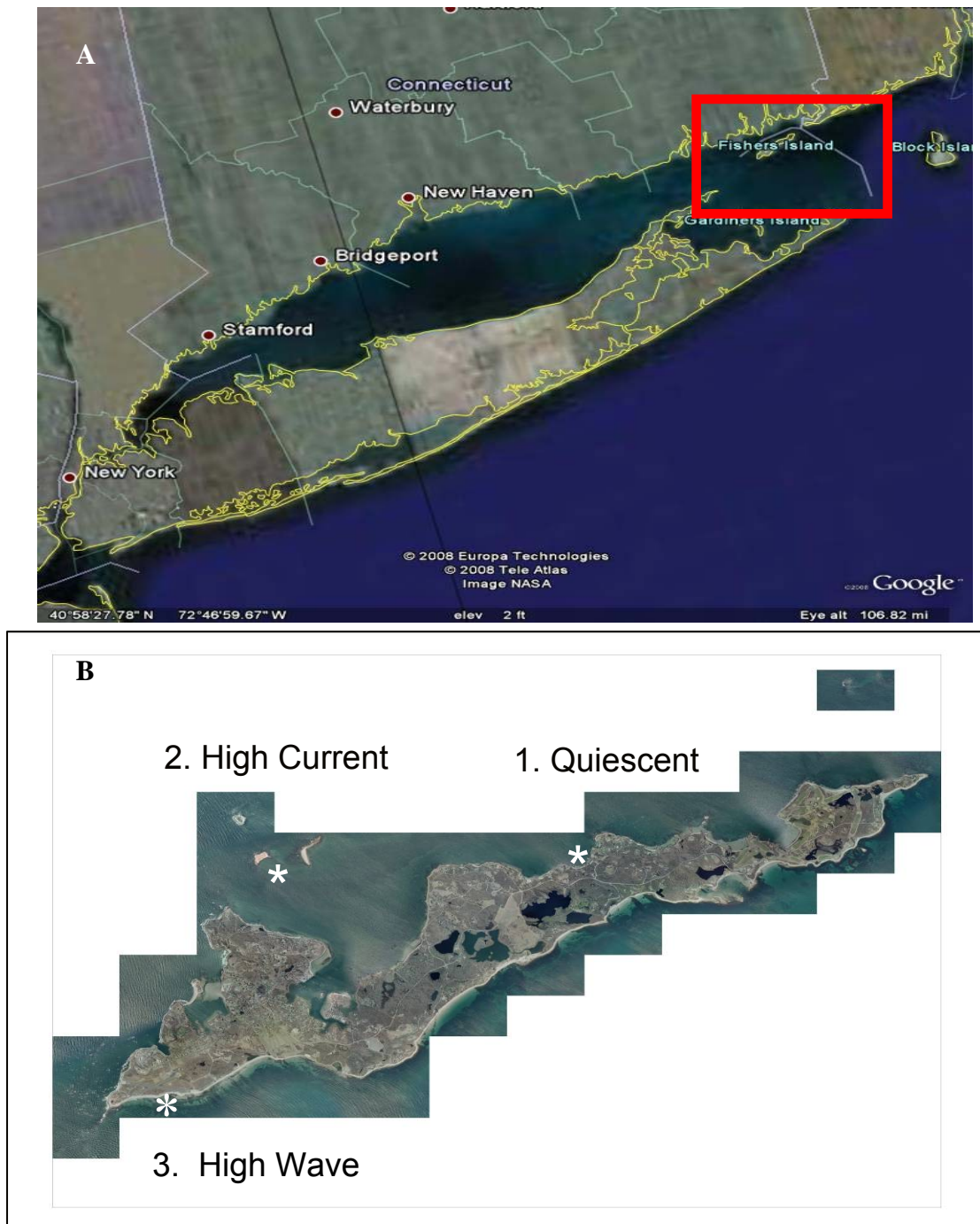


Figure 1.1 A) Location of Fisher's Island, NY within Long Island Sound, note the extremely long fetch in the SE direction, and B) location of three field sites around Fisher's Island, NY: 1) quiescent site which is protected from currents and waves, 2) high current site as tidal currents are increased between the island and 3) high wave site with oceanic swell.

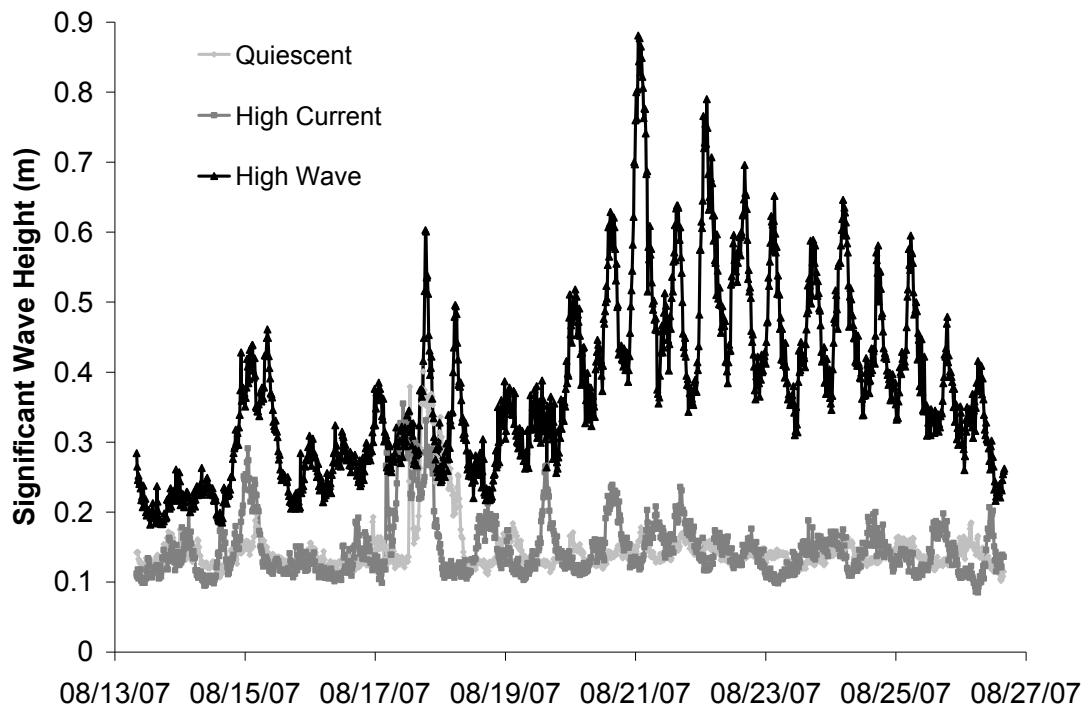


Figure 1.2. Significant wave height (m) at the quiescent (light grey triangles), high current (dark grey squares) and high wave (black triangles) sites measured over a two week period in August, 2007. The tidal signal present at the high wave site was found to be significantly related to water depth ($p < 0.0001$) such that when the tide was low, significant wave height decreased, and when the tide was high, significant wave height increased.

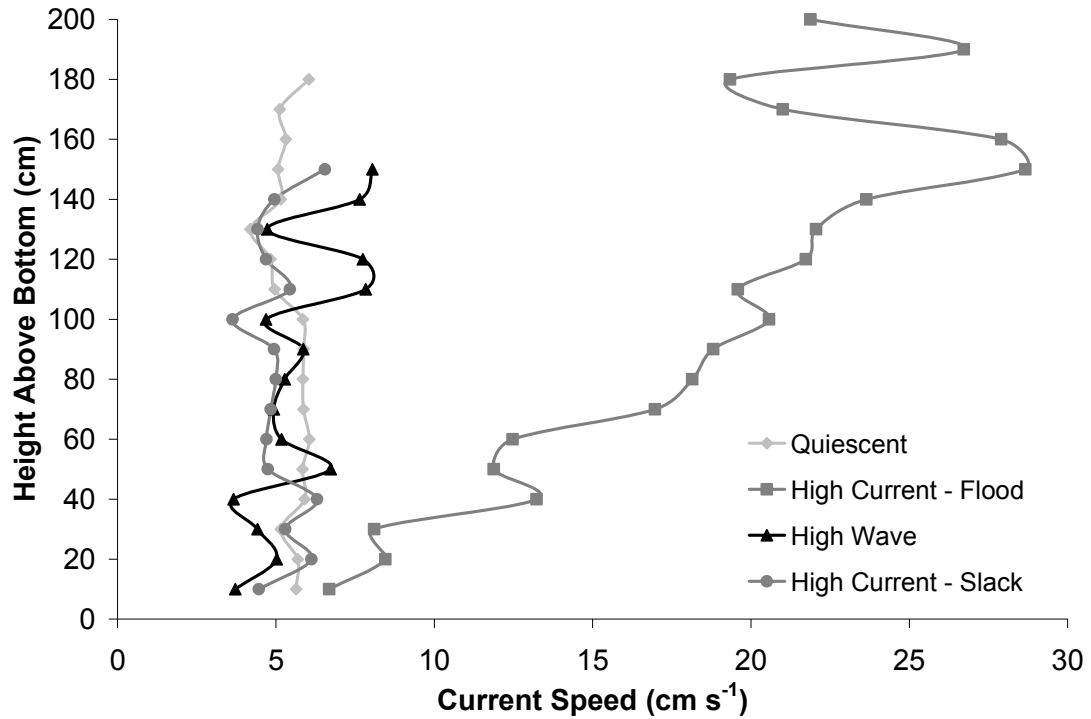


Figure 1.3. Average current speed (m s^{-1}) plotted over water depth for the quiescent (light grey diamonds), high wave (black triangles), and high current (dark grey, slack tide – circles, flood tide - squares) sites over a six hour period in June, 2008. Tidal phase was a neap tide. Canopy height was 29.5 cm, 4.8 to 27.8 cm, 103 cm, and 41.5 cm for the quiescent, high wave, and high current slack or high current flood tide.

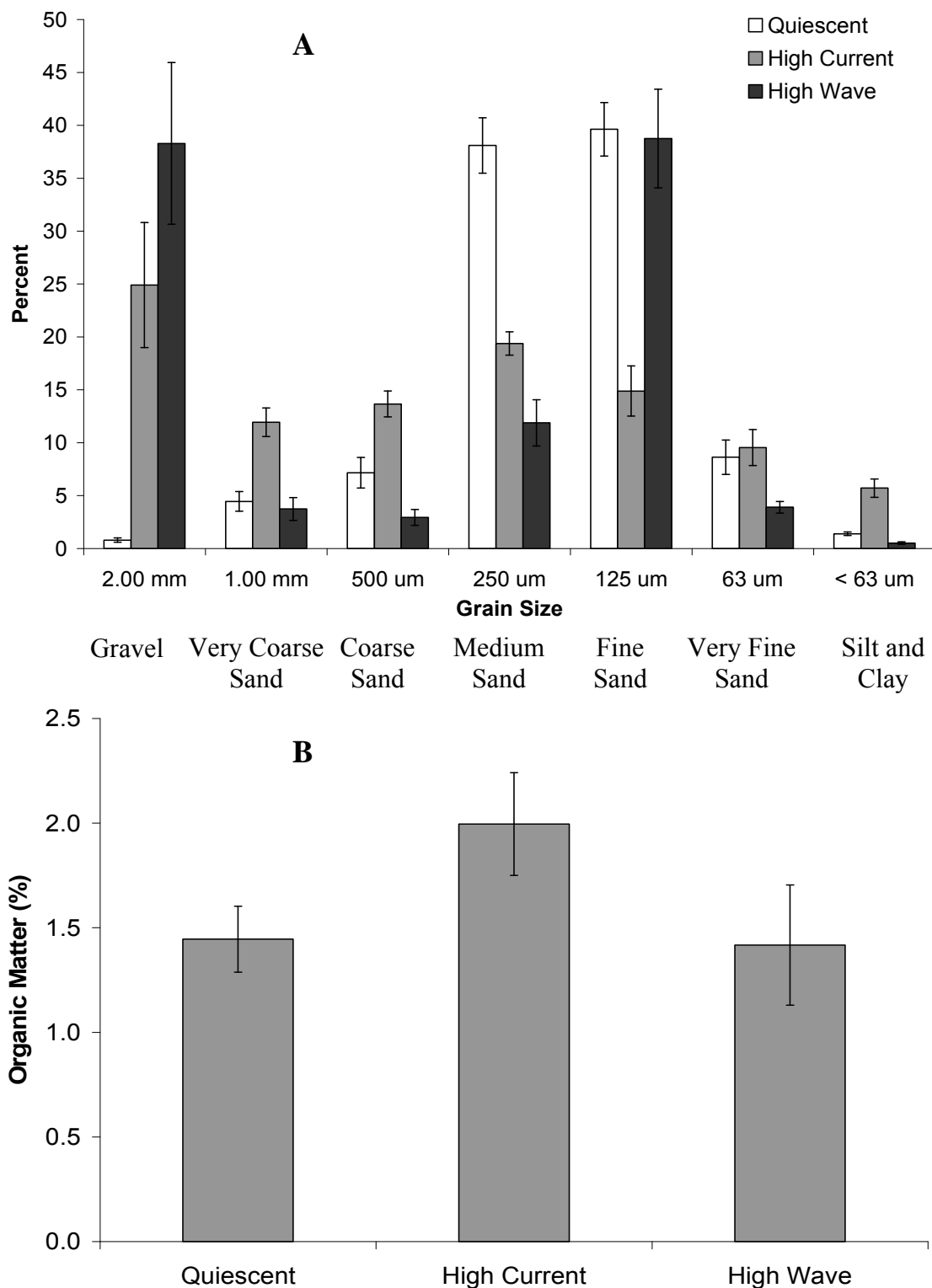


Figure 1.4. A) Average grain size distribution and B) average percent organic matter of sediment cores collected in July, 2007 from the quiescent, high current, and high wave sites off Fisher's Island, NY. Error bars represent \pm S.E., $n = 7$.

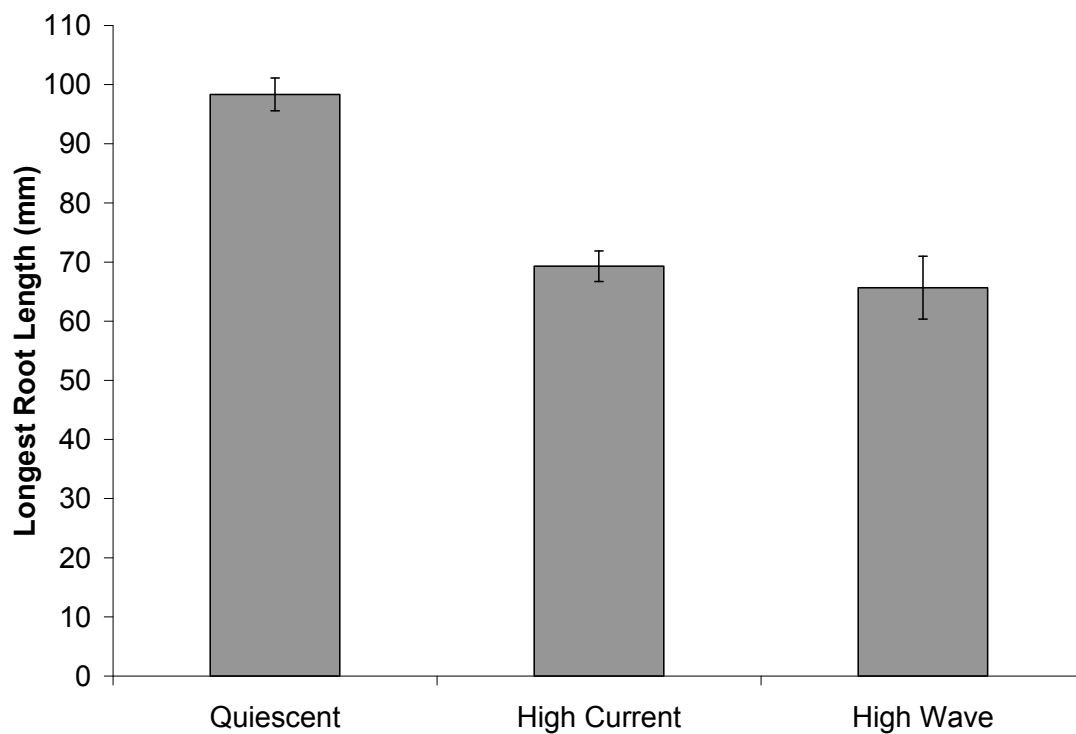


Figure 1.5. Average length of the longest root of *Z. marina* collected from the quiescent, high current, and high wave sites off Fisher's Island, NY in July, 2007. Error bars represent \pm S.E., $n = 7$ for high current and high wave sites, $n = 4$ for quiescent site. Quiescent $>$ (High Current = High Wave).

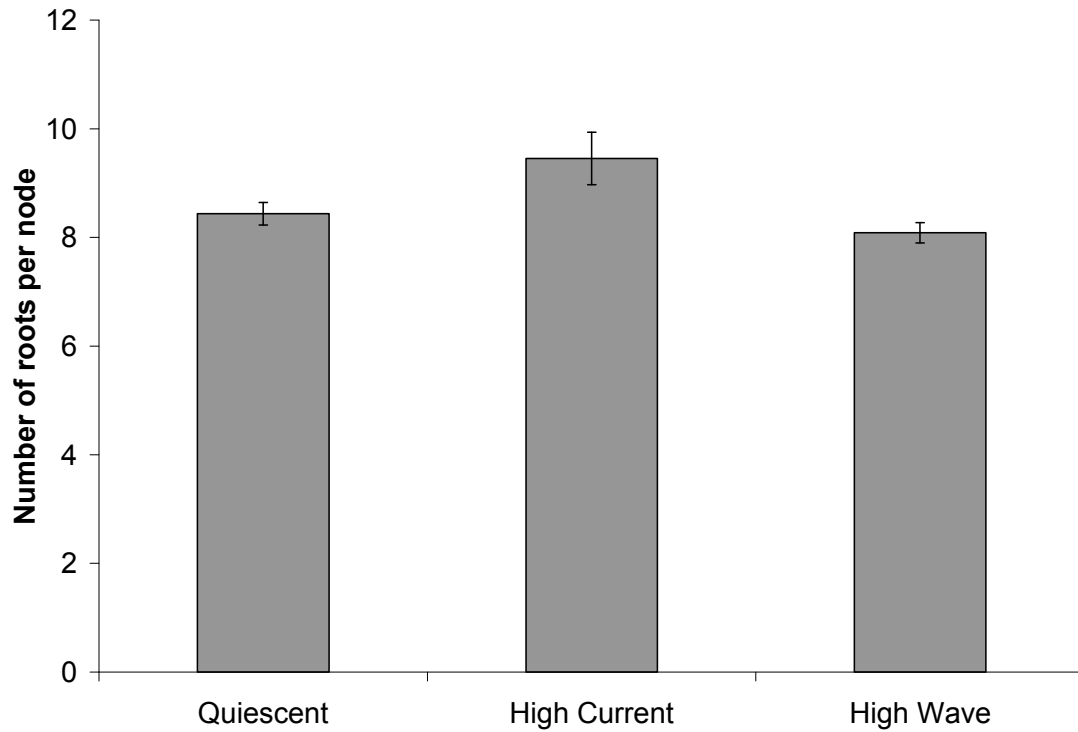


Figure 1.6. Average number of roots per node of *Z. marina* collected from the quiescent, high current, and high wave sites in July, 2007. Error bars represent +/- S.E., $n = 7$ for high current and high wave sites, $n = 4$ for quiescent site. High Current > High Wave but High Current = Quiescent.

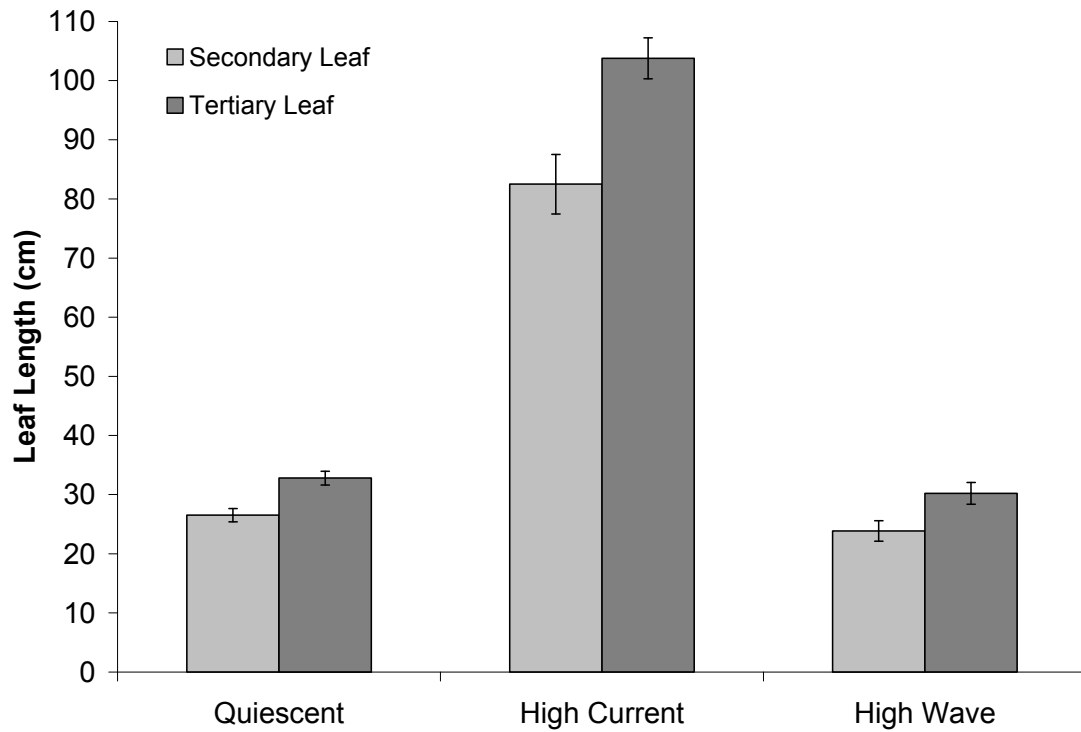


Figure 1.7. Average secondary (light grey) and tertiary (dark grey) leaf length (cm) of *Z. marina* collected from the quiescent, high current, and high wave sites in July, 2007. Error bars represent +/- S.E., $n = 7$ for high current and high wave sites, $n = 4$ for quiescent site. High Current \gg (Quiescent = High Wave).

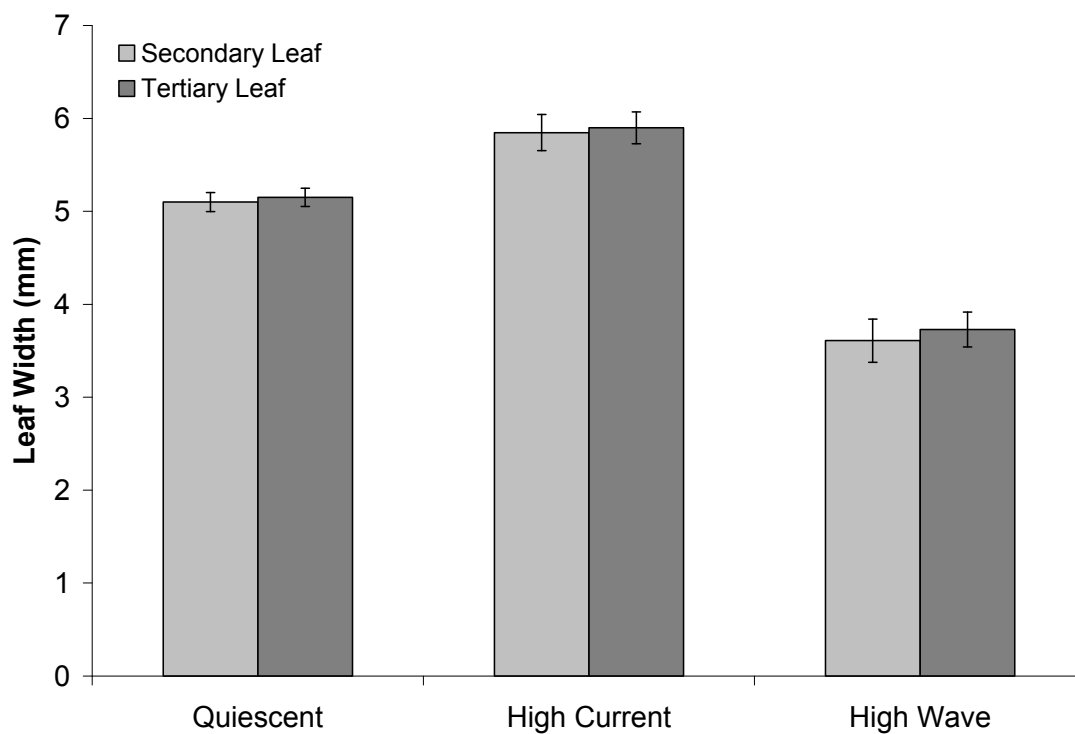


Figure 1.8. Average secondary (light grey) and tertiary (dark grey) leaf width (mm) of *Z. marina* collected from the quiescent, high current, and high wave sites in July, 2007. Error bars represent +/- S.E., $n = 7$ for high current and high wave sites, $n = 4$ for quiescent site. High Wave \ll Quiescent $<$ High Current.

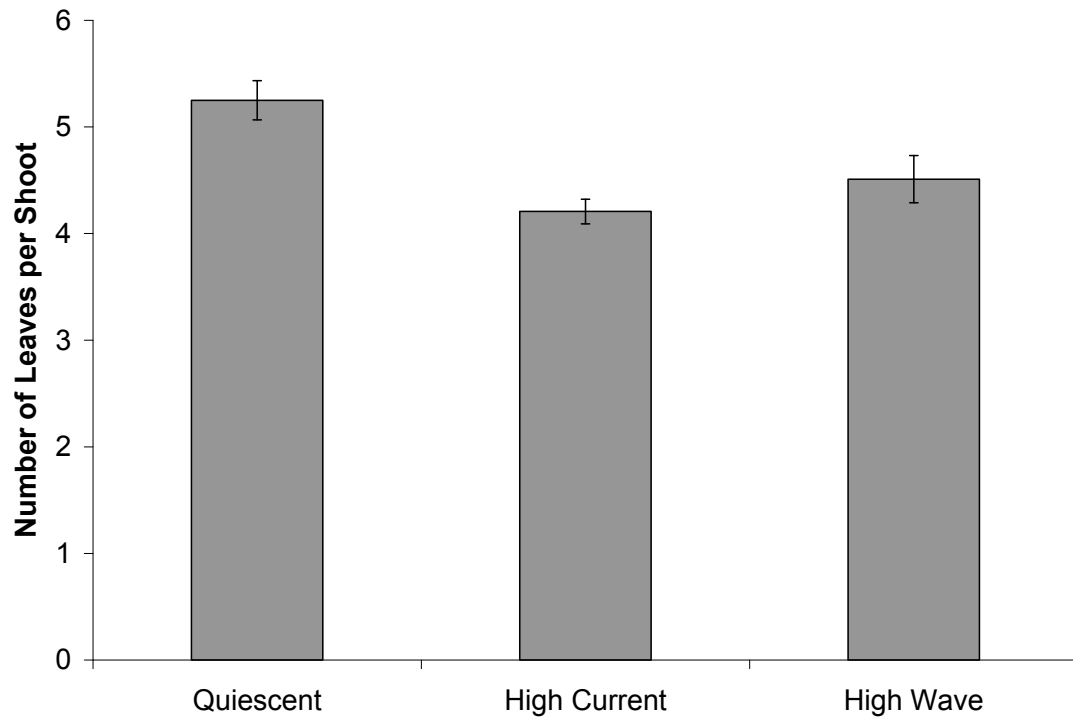


Figure 1.9. Average number of leaves of *Z. marina* shoots collected from the quiescent, high current, and high wave sites in July, 2007. Error bars represent +/- S.E., $n = 7$ for high current and high wave sites, $n = 4$ for quiescent site. Quiescent > (High Current = High Wave).

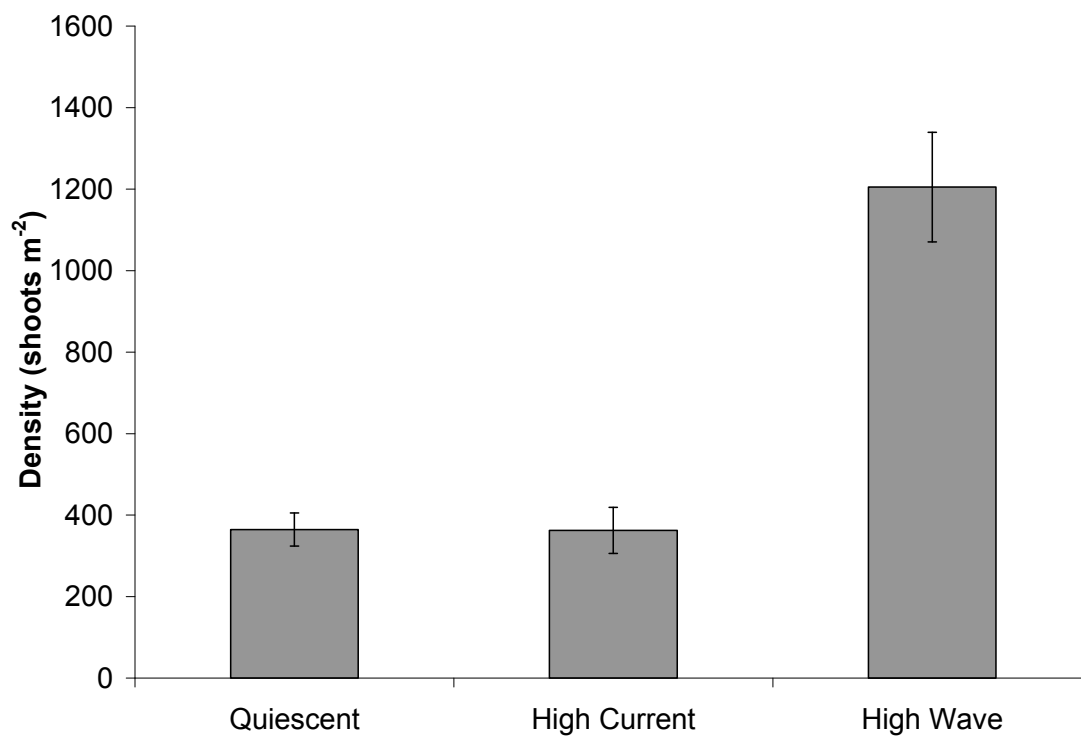


Figure 1.10. Average shoot density of *Z. marina* at the quiescent, high current, and high wave sites in July, 2007. Error bars represent +/- S.E., n = 7. High Wave >> (Quiescent = High Current).

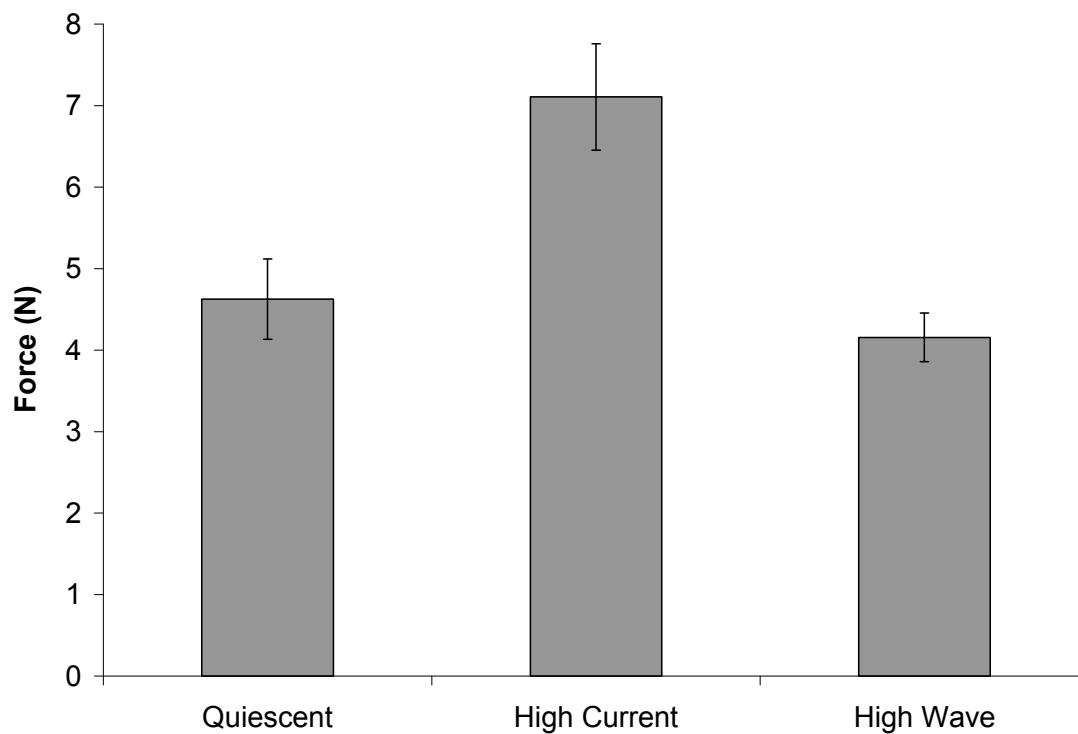


Figure 1.11. Average force in Newtons (N) required to break the tertiary leaf of *Z. marina* collected from the quiescent, high current, and high wave site in July, 2007. Error bars are +/- SE, n = 7. High Current > (Quiescent = High Wave).

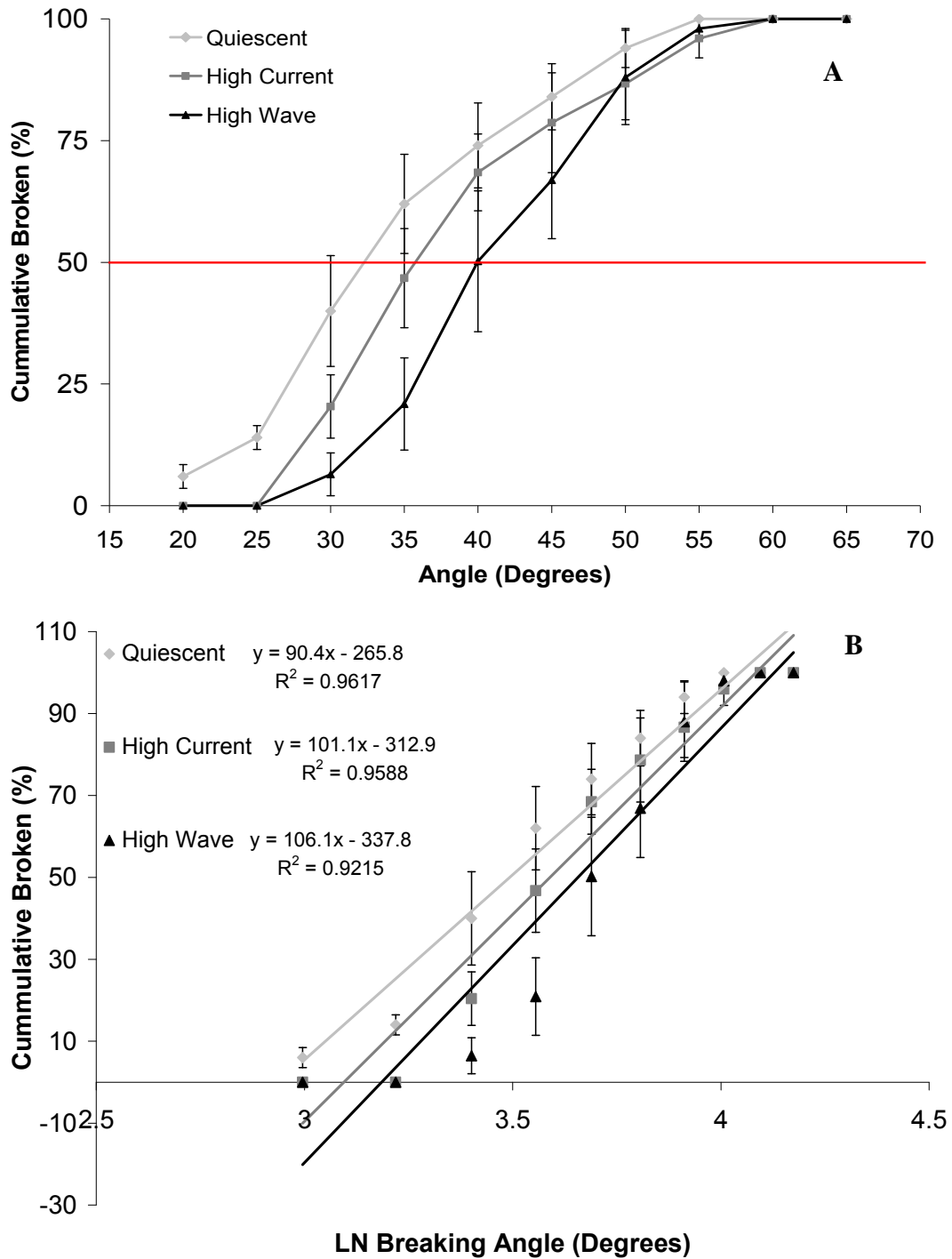


Figure 1.12. A) Cumulative distribution and B) the natural log of the cumulative distribution of the angle (degrees) required to break the tertiary leaf of *Z. marina* collected in July, 2008 from the quiescent (light grey diamonds), high current (dark grey squares), and high wave (black triangles) sites off Fisher's Island, NY. Error bars represent \pm S.E., $n = 5$. A: Quiescent = High Current = High Wave. B: Quiescent < (High Current = High Wave).

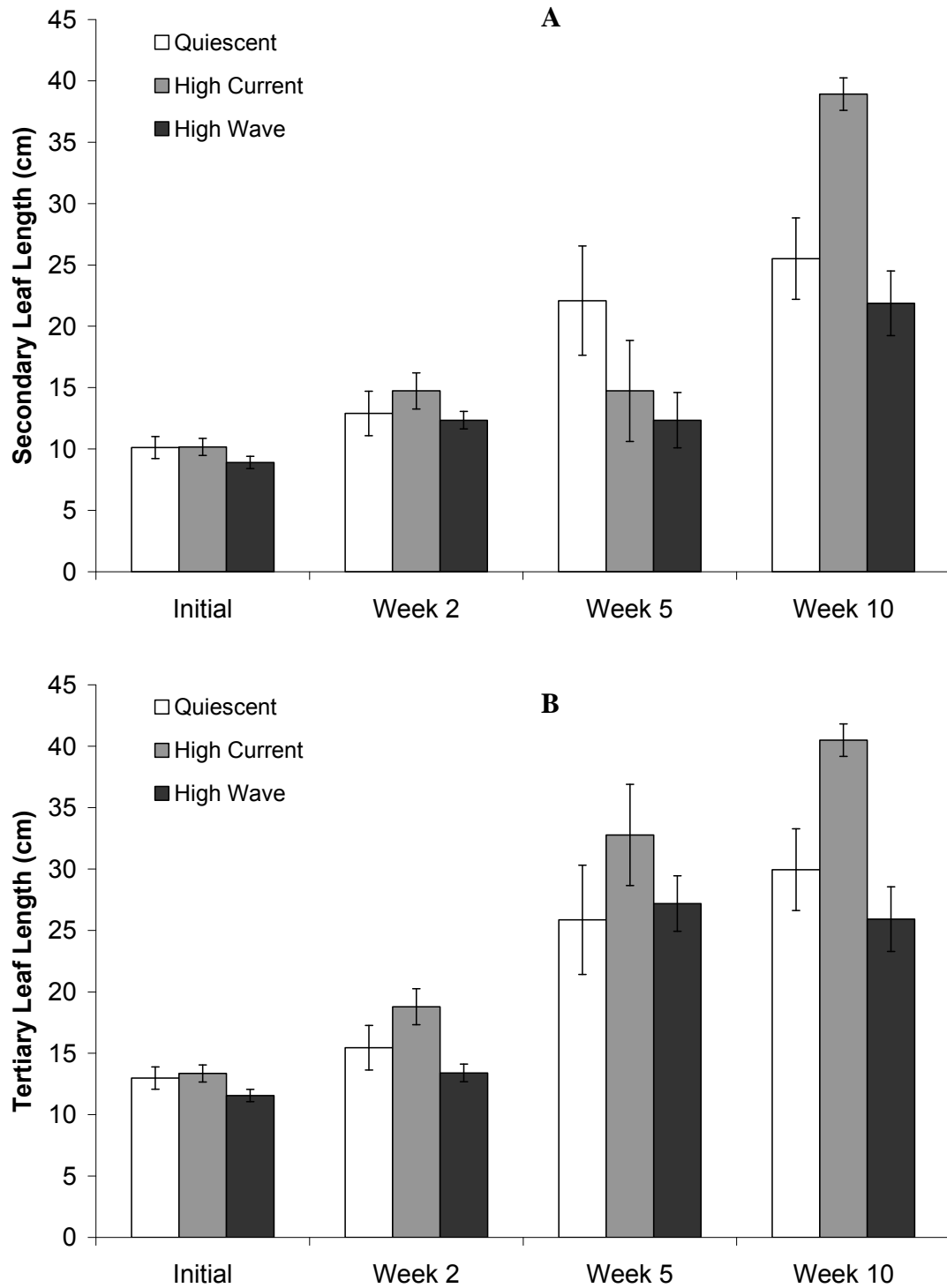


Figure 1.13. Average secondary (A) and tertiary (B) leaf lengths (cm) of *Z. marina* collected from the quiescent (white), high current (grey), and high wave (black) sites in April 2008 and grown in outdoor flow tanks under common garden conditions for 10 weeks. Error bars represent \pm S.E., n = 4.

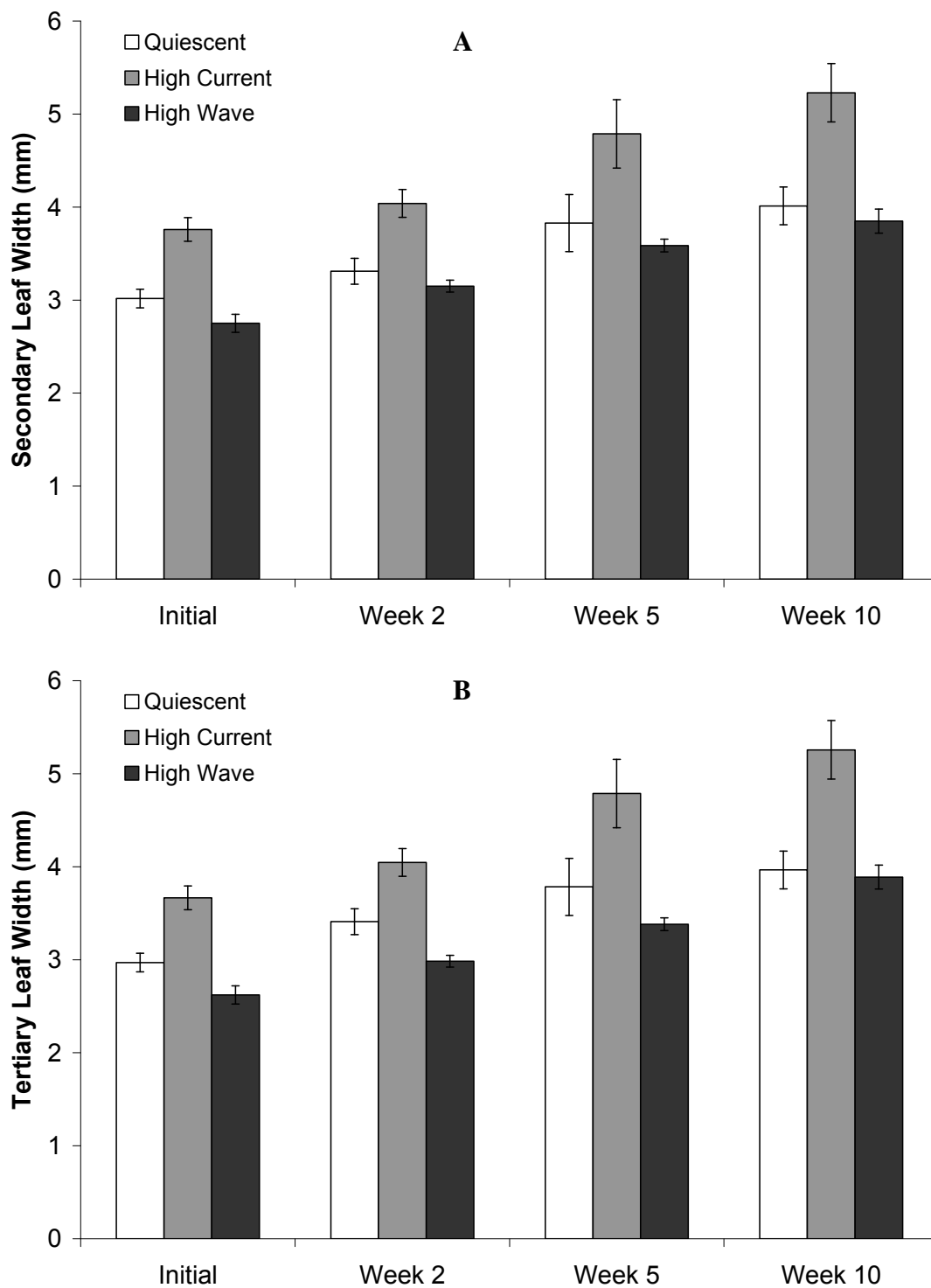


Figure 1.14. Average secondary (A) and tertiary (B) leaf widths (mm) of *Z. marina* collected from the quiescent (white), high current (grey), and high wave (black) sites in April, 2008 and grown in outdoor flow tanks under common garden conditions for 10 weeks. Error bars represent \pm S.E., $n = 4$.

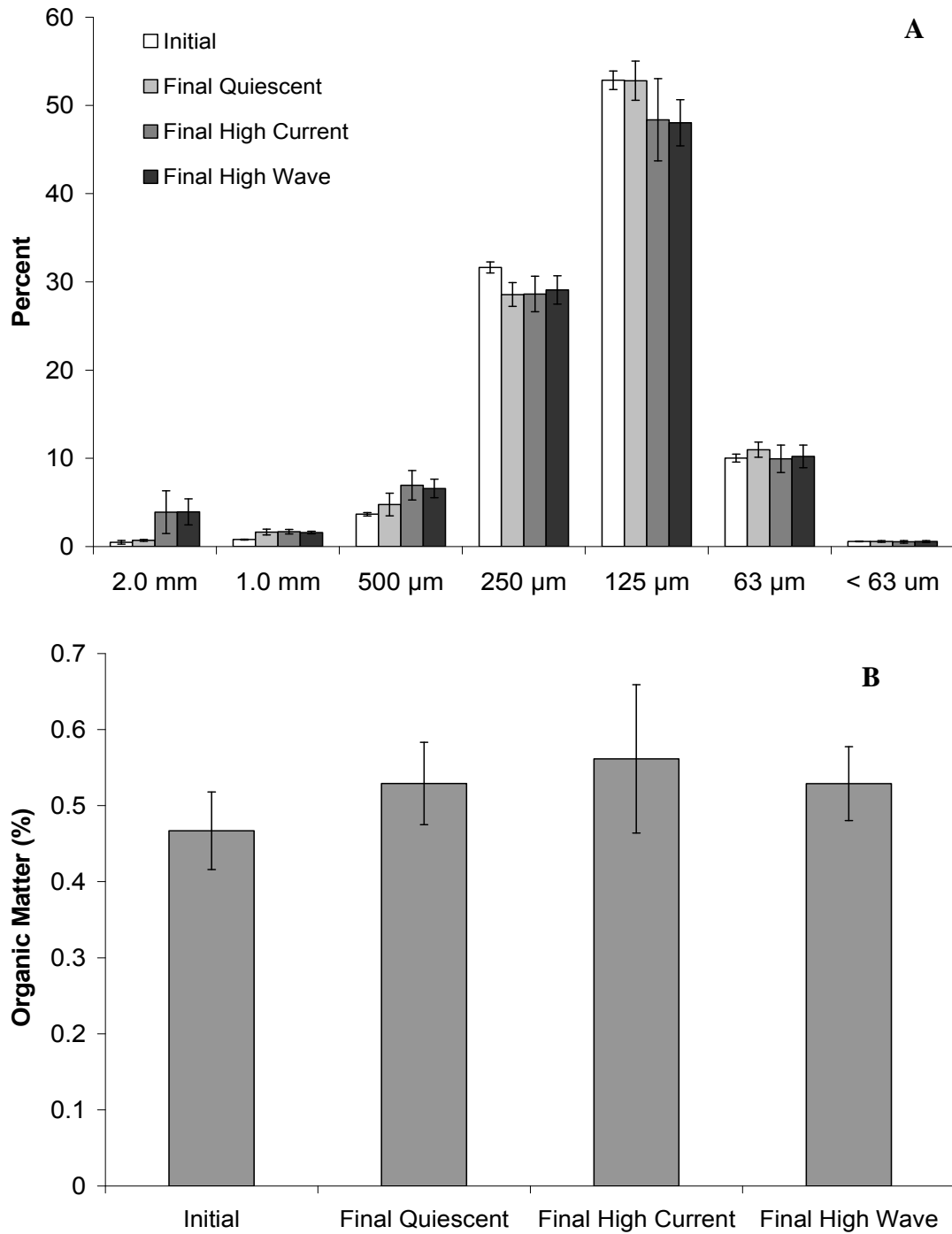


Figure 1.15. A) Average grain size distribution of sediment cores collected from flow tank trays initially, before *Z. marina* was transplanted, and at the end of the 10 week flow tank experiment. B) Average percent organic matter of sediment collected via cores from flow tank trays initially, before *Z. marina* was transplanted, and at the end of the 10 week flow tank experiment. Error bars represent \pm S.E., $n = 4$ for final conditions and 6 for initial conditions.

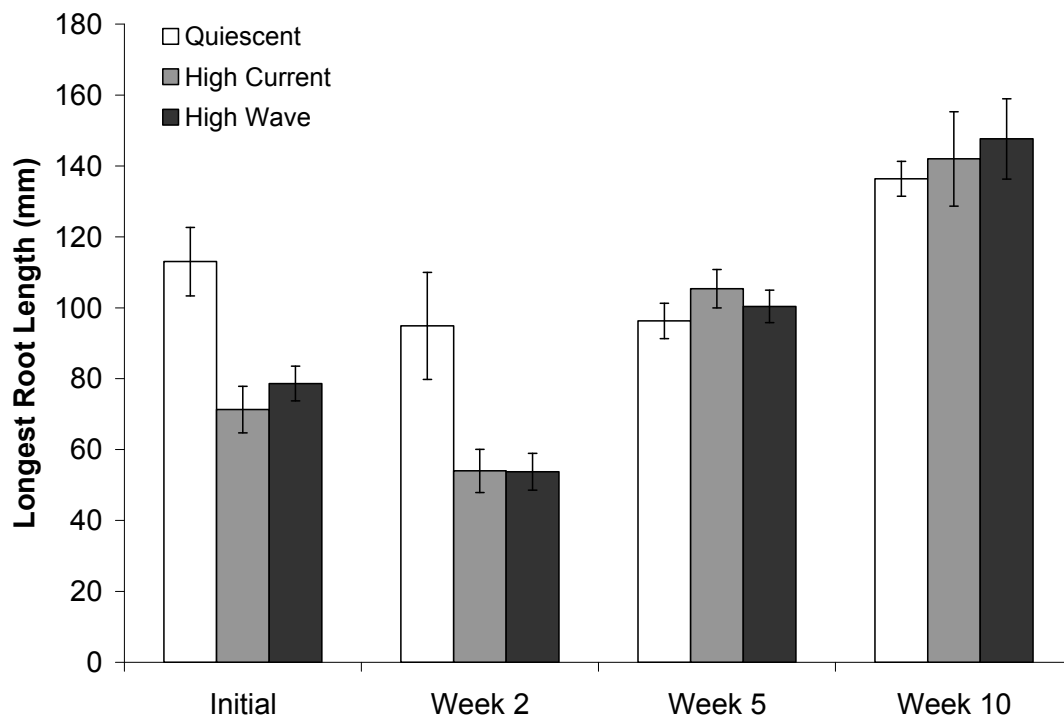


Figure 1.16. Average length of the longest root of *Z. marina* collected from the quiescent (white), high current (grey), and high wave (black) sites in April, 2008 (Initial) and grown in outdoor flow tanks for 10 weeks. Error bars represent +/- S.E., n = 4.

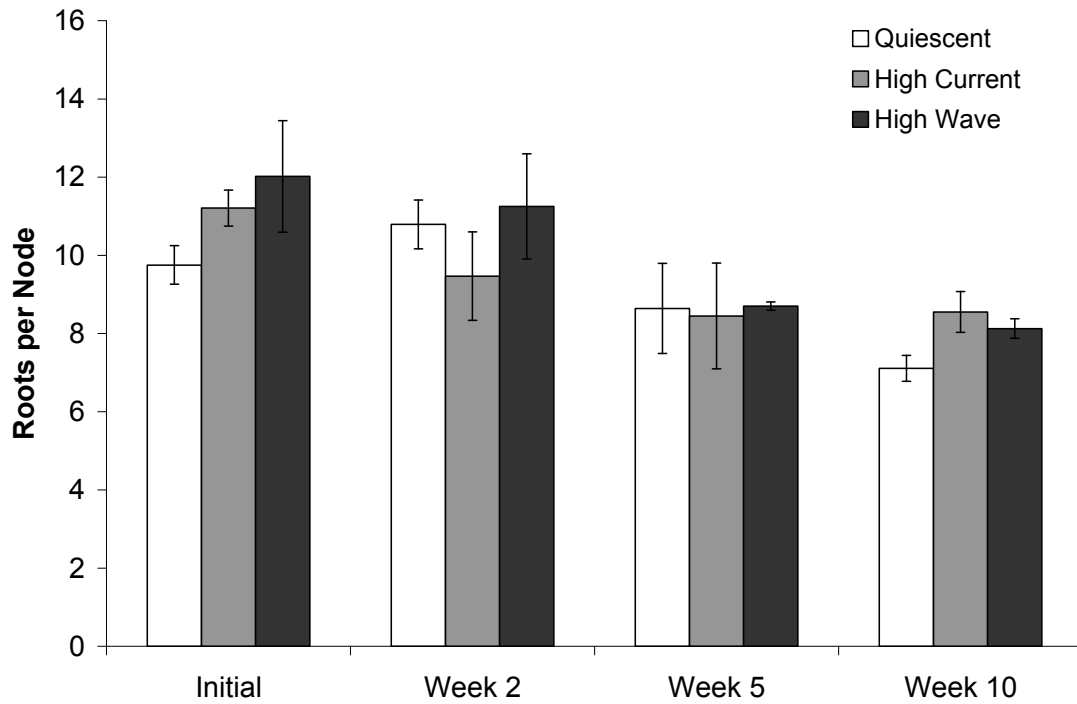
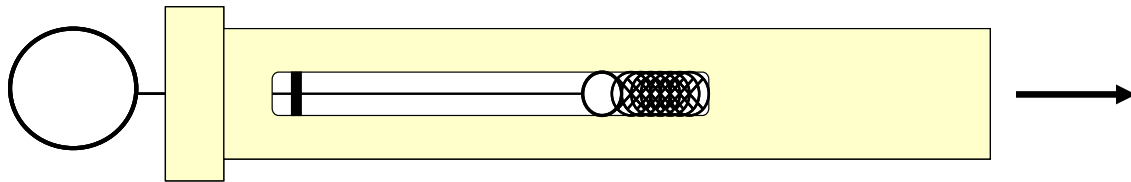


Figure 1.17. Average number of roots per node of *Z. marina* collected from the quiescent (white), high current (grey), and high wave (black) sites in April, 2008 (Initial) and grown in outdoor flow tanks for 10 weeks. Error bars represent \pm S.E., $n = 4$.

Illustrations



Legend:



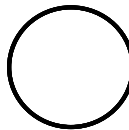
Spring



Rubber Piece



Fishing Line



Clip

Illustration 1.1. Illustration of modified dynamometer used to measure the strength of the tertiary leaf of *Z. marina* collected from the quiescent, high current, and high wave sites. The base of the tertiary leaf was secured with the clip, while the tip of the leaf was held in place. The end of the dynamometer was pulled, moving the black rubber piece along the length of the fishing line. When the leaf broke, the distance that the rubber piece had moved was recorded, and used to calculate force from a linear regression achieved from a calibration.

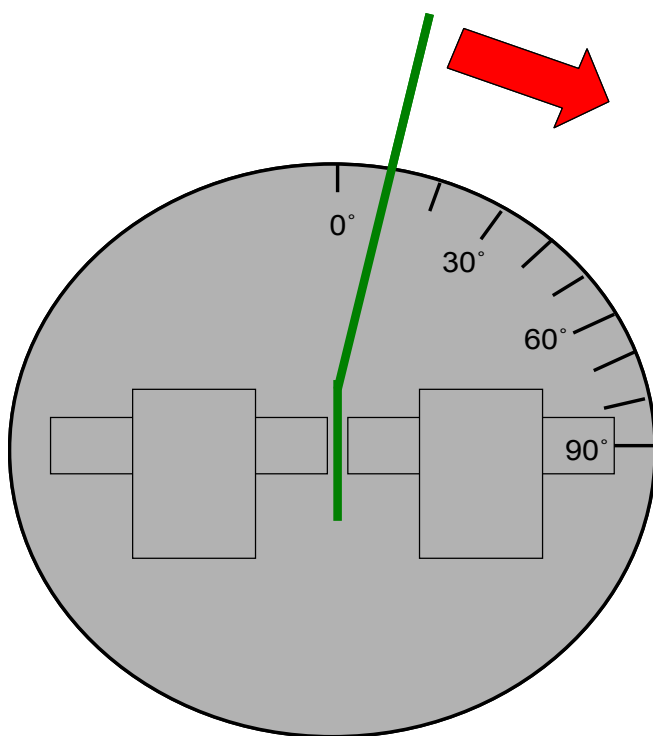
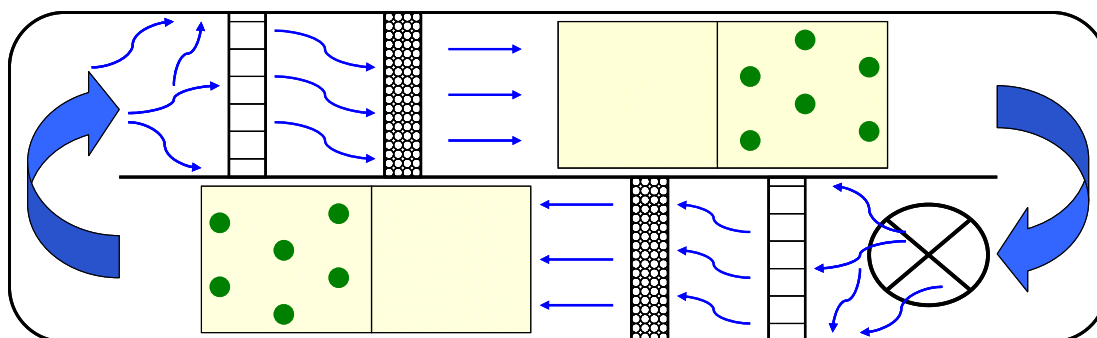


Illustration 1.2. Diagram of the apparatus used to measure the breaking angle of the tertiary leaf of *Z. marina* collected from the quiescent, high current, and high wave site. Base of tertiary leaf was secured in the center of the circular base. The tip was then rotated around the circle with equal tension until the leaf broke. The angle at which the leaf broke was recorded to the nearest 5°.



Legend:



Tray of sand with 6 *Z. marina* shoots



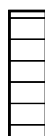
Tray of sand without plants



Trolling Motor



Collimator



Flow Straightener

Illustration 1.3. Schematic of flow tank set-up used for the common garden experiment. Current was generated with a trolling motor, which circulated water around the flow tank. Water flow was directed through a flow straightener and collimator before flowing over *Z. marina* shoots. There were 6 of these flow tanks, making a total of 12 trays with transplanted seagrass, which contained 6 *Z. marina* shoots each.

Chapter 2: Light availability in *Zostera marina* beds exposed to currents and waves: the importance of leaf morphology, shoot density, and self-shading.

Abstract

The role of hydrodynamic conditions on light availability to the seagrass *Zostera marina* was quantified. Leaf motion was analyzed for *Z. marina* exposed to currents, waves, and quiescent conditions, and used to calculate area of photosynthetic tissue available to capture downwelling light, the dominant form of light at the study sites. Leaf carbon and nitrogen content were also analyzed, as well as photosynthetic yields, in order to understand how light availability, carbon uptake, and nutrient availability affect productivity of seagrasses. Our calculations indicate that, due to self-shading, seagrass shoots exposed to waves and currents have less tissue available for capturing downwelling light than shoots exposed to quiescent conditions; in agreement, shoots exposed to currents and waves experienced lower photosynthetic yields. Thus, the self-thinning hypothesis proposed by Marbà and Duarte (2003) may not apply in hydrodynamically active environments, and morphological variations, which enhance self-shading, may be a necessary trade-off to ensure survival under dynamic conditions. In contrast, *Z. marina* leaves in quiescent waters experienced minimal self-shading and higher photosynthetic yields than *Z. marina* leaves exposed to currents and waves, but were more carbon limited, possibly due to reduced fluxes through the diffusive boundary layer. Hence, life under different hydrodynamic conditions leads to trade-offs between light and nutrient availability. We hypothesize that, due to the high degree of self-shading,

seagrasses exposed to currents and waves may require better water quality and higher irradiances when compared to those located in quiescent waters, making them more vulnerable to eutrophication.

Introduction

The interaction of flexible organisms with their fluid environment is indeed quite complex. It has been observed that seagrasses sway back and forth with waves and deflect with currents (Grizzle et al. 1996, Ghisalberti and Nepf 2002, Abdelrhman 2007, Fonseca et al. 2007, Morris et al. 2008). The stiffness and buoyancy of a benthic organism then tends to restore it to an upright position (Abdelrhman 2007). As organisms acclimate to hydrodynamic forces exerted upon them by changing their morphology (Peralta et al. 2000, Schanz and Asmus 2003, Peralta et al. 2005) and flexibility (Bouma et al. 2005), they are ultimately affecting how much they sway back and forth and how much they are deflected.

While streamlined leaf morphology may benefit the organism via reduced drag (i.e. a reduced risk of being dislodged), it may also bring disadvantages such as reduced light availability via self-shading (Zimmerman 2003). By bending when exposed to currents, strap-like leaves in a canopy can shade or be shaded by other leaves that are also bending in unidirectional flow (Fonseca et al. 1982, Fonseca and Kenworthy 1987, Koehl and Alberte 1988, Grizzle et al. 1996, Fonseca et al. 2007). Seagrass leaves exposed to waves tend to sway back and forth “opening and closing” the canopy (Koch and Gust 1999) theoretically allowing more light into the seagrass canopy and exposing sections of each leaf to downwelling irradiance over short

fractions of time as the leaf completes its swaying cycle. Therefore, less light limitation is expected in wave-exposed than in current-exposed seagrass canopies. However, seagrasses exposed to waves can also experience self-shading when the canopy is “closed” for a fraction of the wave cycle.

Seagrasses minimize self-shading by decreasing shoot density in large wave or strong current conditions (Bouma et al. 2005, Peralta et al. 2005). It follows that hydrodynamics appear to play a role in the “self-thinning” hypothesis proposed for seagrasses by Marbà and Duarte (2003) where an equilibrium between the minimum distance between shoots and maximum aboveground biomass is achieved. The self-thinning hypothesis assumes density-dependent mortality; however, this does not make sense, evolutionarily speaking, for clonal plants (Marbà and Duarte 2003). Therefore, it was concluded that the scaling of the distances between shoots and leaf and shoot characteristics described by the self-thinning hypothesis is programmed onto the architecture of the seagrass canopy. As a canopy reaches its maximum aboveground biomass, which is accompanied by decreased light availability, the plants may respond by decreasing shoot recruitment, rhizome growth, or shoot size to maximize light availability (Marbà and Duarte 2003). Consequently, the degree of self-shading imposed by bending leaves, which is a result of local hydrodynamic conditions, could lead to a change in seagrass morphology and canopy density.

For *Zostera marina* it was reported that maximum canopy bending occurred by a current velocity between 40 and 50 cm s⁻¹ (Fonseca et al. 1982). Any increase in current velocity above 50 cm s⁻¹ did not significantly change the bending angle of *Z. marina* (Fonseca et al. 1982), but was reported to drastically reduce *Z. marina*

densities (Fonseca and Kenworthy 1987) despite being tolerant of current velocities up to $120 - 150 \text{ cm s}^{-1}$ (Fonseca et al. 1983). Similarly, flows of 80 cm s^{-1} in a field flow tank experiment significantly reduced shoot density in an area characterized by slower current velocities (Schanz and Asmus 2003). However, currents in seagrass beds are often below these values (Koch 2001), and while these values are helpful, they are not yet coupled with morphological characteristics such as leaf length, width and number, and shoot density, which could drastically change the effective bending, and hence light availability, associated with varying current velocities.

Light availability to seagrass leaves as a function of the angle of bending under different current velocities was explored in a theoretical bio-optical model (Zimmerman 2003). Horizontally projected leaf area (l_p) was used to determine how much green tissue is exposed to adjusted downwelling irradiance at different angles of bending (Zimmerman 2003). Light availability reached its maximum at a bending angle between 10° and 20° for both *Thalassia testudinum* and *Zostera marina*. At a bending angle $<10^\circ$, photosynthesis was limited by a small projected leaf area as the leaf presented a very small target to the downwelling irradiance, whereas a bending angle $>20^\circ$ limited photosynthesis as most of the light was absorbed by the upper layers of the canopy (Zimmerman 2003). It is important to note that, since light in the marine environment is diffuse, Zimmerman characterized the light properties and adjusted for the scattering of light by correcting for angular distribution of downwelling irradiance in his model. Our study characterizes the light properties and uses Zimmerman's model to calculate l_p of seagrasses exposed to quiescent

conditions, tidally influenced current, and high wave action in order to quantify the role of hydrodynamics in light availability to the seagrass *Z. marina*.

Objectives and Hypotheses

In chapter 1, morphological variation among *Zostera marina* exposed to currents, waves, or quiescent conditions was described, yet a mechanism for this variation was not demonstrated. Water flow could directly cause changes in morphology in response to the mechanical stress that water flow imposes on seagrass leaves, or water flow could indirectly affect seagrass morphology via nutrient uptake, carbon availability, or light availability. Therefore, the objective of this chapter was to examine the influence of water flow, in the form of waves, currents, or the lack there of, on nitrogen and carbon uptake, and how these varying hydrodynamic forces affect leaf bending and light availability to the canopy. Thus, an understanding of the potential productivity of a seagrass bed under different hydrodynamic conditions, as well as what may be limiting productivity, is achieved, while also gaining a better understanding of possible mechanisms driving the observed morphological variation.

Hypothesis 1: Differences in *Zostera marina* leaf morphology and shoot density determine the degree of self-shading in a seagrass canopy.

Rationale for Hypothesis 1: *Zostera marina* leaf morphology and shoot density should reflect the amount of self-shading occurring as a result of the local hydrodynamics, as stated in the self-thinning hypothesis by Marbà and Duarte (2003). Therefore, as plants bend with currents and sway with waves, the shoot density should decrease in order to minimize self-shading and optimize light availability.

Under oscillatory flows (waves), the bed may remain dense as it is likely to benefit from the “opening and closing” of the canopy as the leaves sway back and forth with the passage of each wave, which brings us to our second hypothesis.

*Hypothesis 2: Leaves of *Zostera marina* exposed to waves will receive more light, although during shorter intervals of time, than leaves exposed to currents and quiescent conditions.*

Rationale for Hypothesis 2: There should be an optimal leaf length and width and shoot density that maximizes light availability as a result of the bending angle that occurs due to the local hydrodynamic conditions (Dennison and Alberte 1982, Fonseca et al. 1982, Fonseca and Kenworthy 1987, Zimmerman 2003). The question is whether this theoretical optimum is indeed reached in nature.

*Hypothesis 3: *Zostera marina* leaves exposed to waves will experience photosynthetic saturation at higher irradiances than *Z. marina* exposed to currents or low water flow.*

*Rationale for Hypothesis 3: If *Zostera marina* leaves exposed to waves do indeed receive more light, than it will be reflected in photosynthetic measurements.*

*Hypothesis 4: The photosynthetic properties of *Zostera marina* grown under the same hydrodynamic conditions (“common garden”) will converge over time.*

*Rationale for Hypothesis 4: *Zostera marina* grown under common garden conditions will develop similar morphological characteristics and therefore will have*

the same light availability due to the same degree of self-shading (or lack thereof), which will result in identical photosynthetic capacity.

Methods

Site Location

Field sites were located in Long Island Sound off Fisher's Island, NY (Figure 1.1 A) due to the broad range of hydrodynamic conditions under which *Zostera marina* is found there. Three sites were studied: 1) a quiescent site that experienced minimal waves and currents, which was located on the north side of the island within a protected cove, 2) a high current site located on the northwest side of the island between Fisher's Island and South Dumpling Island, such that as the tide comes in and out, water is forced between these two land masses, thereby increasing current speed, and 3) a high wave site located on the southwest side of the island that was continually exposed to oceanic swell (Figure 1.1 B). At each of the three sites, 4 to 7 patches (quiescent and high wave site), or when patches were not present (high current site), 4 to 7 areas within a bed separated by at least 3 m were used as replicates. All replicate patches at the same site and between sites were located at approximately the same depth (mean water level = 2.0 m +/- 0.2 m, tidal range = 0.8 m). Sampling events took place in July and August, 2007 and June and July, 2008. During this time salinity ranged between 30 and 35 and water temperature ranged between 15 and 23° C.

Hydrodynamics and Seagrass Leaf Motion

At each sampling site seagrasses were videotaped in motion using a digital underwater camera (Sony PC100 mini DV recorder, Gates Housing) mounted on a tripod (Design and Construction, Chris Pickerell and Kevin Cahill, Cornell University, Cooperative Extension of Suffolk County, Marine Program) to ensure that the height above the bottom and angle which the video was taken from were consistent. A 1.5 m reference pole sub-divided into 10 cm intervals was visible in each frame. Simultaneously we record currents (AquaDopp Current Profiler, Nortek AS) and waves (MacroWave pressure gauge, Coastal USA) in an unvegetated area adjacent to the patches or directly in the area being video taped. The current profiler recorded at 2 Hz and averaged current velocity measurements for 5 minutes every 15 minutes for 6 hours over 10 cm depth intervals throughout the water column starting 5 cm above the instrument (15 cm above the bottom). Current measurements were taken during the weeks of July 17th – 20th, 2007, and June 9th – 13th, 2008. The wave gauges recorded pressure at 5Hz, and averaged data for 13.5 minutes every 15 minutes for 5 days (July 17th – 20th, 2007). The pressure data was then Fast-Fourier transformed (Denman 1975) to obtain wave parameters such as significant wave height (H_s) and wave period (P) in addition to average water depth (z). Wave period was used to calculate wavelength (L) from the equation: $L = \frac{gP^2}{2\pi}$, which assumes the waves are deep water waves (Open University 1999). L , P , H_s and z were used to calculate the maximum near-bottom orbital velocity (U_b) (Infantes et al. 2009), giving further insight as to how the waves were affecting the bottom, and the seagrass beds inhabiting the benthos.

Light

Downwelling plane [$E_d(z)$] and scalar ($[E_o(z)]$ irradiance (PAR) were measured at 0.5 m intervals from the surface to the sea floor adjacent to the studied seagrass beds using both LiCor Inc. UWQ5108 and SPQA1876 radiometers, which allowed us to calculate the average cosine for downwelling ($\overline{\mu_d}$) light. $\overline{\mu_d}$ is defined as the downwelling plane irradiance (E_d) divided by the downwelling scalar irradiance (E_{0d}) (Kirk 1983). E_d was measured with a cosine LiCor irradiance sensor, whereas E_{0d} was measured with a spherical LiCor sensor fitted with a black plate positioned directly below the base and was 10 times the diameter of the spherical irradiance sensor in order to block upwelling irradiance (Højerslev 1975).

A chain of plane irradiance sensors (Odyssey Data Recording Systems, Christchurch, New Zealand) were used to quantify light attenuation (K_d) in the water column in relation to turbidity as a result of local hydrodynamic conditions. Four sensors were placed 12, 47, 82, and 117 cm above the seabed, and PAR was recorded every 15 minutes for 6 hours concurrently with current and wave data collection.

Seagrass Morphology

From each replicate patch we collected *Zostera marina* for morphological measurements (leaf length and width of secondary and tertiary leaves, number of leaves per shoot) (n=4 at the quiescent site, n=7 at the high current and high wave site), and leaf tissue for carbon and nitrogen content and $\delta^{13}\text{C}$ and $\delta^{15}\text{N}$ analyses (UC Davis Stable Isotope Facility) (n=4). *Z. marina* shoot density was also quantified at each replicate patch (n=7) using the quadrat method (25 x 25 cm) according to Duarte

and Kirkman (2003) in which the quadrat was randomly placed within the designated replicate area such that the entire quadrat contained *Z. marina* shoots.

Video Analysis

Upon returning to the lab, video data were analyzed frame-by-frame for seagrass leaf bending angle during selected time periods. Still images from the video were analyzed with ImageJ [National Institute of Health (NIH)] to calculate leaf bending angle and the proportion of the leaf bent at that particular angle, as often times the leaf was bent into multiple angles. In order for a segment of video to be used, water quality had to be good enough that individual shoots could be seen, and only shoots that could be followed from the base to the tip without interruption were used.

For the quiescent site, 5 - 15 leaves were measured for bending angle in each of the 7 replicate videos. For the high current site, the video was supplemented with still images because the leaves were too long (>1m) to fit in the video frame at a distance where the video camera could focus on the seagrasses. This approach was acceptable as currents were relatively steady and angle of bending changed very slowly over time. Close up images were taken of the seagrass canopy, section by section, following a single leaf from the base to the tip, which were pieced together and used in conjunction with the video to measure bending angle, and the proportion of the leaf associated with that angle. Furthermore, since the current velocity was tidally influenced, it varied over time. To account for this, the acoustic Doppler profiler (AquaDopp) was deployed over a half-tidal cycle, and images of the plants, as described above, were taken every 1.5 hours for 6 hours to understand how the

canopy shape and leaf bending angle change as a function of current velocity. Based on these data we calculated the fraction of time the shoots were oriented at a particular bending angle.

At the high wave site, seagrass leaf motion was much more variable than originally expected. In order to take into account this variability, the shape of the shoot, as comprised of multiple bending angles, was determined from the video every 0.5 seconds for 45 seconds in order to achieve a detailed understanding of how the plants were moving under the influence of waves due to wave height and period, and depth of the seagrass bed. Then, plant motion was divided into 7 key phases. Each phase was characterized by a key leaf position within the cycle covered by the passage of a wave. Therefore, the amount of time the canopy spent in each of these phases, which varied on a second time scale, could be determined.

Horizontally Projected Leaf Area (l_p)

Bending angle, leaf length, and leaf width data were used to calculate the horizontally projected leaf area (l_p) (see “Calculations”), that is, the area of plant tissue adjusted to a horizontal orientation, for each site as described in Zimmerman (2003) (Illustration 2.1) . At the quiescent site, l_p was calculated from the average bending angles and the length of leaf associated with those angles. At the high current site, we calculated the fraction of time that seagrass leaves spent at a particular bending angle, and applied a time weight to the l_p calculations in order to estimate an l_p over a 12-hour light cycle (see “Calculations”). For the high wave site, l_p was calculated for the 7 chosen representative leaf shapes (as described by bending angles). Similar to the high current site, the fraction of time that seagrass leaves spent

in each of these shapes was also calculated, which was applied as a time weight to the l_p calculations in order to calculate an appropriate l_p over a 12-hour light cycle (see “Calculations”).

Calculations of Biomass and l_p

Shoot specific leaf area (L_s) was calculated as the sum of the secondary and tertiary one-sided area (width (m) x length (m)), noting that leaf length was measured from the top of the sheath to the tip of the leaf; i.e. sheath was not included in the leaf length measurements. L_s was multiplied by the shoot density to determine the leaf area index (L) for the canopy (m^2 leaf m^{-2} seabed).

$$L = L_s * \text{shoot density} \quad (1)$$

Note that in this particular situation L is an underestimation of the total leaf area in a seagrass canopy as it does not include primary (usually short and pale), quaternary (usually covered by epiphytes and senescent), etc leaves of *Zostera marina* shoots, but it does include the most photosynthetically active leaf tissue.

The water column that the seagrass canopy occupied from the sheath to the leaf tip when the longest leaf was exactly perpendicular to the sediment (H_c) was divided into 100 segments (z_n). As a seagrass leaf bends over, fewer z are occupied by seagrass, but there is more seagrass biomass within each occupied z . The relative biomass [$B(z)$] (dimensionless) of the seagrass canopy was distributed vertically throughout the water column that could potentially be occupied by seagrass as a sigmoid function such that:

$$B(z) = \frac{\psi}{\left(1 + \left[\frac{h(z)}{I}\right]^s\right)} \quad (2)$$

where ψ is the percentage of biomass at the base of the canopy,
defined as where the leaves emerge from the sheath (%)

$h(z)$ is the height above the sheath (m)

I is the intermediate point of the canopy when the canopy is
occupying a particular percent of the water column (m)

s is the shape factor, defined as 3.43 for this study based on
Zimmerman (2003).

Leaf area index (L) was then distributed throughout the water column that
could potentially be occupied by a seagrass canopy as a function of the relative
amount of biomass $[B(z)]$; $l(z)$ represents the leaf area index at a height z above the
sheath ($\text{m}^2 \text{ leaf m}^{-2} \text{ seabed}$):

$$l(z) = L * B(z) \quad (3)$$

The leaf area index was adjusted for the orientation and shape of the leaf due to the
local hydrodynamic conditions, and the resulting nadir bending angle (β) (radians)
such that $l_p(z)$ was the horizontally projected leaf area (l_p) at each z :

$$l_p(z) = l(z) * \sin \beta \quad (4)$$

$L_p(z)$ ($\text{m}^2 \text{ leaf m}^{-2} \text{ seabed}$) was then summed over the canopy height (z) in order to
achieve a vertically integrated l_p ($\text{m}^2 \text{ leaf m}^{-2} \text{ seabed}$):

$$l_p = \sum_1^z l_p(z) \quad (5)$$

Finally, for the sites that had multiple shapes associated with their movement, (high current and high wave sites) l_p for each shape was multiplied by its appropriate time weight. These time weighted l_p were then summed to achieve l_p over a 12-hour light cycle [$l_p(12)$] (m^2 leaf m^{-2} seabed):

$$l_p(12) = \sum_1^n \left[(tw_1 * (l_p)_1) \dots (tw_n * (l_p)_n) \right] \quad (6)$$

Where n = shape number

tw = time weight

Additionally, an epiphyte factor was determined. Epiphytic coverage at the three field sites was dominated by the polychaete *Spirorbis spirorbis*, grazing snails, and colonial tunicates of the genus *Botrylloides*. Shoots were collected from 5 patches at each of our three sites; secondary and tertiary leaves were photographed and analyzed for area covered by epiphytes using the software ImageJ (NIH). This analysis was achieved by increasing the contrast of the image such that the leaves became black, and the epiphytes became white, allowing the program to calculate the area of each white section. The areas were summed to achieve total area covered by epiphytes (EA). This area was then used to calculate an epiphyte factor (EF) such that:

$$EF = \left(\frac{EA}{l_p} \right) * 100 \quad (7)$$

Similarly, a self-shading factor was established. In order to determine the degree of self-shading, the average distance between seagrass shoots was calculated based on field shoot density data. The average distance between shoots, leaf length, and bending angle could be used to calculate the shaded l_p (m^2 leaf m^{-2} seabed) (Illustration 2.2). This shaded l_p was related to the total l_p , such that a self-shading factor (SSF) was established:

$$SSF = \left(\frac{l_p - shaded(l_p)}{l_p} \right) * 100 \quad (8)$$

For the sites that had multiple shapes associated with their movement, (high current and high wave sites) a SSF for each shape was multiplied by its appropriate time weight. These time weighted SSF were then summed to achieve SSF over a 12-hour light cycle [SSF(12)] (m^2 leaf m^{-2} seabed):

$$SSF(12) = \sum_1^n [(tw_1 * (SSF)_1).....(tw_n * (SSF)_n)] \quad (9)$$

Where n = shape number

tw = time weight

Finally, these factors [EF, SSF(12)] could be applied to $l_p(12)$ by reducing the potential amount of tissue oriented toward downwelling light by the percent of leaf tissue that epiphytes occupied and by the percent of the canopy that was potentially self-shade.

Bio-optical Properties of the Seagrasses

At 5 replicate patches, 5 – 10 *Zostera marina* shoots were collected for yield ($\mu\text{mol electrons m}^{-2} \text{ s}^{-1}$) measurements using a diving pulse amplitude modulated (PAM) fluorometer (Walz, Germany), and analysis of leaf absorbance and reflectance. Due to the extreme motion present at the high wave site, the diving PAM fluorometer would not work *in situ*. Therefore, collected *Z. marina* shoots were brought onto the boat where they were placed in ambient water and dark-adapted in the middle of the tertiary leaf for a minimum of 20 minutes. After dark adaptation was complete, yield was measured over 9 light levels between 0 and 1000 ($\mu\text{mol photons m}^{-2} \text{ s}^{-1}$).

Absorbance [$D(\lambda)$] and reflectance [$R(\lambda)$] of the tertiary leaf of *Z. marina* were processed at Old Dominion University in Norfolk, VA using an integrating sphere (60mmDIA.) in a Recording Spectrophotometer (UV-2401PC, Shimadzu) (350 to 800 nm). The absorbance [$D(\lambda)$] was used to calculate the absorbance [$A(\lambda)$] and was corrected for reflectance [$R(\lambda)$] and non-photosynthetic absorbance from 720 to 800 nm (Cummings and Zimmerman 2003), such that:

$$A(\lambda) = [1 - 10^{-D(\lambda)}] - R(\lambda) - \text{Average } A(800 - 720) \quad (10)$$

Average photosynthetic absorbance from 700 to 400 nm was used to calculate leaf absorbance ($A_L(\lambda)$), such that:

$$A_L(\lambda) = \text{Average } A(700 - 400) \quad (11)$$

Flow Tank Experiment

In order to address if water flow induced changes in *Zostera marina* are an acclimation or an adaptation, a “common garden” experiment was conducted. *Z.*

marina shoots from the 3 study sites in Long Island Sound were collected on April 1st, 2008 and grown for 2.5 months in 6 outdoor flow tanks (3.0 m L X 0.7 m W X 0.6 m D) located at Horn Point Laboratory, Cambridge, MD. Salinities between 28 and 30 were obtained by mixing Choptank River water and sea salts (Crystal Sea Marine Mix), and the temperature throughout the experiment ranged from 8.8 °C in April to 35.1 °C in June.

Each of the 6 flow tanks were split down the middle with a divider (Illustration 2.3) such that water circulated in a race track fashion at a current speed of $9 \text{ cm s}^{-1} \pm 2 \text{ cm s}^{-1}$, which was achieved with a 2 pound thrust Sevylor trolling motor. Two trays were placed on each side of the divider, such that there were 4 trays per flow tank (Illustration 2.3) achieving a total of 24 trays. All trays contained sediment dominated by fine sand that had an organic content of 0.52% collected from Chincoteague Bay; a location where *Z. marina* is naturally occurring, and therefore the sediment is suitable for seagrass growth. The first tray on each side was filled with only sediment in order to homogenize the water flow before it reached the second tray where *Z. marina* was planted at a density of 6 shoots tray⁻¹ (Illustration 2.3). Each of the three sites was randomly assigned 4 replicate trays; the 6 *Z. marina* shoots from each tray were considered sub-replicates while the tray itself was considered a true replicate.

Yield was measured as described previously at weeks 1, 3, 5, 7, and 9 in order to understand how *Z. marina* was acclimating to its new light levels and environment. Furthermore, to ensure that the plants did not become nutrient limited, a water change was done every two weeks for the duration of the experiment. Two-thirds of the

water was replaced with Choptank River water mixed with sea salts to bring the salinity between 28 and 30.

Statistical Analysis

The statistical program SAS (9.1) was used to run all statistical analyses. Data that were not normally distributed were transformed with a natural log, which achieved normality for all skewed data. One-way ANOVA was performed on field data (significant difference defined as $p < 0.05$) with a Tukey's Test for comparison of treatment means. Regression analysis was performed on data that related light levels and hydrodynamic conditions as well as wave height and water depth in order to test for significant relationships. Two-way ANOVA was performed on data collected from the flow tank experiment as the variable of time was introduced. If no significant interaction was present, the effects of time and site were analyzed separately using one-way ANOVA and a Tukey's Test.

For the l_p calculations, statistical analysis was not possible, but instead a range of possibility for l_p was defined. This range of possibility was established by assuming that all plants were bent at the average minimum angle measured to establish a minimum l_p and by assuming that all plants were bent at the average maximum angle measured to establish a maximum l_p . Therefore, overlap between sites based on minimum or maximum l_p the canopy may achieve could be compared.

Results

Hydrodynamic conditions varied between sites, and as a result, *Zostera marina* leaves moved differently through space and time, resulting in different light availability to *Z. marina* leaves exposed to currents, waves, or a lack thereof.

Hydrodynamics

The high wave site experienced larger waves than the quiescent and high current sites. Over a 5 day period in July 2007, significant wave height (H_s) at the high wave site ranged from 0.15 to 0.37 m with an average of 0.24 m, whereas H_s at the quiescent and high current sites ranged from 0.078 to 0.19 m and 0.09 to 0.19 m with an average wave height of 0.10 and 0.12 m, respectively (Figure 2.2). Wind was dominantly from the south-southwest and was between 0 and 10 knots. Wave period at the high wave site was 8.3 seconds, while it was 3.1 and 2.7 seconds at the quiescent and high current sites, respectively (Table 2.1).

Using the equations developed by Infantes et al. 2009, maximum near-bottom orbital velocity (U_b) at the high wave site was 1.21 m s^{-1} , whereas U_b at the quiescent and high current sites was 0.11 and 0.10 m s^{-1} , respectively (Table 2.1); a full magnitude slower. Lastly, the tidal signal present in the significant wave height (Figure 2.2) was significantly related to water depth (regression analysis, $p < 0.0001$), such that when the tide was low, the wave height was reduced, and when the tide was high, the wave height increased. Therefore, the waves were shoaling at low tide, which reduced the energy associated with the wave.

The quiescent and high wave sites, which had consistent current profiles over depth, both experienced an average current speed of 6 cm s^{-1} (Figure 2.3). The high

current site was more tidally influenced than the other two sites. During slack water, the vertical current speed profile was consistent over depth (unvegetated area) and averaged 6 cm s^{-1} . During the beginning of the flood phase of a neap tide, the average current speed over depth was 8 cm s^{-1} with a maximum current speed of 16 cm s^{-1} occurring 130 cm above the bottom. Additionally, the vertical profile started to show the influence of the benthic boundary layer and/or the presence of seagrasses nearby as seen by the slower current speeds near the bottom. As the tide continued to flood, speed began to increase and at the intermediate phase of the flood the average current speed over the water column was 17 cm s^{-1} with a maximum current speed of 25 cm s^{-1} occurring 160 cm above the bottom. When the current speed was at its maximum, the average current speed over depth was 22 cm s^{-1} with a maximum of 38 cm s^{-1} occurring 150 cm above the bottom. From this point on, when bending angle or l_p are referred to in respect to current speed, the maximum, not average, current speed will be referenced.

Light: Downwelling vs. Diffusive

The average cosine for downwelling irradiance ($\overline{\mu_d}$) at the quiescent site was 0.68 with a maximum of 0.74 occurring 1.0 m below the surface. The high current site had an average $\overline{\mu_d}$ of 0.71 with values above 0.80 occurring at the surface and a depth of 1.5 m below the surface. The high wave site had an average $\overline{\mu_d}$ of 0.86 with a maximum of 0.96 occurring 1.5 m below the surface (Figure 2.4). As $\overline{\mu_d}$ represents the angular structure of the downwelling irradiance field, the quiescent site appears to be the most diffusive with an average angle of 47° from the vertical, while

the high current site is intermediate with an average angle of 45° from the vertical, and the high wave site is the least diffusive with an average angle of 30° from the vertical.

Light vs. Turbidity

At the quiescent site, K_d ranged between 0.6 and 1.0 m^{-1} when measured between 13:30 and 16:00 in July 2008 (Figure 2.5). At the high wave site, K_d ranged between 0.4 and 0.8 when measured between 10:30 and 12:30 in July 2008 (Figure 2.6 A). The variation in K_d did not fluctuate with significant wave height, as a regression analysis demonstrated a non-significant linear relationship between significant wave height and K_d ($p=0.5132$, Table 2.2) (Figure 2.6 B).

At the high current site, K_d ranged between 0.6 and 0.8 m^{-1} (Figure 2.7 A). The variation in K_d fluctuated with current speed, as a regression analysis demonstrated a significant positive linear relationship between current speed and K_d ($p=0.0006$, $R^2=0.6059$, Table 2.2) such that as current speed increased by 10 cm s^{-1} , K_d increased by 0.02 m^{-1} (Figure 2.7 B)

Seagrass Morphology

Zostera marina leaves from the high current site were longer and wider than leaves from the quiescent and high wave site. *Z. marina* from the high wave site had a higher shoot density than seagrasses from the quiescent and high current site. These morphological variations result in varying leaf area indices between sites, which were calculated based on secondary and tertiary leaf morphology and shoot density. The quiescent site had a leaf area index (LAI) of 1.1 $\text{m}^2 \text{ leaf m}^{-2} \text{ seabed}$, the high current site had a LAI of 4.0 $\text{m}^2 \text{ leaf m}^{-2} \text{ seabed}$, and the high wave site had a LAI of

2.5 m² leaf m⁻² seabed (Table 2.1). For more detail about leaf morphology, see section entitled “Chapter 1: Results”.

Zostera marina leaves from the quiescent site had significantly higher carbon content (35.4%) ($p=0.0083$, Table 2.3) than plants from the high current site (33.4%) but not the high wave site (34.1%). Additionally, *Z. marina* from the quiescent site had significantly higher (less negative) ($p=0.0006$, Table 2.3) $\delta^{13}\text{C}$ than plants from both the high current and high waves sites (Figure 2.8). *Z. marina* from the quiescent site had significantly lower percent N (0.99%) ($p=0.0232$, Table 2.3) than plants from the high wave site (1.16%) but not the high current site (1.08%); similarly, *Z. marina* from the quiescent site had significantly higher ($p=0.0155$, Table 2.3) $\delta^{15}\text{N}$ than plants from the high wave site but not the high current site (Figure 2.9).

Video Analysis

Zostera marina leaves from the quiescent site were found to bend lightly (7.2°) near the bottom (lower 25.1 cm of the leaf), while the tip (top 5.5 cm of the leaf) was bent further (26.6°) (Figure 2.10). *Z. marina* leaves from the high current site, which were quite long (>1m), were classified into four shapes based on the current speed affecting the leaf orientation. When the current was 6 cm s⁻¹, the bottom 58.0 cm of the leaves were bent at 4.4° and the top 46.0 cm were bent at 16.1°. The seagrass canopy spent 33% of its time in this position. When the current speed was 16 cm s⁻¹, the bottom 50.5 cm of the leaves were bent at 18.3° and the top 53.5 cm was bent at 36.1°; the seagrass canopy was in this position 33% of the time. When the current speed was 25 cm s⁻¹, the bottom 35.6 cm was bent at 24.3°, the

middle 39.5 cm was bent at 45.2°, and the top 28.6 cm was bent at 80.1°; the seagrass canopy experienced this current speed 25% of the time. Lastly, when the current speed was 38 cm s⁻¹ the bottom 58.4 cm was bent at 64.0° and the top 45.7 cm was bent at 69.5°; however, the seagrass canopy only experienced this current speed 8.3% of the time (Figure 2.11).

The movement of *Zostera marina* exposed to waves was classified into seven shapes such that the plants motion through space and time could be accurately represented. The shapes that *Z. marina* spent most of its time in were “dancing upright”, “bent shoreward”, and “transition closed” (Figure 2.12) which it experienced 31.8, 27.6, and 16.2% of the time, respectively. The other four shapes, “almost flat open”, “completely flat”, “transition compressed”, and “almost flat closed”, were experienced 8.8, 7.6, 4.5, and 3.4% of the time, respectively (Figure 2.12).

Calculations of Biomass and I_p

For each site the biomass distribution of *Zostera marina* was highest just above the sheath and decreased in a sigmoid fashion away from the sheath toward the top of the canopy (Figure 2.13). As leaves at the quiescent site only occupied one position in time, only one form of vertical biomass distribution occurred (Figure 2.13 A). For the high current site, as current speed increased, and *Z. marina* was bent at a greater angle, the biomass occupied a smaller proportion of the water column (Figure 2.13 B). As was seen for both the quiescent and high current sites, the biomass distribution of the high wave site decreased from the sheath to the top of the canopy, with maximum biomass occurring just above the sheath. Similarly to the high current

site, when a phase of the wave caused *Z. marina* to be more bent over, the biomass occupied a smaller proportion of the water column (Figure 2.13 C). While the biomass distribution for the quiescent site did not change over time, biomass distributions fluctuated every few hours for the high current site and in a matter of seconds or fractions of a second at the high wave site.

At the quiescent site, $l_p(z)$ followed a similar pattern as the biomass distribution with decreasing $l_p(z)$ away from the sheath toward the top of the canopy as there was less biomass available to be horizontally projected (Figure 2.14 A). However, near the top of the canopy $l_p(z)$ suddenly increased again as a result of a steeper bending angle that the tips of *Z. marina* experienced. This sudden change in $l_p(z)$ also occurs for *Z. marina* at the high current and high wave sites each time measured angles change throughout the canopy and is a consequence of the mathematics.

At the high current site, when current speed increased over the tidal cycle, *Zostera marina* leaves were compressed into a smaller area thereby occupying fewer z , but the biomass that occupied each z increased. As a result, $l_p(z)$ increased with increasing current speed due to increasing bending angle (Figure 2.14 B). Similarly, at the high wave site, when *Z. marina* was more bent over and occupied less of the maximum canopy height (z) due to a particular wave phase, $l_p(z)$ increased but fewer z were occupied by *Z. marina* leaf tissue (Figure 2.14 C). When $l_p(z)$ is vertically integrated and a time weight is applied, $l_p(12)$ at the high current ($1.65 \text{ m}^2 \text{ leaf m}^{-2}$ seabed) and the high wave sites ($1.22 \text{ m}^2 \text{ leaf m}^{-2}$ seabed) is greater than at the quiescent site ($0.16 \text{ m}^2 \text{ leaf m}^{-2}$ seabed) (Figure 2.15).

Although *Zostera marina* from the high current and high wave site had more tissue oriented toward downwelling light, leaves from these two sites experienced a high degree of self-shading. At the quiescent site, the SSF was 1.89%, such that the area of tissue oriented toward downwelling light could be reduced by 1.89% as a result of shading by other leaves (Table 2.4). At the high current site, when *Z. marina* leaves were positioned in a more upright orientation, as they were when the current speed was at a maximum of 6 or 16 cm s⁻¹, the SSF was 97.26% and 97.32%, respectively. When *Z. marina* was positioned in a more horizontal orientation, as they were when the current speed was at a maximum of 25 or 38 cm s⁻¹, the SSF was 98.12% and 97.04%, respectively (Illustration 2.4, Table 2.4). At the high wave site, when a particular phase of the wave caused *Z. marina* to become more upright (but still bent at a slight angle), the SSF was between 90.20% and 95.90% (Table 2.4). Conversely, when a particular phase of the wave caused *Z. marina* to become more horizontally oriented, the SSF increased and was between 99.12% and 99.40% (Illustration 2.4) (Table 2.4). When these SSFs are integrated over time, the quiescent site has a very low SSF(12) of 1.89%, while the high current and high wave sites have large SSF(12)s of 97.47% and 94.78%, respectively (Table 2.4).

Although *Zostera marina* leaves from the high current and high wave sites had large SSFs, leaves of *Z. marina* from the quiescent site had a larger EF. At the quiescent site, the EF was 21.48%, while the high current and high wave sites had an EF of 0.68% and 0.00% respectively, as leaves from the high wave site had no epiphytes (Table 2.4). When the SSF and the EF are applied to $I_p(12)$, the area of tissue oriented toward downwelling light is greatly reduced by self-shading at the

high current and high wave sites, and is reduced slightly by epiphytes at the quiescent site (Figure 2.16).

Lastly, a range of possibility was defined for each site. A maximum and minimum $l_p(12)$ that *Z. marina* from each site could experience was calculated based on the replicate video that resulted in the largest and smallest angle, respectively. It was found that the minimum $l_p(12)$ for the quiescent site was $0.077 \text{ m}^2 \text{ leaf m}^{-2}$ seabed, whereas the maximum $l_p(12)$ for the high current and high wave sites were 0.059 m^2 and $0.078 \text{ m}^2 \text{ leaf m}^{-2}$ seabed, respectively (Figure 2.17).

Bio-optical Properties

Zostera marina leaves from the high wave site had significantly higher photosynthetic leaf absorbance than *Z. marina* leaves from the quiescent and high current sites ($p=0.0104$, Table 2.3) (Figure 2.18). The average photosynthetic leaf absorbance of leaves from the high wave site from wavelength 400 to 700 nm was 0.62; it was found to be 0.59 for leaves from the high current site and 0.54 for leaves from the quiescent site.

Zostera marina leaves from the quiescent site had significantly higher photosynthetic yields than *Z. marina* leaves from high current and high wave sites when PAR was 113 or greater ($p<0.05$, Table 2.5 A). Furthermore, *Z. marina* leaves from the quiescent site had significantly higher yields than the high wave site, which had significantly higher yields than the high current site when PAR was greater than or equal to 601 ($p<0.0001$, Table 2.5 A) (Figure 2.19).

Flow Tank Experiment

When *Zostera marina* from each site was planted into flow tanks and exposed to similar current speed and sediment type, plants from each site were found to photosynthesize similarly as yield of *Z. marina* leaves from each site were not significantly different from one another on a bi-weekly basis throughout the course of the experiment ($p>0.05$, Table 2.5 B). For the sake of space, only weeks 3 and 5 are shown in Figure 2.20 and are representative of the entire data set. Although significant differences between sites were not observed, there were significant differences over time, ($p<0.002$, Table 2.5 B) as yield measurements also depend upon ambient light conditions, and as cloud cover changed on a daily to weekly basis, yield measurements measured *in situ* on a biweekly basis also varied (Figure 2.20), yet leaves from each field site had similar photosynthetic capacity under the same environmental conditions.

Discussion

Our results indicate that *Zostera marina* exposed to currents and waves have a much higher self-shading index than do *Z. marina* inhabiting a quiescent environment. Consequently, *Z. marina* from the quiescent site acclimated to higher irradiances and had a higher photosynthetic yield than *Z. marina* from the high current and high wave sites. Hence, observed differences in photosynthetic capability measured *in situ* are a result of differences in morphology and local hydrodynamic conditions that cause different leaf motion and therefore orientation to downwelling irradiance and light availability. Yet, despite reduced light availability, *Z. marina*

exposed to waves and currents are less carbon and nitrogen limited than *Z. marina* exposed to quiescent conditions due to the benefits associated with water flow such as reduced diffusive boundary layer thickness (Koch 1994) and increased flux of dissolved and particulate matter (Huettel et al. 1996, Koch and Huettel 2000, Huettel et al. 2003, Huettel and Rusch 2003, Wilson et al. 2008). Additionally, leaves that experience low light levels such as those exposed to high currents and waves have a lower carbon demand (Grice et al. 1996). Therefore, seagrasses that inhabit areas with hydrodynamically active conditions have different habitat and morphological requirements than seagrasses in quiescent conditions.

Hydrodynamics and Light Availability

The self-thinning hypothesis proposed by Marbà and Duarte (2003) for seagrasses only applied at the quiescent site as the average distance between shoots of *Zostera marina* located there was almost exactly equal to the length component of l_p , such that there was essentially no self-shading due to an optimized shoot density. However, due to the high degree of self-shading observed when *Z. marina* was exposed to currents or waves, our results suggest that the self-thinning hypothesis does not apply in hydrodynamically influenced environments, and that seagrass beds exposed to currents or waves do not have a shoot density that optimizes light availability. Fonseca et al. (2007) also concluded that water motion, not the ability of a canopy to capture light, was the dominant mechanism for shoot arrangement. Therefore physical parameters, while increasing self-shading, may be driving seagrass shoot density.

The long and wide leaves and high shoot density of *Zostera marina* at the high current and high wave sites, respectively, may be necessary morphological variations to ensure survival under a dynamic environment at the expense of reduced light availability. The same trade-off was demonstrated for the alga *Pachydictyon coriaceum*, such that the wave-exposed morphology had lower biomass-specific net production presumably because the compact shape and densely-bladed morphotype, which made it tolerant to wave action, shaded the internal blades thus reducing light availability (Haring and Carpenter 2007).

In our study we calculated the amount of tissue available to capture downwelling light, when in fact, light in the marine environment is quite diffuse. Therefore, we could have potentially underestimated light availability on a canopy level. Tissue that was not horizontally projected could have been receiving light that was coming from some angle as light becomes scattered as it travels through the water column. At our particular study sites, light was dominantly downwelling, and having tissue available to capture this light is of high importance for *Zostera marina* located off Fisher's Island, NY in Long Island Sound. However, not all seagrass beds are located in areas where downwelling light dominates, and therefore our results could have different implications on a regional basis. However, Zimmerman (2003) did correct I_p for the scattering of light by correcting for angular distribution of downwelling irradiance in his model. He used this corrected I_p to calculate the daily integrated biomass-specific photosynthesis of a seagrass canopy over varying canopy architecture (bending angles) (Zimmerman 2003). Despite the differences between our two studies, we came to a similar conclusion: bending leaves reduce the amount

of light available to a seagrass canopy, which reduces photosynthetic capacity, and that this reduction is greater in denser beds.

Other studies have also found that photosynthetic communities that are bent experience self-shading, which causes reduced light availability (Binzer and Sand-Jensen 2002, Zimmerman 2003, Abdelrhman 2007, Fonseca et al. 2007) and lowered photosynthetic capacity (Binzer and Sand-Jensen 2002, Zimmerman 2003). Binzer and Sand-Jensen (2002) found horizontal communities of algae received an uneven distribution of light due to high degrees of self-shading and were found to saturate at lower irradiances, as was seen for *Z. marina* located at the high current and high wave sites. Additionally, Abdelrhman (2007) demonstrated that when leaves of *Z. marina* become more bent over with increasing current velocity, leaves act as physical barriers to leaves below them, thereby greatly reducing light availability within the canopy.

The extent to which self-shading occurred when *Zostera marina* leaves were exposed to currents and waves in our study differed, such that leaves exposed to currents experienced more self-shading than leaves exposed to waves. The continual opening and closing of the canopy that occurred at the high wave site seems to result in increased light availability when compared to seagrasses exposed to currents. Hence, our results support the hypothesis suggested by Koch and Gust (1999) that seagrasses exposed to waves, which cause the leaves to sway back and forth thereby “opening and closing” the canopy (Koch and Gust 1999), may be benefiting from the small time scale the canopy is open (“dancing upright” and “almost flat open”, which occurs multiple times a minute.

Our results demonstrate that a more vertical orientation is beneficial because light is available to a larger proportion of a seagrass leaf (reduced self-shading), thereby increasing the total area of photosynthetic tissue exposed to downwelling light and net production. When leaves of *Zostera marina* exposed to waves and currents were in a more upright position, that being a position more similar to *Z. marina* from the quiescent site, they may resemble a vertical community for a given time interval. More vertically oriented communities have higher production rates (Binzer and Sand-Jensen 2002, Zimmerman 2003) indicating that a vertical orientation of *Z. marina* located at the quiescent site, during slack water at the high current site, and during a wave phase that causes an upright position at the high wave site, is of the utmost importance for capturing light, just as Zimmerman (2003) found that the optimum bending angle to maximize light availability and production was between 10° and 20° in his bio-optical model. Indeed, this is why trees in a forest grow tall, as they can avoid self-shading and pack more biomass into an area, by growing taller than a neighboring tree (Holbrook and Putz 1989).

Broadening our attention from the leaves to the entire seagrass meadow, the architecture of the canopy that results from local hydrodynamic conditions, which determines how much of the canopy is exposed to downwelling light, has been demonstrated to affect light utilization. When light is evenly distributed due to an upright position, photosynthetic communities have a near linear response to increasing irradiance (Binzer and Sand-Jensen 2002). However, when light is unevenly distributed due to a more horizontal position, photosynthetic communities benefit more from increased irradiance as there are more photons available to be

transmitted throughout the canopy (Binzer and Sand-Jensen 2002). Therefore, seagrass beds exposed to currents and waves may require good water quality and high light irradiances such that more photons can be transmitted throughout the dense canopy making light available to previously shaded leaves.

Moreover, seagrasses photosynthetically acclimate to self-shading conditions that reduce light availability to photosynthetic tissue. For example, *Zostera marina* leaves from both the high current and high wave sites experienced reduced light availability due to increased self-shading, and were both found to have lower photosynthetic yields than *Z. marina* leaves from the quiescent site, suggesting that they were more light-limited. A lower yield would benefit *Z. marina* exposed to currents and waves as it would reduce the photon demand necessary to achieve photosynthetic saturation in a canopy characterized by reduced light availability. Therefore, our results demonstrate the interaction between water flow, leaf motion, and light availability, and that as water flow and leaf motion increase, light availability and photosynthetic yield decrease.

Lastly, water flow does not only affect the angle at which seagrass leaves bend, but can also potentially affect water turbidity as was seen in our field measurements. Since seagrasses exposed to currents or waves experience a high degree of self-shading, and may also experience increased turbidity resulting in brief periods of reduced light levels, it follows that seagrasses found in high water flow environments may be at more risk with eutrophication and decreased water quality than seagrasses found in quiescent waters.

Hydrodynamics, Epiphytes, and Nutrient Uptake

While leaf bending and self-shading play a major role in the amount of light that is available for seagrasses exposed to current and waves, epiphytes under these dynamic conditions may only play a minor role. As leaves move back and forth with water flow, epiphytes are removed, potentially increasing light availability several-fold due to the reduced leaf area occupied by epiphytes (Lavery et al. 2007). In contrast, seagrass leaves exposed to weak currents and waves, such as our quiescent site, tend to have more epiphytes (Lavery et al. 2007). As a result, epiphytes could potentially play a major role in light availability to seagrasses located in quiescent water, while leaf bending and self-shading may only play a minor role due to the average distance between shoots that optimizes light availability.

It is important to remember that *Zostera marina* located at each field site was healthy and thriving; there was no sign of stress or diebacks, and each year the extent of the seagrass bed was unchanged (Chris Pickerell, pers. com.). Indeed, *Z. marina* from the quiescent site was found to have a larger area of photosynthetic tissue exposed to downwelling light and a higher photosynthetic capacity, yet seagrasses from the quiescent site had a different suite of challenges to overcome. For example, although the tissue carbon content for *Z. marina* from the quiescent site was within the normal range of carbon content (28% - 43% with an average around 36%) for this species (Duarte 1990), leaves from the quiescent site were more carbon limited than leaves from the high current and high wave site, as demonstrated by the isotopically heavier $\delta^{13}\text{C}$ signatures.

It is well understood that the inherent carbon limitation of seagrasses (Beer 1989, Beer and Koch 1996, Zimmerman et al. 1997, Invers et al. 2001, Palacios and Zimmerman 2007) can be reduced by water flow as the production of seagrasses increases with increasing current velocity due to a reduction in the leaf diffusive boundary layer (DBL) and an increased flux of CO₂ and nutrients (Koehl and Alberte 1988, Koch 1994, Koch and Beer 1996). The high availability of carbon to *Z. marina* from the high current and high wave sites could also potentially explain why *Z. marina* from the high current site was so long and wide and why *Z. marina* from the high wave site was so dense.

Zostera marina from the quiescent site was also more nitrogen limited, as demonstrated by the isotopically heavier $\delta^{15}\text{N}$ signatures, than plants from the high current (not significantly) and high wave site (significantly), as the uptake of nutrients (specifically ammonia) is dependent on water flow (Thomas et al. 2000, Thomas and Cornelisen 2003, Cornelisen and Thomas 2004, Barr et al. 2008, Morris et al. 2008), and is greater in oscillatory flow when compared to unidirectional flow (Koch and Gust 1999, Thomas and Cornelisen 2003). The nitrogen content of *Z. marina* from the quiescent site was below the normal range of nitrogen content (1.2% to over 5% with an average of 2.6%) for *Z. marina* (Duarte 1990) and therefore may be limiting. The leaf nitrogen content for *Z. marina* from the high current and high wave sites was just below or at, respectively, the observed range for saturating percent nitrogen (Duarte 1990), demonstrating that although seagrass from the high current and high wave sites were potentially less limited by the uptake of nitrogen than *Z. marina* from the quiescent site, nutrient content may have been limiting productivity.

Zostera marina from the quiescent site was found to be more carbon and nitrogen limited when compared to *Z. marina* exposed to currents or waves. However, according to Liebig's Law, only the scarcest constituent can limit growth. Since there is no luxury uptake of carbon, but can exist for nitrogen, carbon is potentially more limiting than nitrogen for seagrasses exposed to quiescent conditions. Additionally, seagrasses that experience high irradiance and therefore have higher productivity, as was observed for *Z. marina* at the quiescent site, tend to be more carbon limited because high productivity rates increase the carbon demand (Grice et al. 1996). Therefore, while carbon, not light availability, may be limiting productivity of seagrasses exposed to quiescent conditions, under active current and wave conditions, this limitation may be eased.

Zostera marina from the quiescent site may have also experienced a reduction in the uptake of carbon and nitrogen due to a reduced area available for nutrient delivery as a result of the high abundance of epiphytes on the leaves of *Z. marina* located at this field site (Cornelisen and Thomas 2004). A negative relationship between epiphyte colonization and ammonium uptake has been demonstrated for seagrass leaves and that uptake was reduced proportional to the amount of space that epiphytes occupied (Cornelisen and Thomas 2004).

Lastly, a lack of leaf movement could also limit mixing and therefore nutrient availability to *Zostera marina* located at the quiescent site. The synchronized movements of seagrass leaves, termed "monami" by Ackerman and Okubo (1993), has been shown to increase shear stress and turbulence at the water-canopy interface, thereby promoting mixing (Gambi et al. 1990, Grizzle et al. 1996, Koch and Gust

1999, Ghisalberti and Nepf 2002, Hendriks et al. 2008, Widdows et al. 2008), while the further swaying and flapping of seagrass leaves exposed to currents and waves “opens and closes” the canopy for periods of seconds to hours (Koch and Gust 1999) promoting turbulent mixing within the canopy (Grizzle et al. 1996). As turbulent mixing has been shown to play a key role in nutrient uptake rates in denser vegetation (Morris et al. 2008), it follows that a lack of leaf movement could limit mixing and therefore nutrient availability to *Z. marina* from the quiescent site.

Conclusions

Hydrodynamic conditions in seagrass habitats bring both advantages and disadvantages; however, seagrasses may have the ability to acclimate to the challenges established by varying hydrodynamic conditions in order to reduce the associated detriments. For seagrass communities found in low water flow environments with high levels of downwelling irradiance, light availability may be high, yet the uptake of DIC and DIN may be limited by a thick diffusive boundary layer, epiphyte colonization, and reduced mixing between inter- and above- canopy water masses. Conversely, seagrass communities found in high water flow environments may experience a high degree of self-shading resulting in reduced light availability, yet the uptake of DIC and DIN may be promoted via reduced boundary layer thickness and epiphytic loading. Despite experiencing reduced light availability as a result of extensive self-shading, seagrass communities in high water flow environments were found to cope with this disadvantage by acclimating photosynthetically to flow-induced light conditions, thereby potentially decreasing

photon demand. Hence, the benefits, detriments, and acclimations associated with these hydrodynamic conditions can be useful when managing seagrass communities. Seagrasses found in low-water flow environments may be vulnerable to carbon limitation and less productive in low nutrient environments than seagrasses exposed to currents or waves. Since modern tendencies are to increase CO₂ levels in shallow waters (Beer and Koch 1996, Zimmerman et al. 1997, Palacios and Zimmerman 2007) and nutrient levels in coastal waters (Burkholder et al. 2007), the largest threat to seagrasses growing in quiescent waters comes from epiphytic growth. In contrast, due to the high degree of self-shading experienced by seagrasses found in high water flow environments, they may be more vulnerable to low light levels associated with eutrophication and poor water quality than CO₂ limitation and/or epiphytic growth. These trade-offs suggest that seagrass habitat requirements may need to take hydrodynamic conditions into consideration when protecting and restoring these plant communities.

Bibliography

- Abdelrhman, M.A. 2007. Modeling coupling between eelgrass *Zostera marina* and water flow. *Marine Ecology Progress Series* 228: 81 – 96.
- Ackerman, J.D., and A. Okubo. 1993. Reduced mixing in a marine macrophyte canopy. *Functional Ecology* 7: 305 – 309.
- Barr, G.N., A. Kloeppel, T.A.V. Rees, C. Scherer, R.B. Taylor, and A. Wenzel. 2008. Wave surge increases rates of growth and nutrient uptake in the green seaweed *Ulva pertusa* maintained at low bulk flow velocities. *Aquatic Biology* 3: 179 – 186.
- Beer, S. 1989. Photosynthesis and photorespiration of marine angiosperms. *Aquatic Botany* 34: 153 – 166.
- Beer, S., and E. Koch. 1996. Photosynthesis of marine macroalgae and seagrasses in globally changing CO₂ environments. *Marine Ecology Progress Series*: 199 – 204.
- Binzer, T., and K. Sand-Jensen. 2002. Production in aquatic macrophyte communities: A theoretical and empirical study of the influence of spatial light distribution.
- Bouma, T.J., M.B De Vries, E. Low, G. Peralta, I.C. Tanczos, J. van de Koppel, and P.M.J. Herman. 2005. Trade-offs related to ecosystem engineering: A case study on stiffness of emerging macrophytes. *Ecology* 86: 2187 – 2199.
- Brown, E., A. Colling, D. Park, J. Phillips, D. Rothery, and J. Wright. 1999. *Wave, Tides, and Shallow-Water Processes*, 2nd Edition. Butterworth-Heinemann in association with The Open University, Oxford. Pp 11 – 49.
- Burkholder, J.M., D.A. Tomasko, and B.W. Touchette. 2007. Seagrass and eutrophication. *Journal of Experimental Marine Biology and Ecology* 350: 46 – 72.
- Cornelisen, C.D., and F.I.M. Thomas. 2004. Ammonium and nitrate uptake by leaves of the seagrass *Thalassia testudinum*: impact of hydrodynamic regime and epiphyte cover on uptake rate. *Journal of Marine Systems* 49: 177 – 194.
- Cummings, M.E. and Zimmerman, R.C. 2003. Light harvesting and the package effect in the seagrasses *Thalassia testudinum* Banks ex König and *Zostera marina* L.: optical constraints on photoacclimation. *Aquatic Botany* 75: 261 – 274.
- Denman, K.L. 1975. Spectral analysis: A summary of the theory and techniques. Fisheries and Marine Service, Technical Report N. 539.
- Dennison, W.C. and R.S. Alberte. 1982. Photosynthetic responses of *Zostera marina* L. (Eelgrass) to *in situ* manipulations of light intensity. *Oecologia (Berl)* 55: 137 – 144.
- Duarte, C.M. 1990. Seagrass nutrient content. *Marine Ecology Progress Series* 67: 201 – 207.
- Duarte, C.M. and H. Kirkman. 2003. Methods for the measurement of seagrass abundance and depth distribution. In: Short, F.T. and R.G. Coles (eds.), *Global Seagrass Research Methods*, Elsevier Science, Amsterdam. Pp 141 – 153.

- Fonseca, M.S., J.S. Fisher, J.C. Zieman, and G.W. Thayer. 1982. Influence of the seagrass, *Zostera marina* L., on current flow. *Coastal and Shelf Science* 15: 351 – 364.
- Fonseca, M.S., Zieman, J.C., G.W. Thayer, and J.S. Fisher. 1983. The role of current velocity in structuring eelgrass (*Zostera marina* L.) meadows. *Estuarine and Coastal Shelf Sciences* 17: 367 – 380.
- Fonseca, M.S., and W.J. Kenworthy. 1987. Effects of current on photosynthesis and distribution of seagrasses. *Aquatic Botany* 27: 59 – 78.
- Fonseca, M.S., M.A.R. Koehl, and B.S. Kopp. 2007. Biomechanical factors contributing to self-organization in seagrass landscapes. *Journal of Experimental Marine Biology and Ecology* 340: 227 – 246.
- Gambi, M.C., A.R.M. Nowell, and P.A. Jumars. 1990. Flume observations on flow dynamics in *Zostera marina* (eelgrass) beds. *Marine Ecology Progress Series* 61: 159 – 169.
- Ghisalberti, M., and H.M. Nepf. 2002. Mixing layers and coherent structures in vegetated aquatic flows. *Journal of Geophysical Research* 107: C2, 3011.
- Grice, A.M., N.R. Loneragan, W.C. Dennison. 1996. Light intensity and the interactions between physiology, morphology and stable isotope ratios in five species of seagrass. *Journal of Experimental Marine Biology and Ecology* 195: 91 – 110.
- Grizzle, R.E., F.T. Short, C.R. Newell, H. Hoven, and L. Kindblom. 1996. Hydrodynamically induced synchronous waving of seagrasses: ‘monami’ and its possible effects on larval mussel settlement. *Journal of Experimental Marine Biology and Ecology* 206: 165 – 177.
- Harring, R.N. and R.C. Carpenter. 2007. Habitat-induced morphological variation influences photosynthesis and drag on the marine macroalga *Pachydictyon coriaceum*. *Marine Biology* 151: 243 – 255.
- Hendriks, I.E., T. Sintes, T.J. Bouma, C.M. Duarte. 2008. Experimental assessment and modeling evaluation of the effects of the seagrass *Posidonia oceanica* on flow and particle trapping. *Marine Ecology Progress Series* 356: 163 – 173.
- Højerslev, N. 1975. A spectral light absorption meter for measurement in the sea. *Limnology and Oceanography* 20: 1024 – 1034.
- Holbrook, N.M., and F.E. Putz. 1989. Influence of neighbors on tree form: effects of lateral shade and prevention of sway on the allometry of *Liquidambar styraciflua* (sweet gum). *American Journal of Botany* 76: 1740 – 1749.
- Huettel, M., W. Ziebis, and S. Forster. 1996. Flow-induced uptake of particulate matter in permeable sediments. *Limnology and Oceanography* 41: 309 – 322.
- Huettel, M. and A. Rusch. 2000. Transport and degradation of phytoplankton in permeable sediment. *Limnology and Oceanography* 45: 534 – 549.
- Huettel, M., H. Roy, E. Precht, and S. Ehrenhauss. 2003. Hydrodynamical impact on biogeochemical processes in aquatic sediments. *Hydrobiologia* 494: 231 – 236.
- Infantes, E., J. Terrados, A. Orfila, B. Canellas, and A. Alvarez-Ellacuria. 2009. Wave energy and the upper depth limit distribution of *Posidonia oceanica*. *Botanica Marina* 52: In Press.

- Invers, O., R.C. Zimmerman, R.S. Alberte, M. Perez, and J. Romero. 2001. Inorganic carbon sources for seagrass photosynthesis: an experimental evaluation of bicarbonate use in species inhabiting temperate waters. *Journal of Experimental Marine Biology and Ecology* 265: 203 – 217.
- Kirk, John T.O. 1983. *Light and photosynthesis in aquatic ecosystems*. Cambridge University Press, Cambridge, Great Britain.
- Koch, E.W. 1994. Hydrodynamics, diffusion-boundary layers and photosynthesis of the seagrasses *Thalassia testudinum* and *Cymodocea nodosa*. *Marine Biology* 118: 767 – 776.
- Koch, E.W. 2001. Beyond Light: Physical, geological, and geochemical parameters as possible submersed aquatic vegetation habitat requirements. *Estuaries* 24: 1 – 17.
- Koch, E.W., and S. Beer. 1996. Tides, light and the distribution of *Zostera marina* in Long Island Sound, USA. *Aquatic Botany* 53: 97 – 107.
- Koch, E.W., and G. Gust. 1999. Water flow in tide- and wave-dominated beds of the seagrass *Thalassia testudinum*. *Marine Ecology Progress Series* 184: 63 – 72.
- Koch, E.W., and M. Huettel. 2000. The impact of single seagrass shoots on solute fluxes between the water column and permeable sediments. *Biologia Marina Mediterranea* 7: 235 – 239.
- Koehl, M.A.R., and R.S. Alberte. 1988. Flow, flapping, and photosynthesis of *Nereocystis luetkeana*: a functional comparison of undulate and flat blade morphologies. *Marine Biology* 99: 435 – 444.
- Lavery, P.S., T. Reid, G.A. Hyndes, and B.R. van Elven. 2007. Effect of leaf movement on epiphytic algal biomass of seagrass leaves. *Marine Ecology Progress Series* 338: 97 – 106.
- Marbà, N., and C.M. Duarte. 2003. Scaling of ramet size and spacing in seagrasses: implication for stand development. *Aquatic Botany* 77: 87 – 98.
- Morris, E.P., G. Peralta, F.G. Brun, L. van Duren, T.J. Bouma, and J.L. Perez-Llorens. 2008. Interaction between hydrodynamics and seagrass canopy structure: Spatially explicit effects on ammonium uptake rates. *Limnology and Oceanography* 53: 1531 – 1539.
- Palacios, S.L. and R.C. Zimmerman. 2007. Response of eelgrass *Zostera marina* to CO₂ enrichment: possible impacts of climate change and potential for remediation of coastal habitats. *Marine Ecology Progress Series*: 344: 1 – 13.
- Peralta, G., J.L. Perez-Llorens, I. Hernandez, F. Brun, J.J. Vergara A. Bartual, J.A. Galvez, J., and C.M. Garcia. 2000. Morphological and physiological differences between two morphotypes of *Zostera noltii* Hornem. From the south-western Iberian Peninsula. *Helgoland Marine Research* 54: 80 – 86.
- Peralta, G., F.G. Brun, I. Hernandez, J.J. Vergara, and J.L. Perez-Llorens. 2005. Morphometric variations as acclimation mechanisms in *Zostera noltii* beds. *Estuarine, Coastal and Shelf Science* 64: 347 – 356.
- Schanz, A., and H. Asmus. 2003. Impact of hydrodynamics on development and morphology of intertidal seagrasses in the Wadden Sea. *Marine Ecology Progress Series* 261: 123 – 134.

- Thomas, F.I.M., C.D. Cornelisen, and J.M. Zande. 2000. Effects of water velocity and canopy morphology on ammonium uptake by seagrass communities. *Ecology* 81: 2704 – 2713.
- Thomas, F.I.M., and C.D. Cornelisen. 2003. Ammonium uptake by seagrass communities: effects of oscillatory versus unidirectional flow. *Marine Ecology Progress Series* 247: 51 – 57.
- Widdows, J., N.D. Pope, M.D. Brinsley, H. Asmus, and R.M. Asmus. 2008. Effects of seagrass beds (*Zostera noltii* and *Z. marina*) on near-bed hydrodynamics and sediment resuspension. *Marine Ecology Progress Series* 358: 125 – 136.
- Wilson, A.M., M. Huettel, S. Klein. 2008. Grain size and depositional environment as predictors of permeability in coastal marine sands. *Estuarine, Coastal and Shelf Science* 80: 193 – 199.
- Zimmerman, R.C. 2003. A biooptical model of irradiance distribution and photosynthesis in seagrass canopies. *Limnology and Oceanography* 48: 568 – 585.
- Zimmerman, R.C., D.G. Kohrs, D.L. Steller, and R.S. Alberte. 1997. Impacts of CO₂ enrichment of productivity and light requirements of eelgrass. *Plant Physiology* 115: 599 – 607.

Tables

Table 2.1. Summary of the average field conditions and *Z. marina* morphology \pm standard error from the quiescent, high current, and high wave sites off Fisher's Island, NY. Sites with different letters denote significant differences at $p < 0.05$.

Characteristic	Quiescent	High Current	High Wave
Water Depth (m)	1.8 ± 0.013	1.9 ± 0.013	2.0 ± 0.015
Average Significant Wave Height (m)	0.10 ± 0.0009	0.12 ± 0.0009	0.24 ± 0.0025
Wave Period (sec)	3.1 ± 0.14	2.7 ± 0.11	8.3 ± 0.06
U_b ($m\ s^{-1}$)	0.10 ± 0.003	0.11 ± 0.004	1.21 ± 0.016
Average Current Speed ($cm\ s^{-1}$)	6 ± 0.0017	6 ± 0.77 to 22 ± 8.78	6 ± 0.0054
Light Attenuation (m^{-1})	0.48 ± 0.14	0.47 ± 0.11	0.46 ± 0.10
Density (shoots m^{-2})	364 ± 41 (a)	363 ± 56 (a)	1205 ± 134 (b)
Tertiary Leaf Length (cm)	33 ± 1.2 (a)	104 ± 3.5 (b)	32 ± 1.8 (a)
Tertiary Leaf Width (mm)	5.2 ± 0.1 (a)	5.9 ± 0.2 (b)	3.7 ± 0.2 (c)
Leaf Area Index ($m^2\ leaf\ m^{-2}$)	1.1	4.0	2.5
Leaf Carbon (%)	35.39 ± 0.22 (a)	33.39 ± 0.53 (b)	34.10 ± 0.30 (ab)
Leaf Nitrogen (%)	0.99 ± 0.032 (a)	1.07 ± 0.039 (ab)	1.15 ± 0.036 (b)
Leaf $\delta^{13}C$ (‰)	-7.8 ± 0.30 (a)	-9.69 ± 0.48 (b)	-10.4 ± 0.24 (b)
Leaf $\delta^{15}N$ (‰)	8.74 ± 0.27 (a)	8.00 ± 0.56 (ab)	6.66 ± 0.41 (b)

Table 2.2. The degrees of freedom (DF), mean square (MS), F value (F) and p value (p) from a regression analysis performed of K_d vs. wave height at the high wave site and K_d vs. current speed at the high current site off Fisher's Island, NY in June 2008. Italicized p-values represent significant differences at $p < 0.05$.

Regression	DF	MS	F	p
K_d vs. Wave Height	1	0.0067	0.48	0.51
K_d vs. Current Speed	1	0.0056	19.99	<i>0.0006</i>

Table 2.3. The degrees of freedom (DF), mean square (MS), F value (F) and p value (p) from the ANOVA performed on leaf characteristics of *Z. marina* collected from the quiescent, high current, and high wave sites off Fisher's Island, NY. Italicized p-values represent significant differences at $p < 0.05$.

Variable	DF	MS	F	p
% Carbon	2	5.14	7.32	<i>0.0083</i>
$\delta^{13}\text{C}$	2	9.10	14.59	<i>0.0006</i>
% Nitrogen	2	0.034	5.24	<i>0.0232</i>
$\delta^{15}\text{N}$	2	5.56	6.02	<i>0.0155</i>
Leaf Absorbance	2	0.0049	10.73	<i>0.0104</i>

Table 2.4. The self-shading factor (SSF) (%) for each leaf orientation that is associated with the quiescent, high current, and high wave sites, and the self-shading factor weighted over a 12-hour light cycle [SSF(12)] and the epiphyte factor (EF) for the quiescent, high current, and high wave sites located off Fisher's Island, NY.

Site	Leaf Position	SSF (%)	SSF(12) (%)	EF (%)
Quiescent	Upright	1.89	1.89	21.48
High Current			97.48	0.68
	6 cm s ⁻¹	97.27		
	16 cm s ⁻¹	97.32		
	25 cm s ⁻¹	98.12		
	38 cm s ⁻¹	97.04		
High Wave			94.78	0.00
	Bent Shoreward	95.90		
	Almost Flat Open	90.20		
	Completely Flat	94.90		
	Transition Closed	99.37		
	Almost Flat Closed	99.32		
	Transition Compressed	99.12		
	Dancing Upright	91.62		

Table 2.5. Table of the degrees of freedom (DF), mean square (MS), F value (F) and p value (p) from the ANOVA performed on A) the yield of *Z. marina* leaves collected from the quiescent, high current, and high wave sites off Fisher's Island, NY and B) the yield of *Z. marina* leaves collected from the quiescent, high current, and high wave sites off Fisher's Island, NY and then planted in common garden conditions in outdoor flow tanks for 10 weeks. Italicized p-values represent significant differences at $p < 0.05$.

A)

PAR	DF	MS	F	p
0	2	0.021	9.55	0.0033
49	2	0.0030	1.84	0.2008
79	2	0.0035	2.64	0.1123
113	2	0.0040	3.98	<i>0.0473</i>
177	2	0.0052	9.18	<i>0.0038</i>
250	2	0.0068	18.86	<i>0.0002</i>
397	2	0.0061	40.74	<i><0.0001</i>
601	2	0.0040	54.48	<i><0.0001</i>
923	2	0.0027	60.6	<i><0.0001</i>

B)

	Time				Site			
PAR	DF	MS	F	p	DF	MS	F	p
29	4	0.45	15.97	<i><0.0001</i>	2	0.00018	0.3	0.97
49	4	0.109	7.35	<i><0.0001</i>	2	0.000082	0.04	0.9641
79	4	0.019	7.88	<i><0.0001</i>	2	0.00077	0.37	0.6949
113	4	0.0103	7.3	<i><0.0001</i>	2	0.0006	0.29	0.7512
177	4	0.0057	4.98	<i>0.0018</i>	2	0.00029	0.2	0.8213
250	4	0.0092	6.23	<i>0.0003</i>	2	0.00068	0.33	0.7218
397	4	0.0071	5.76	<i>0.0006</i>	2	0.00063	0.38	0.6881
601	4	0.0072	8.08	<i><0.0001</i>	2	0.000098	0.07	0.9316

Figures

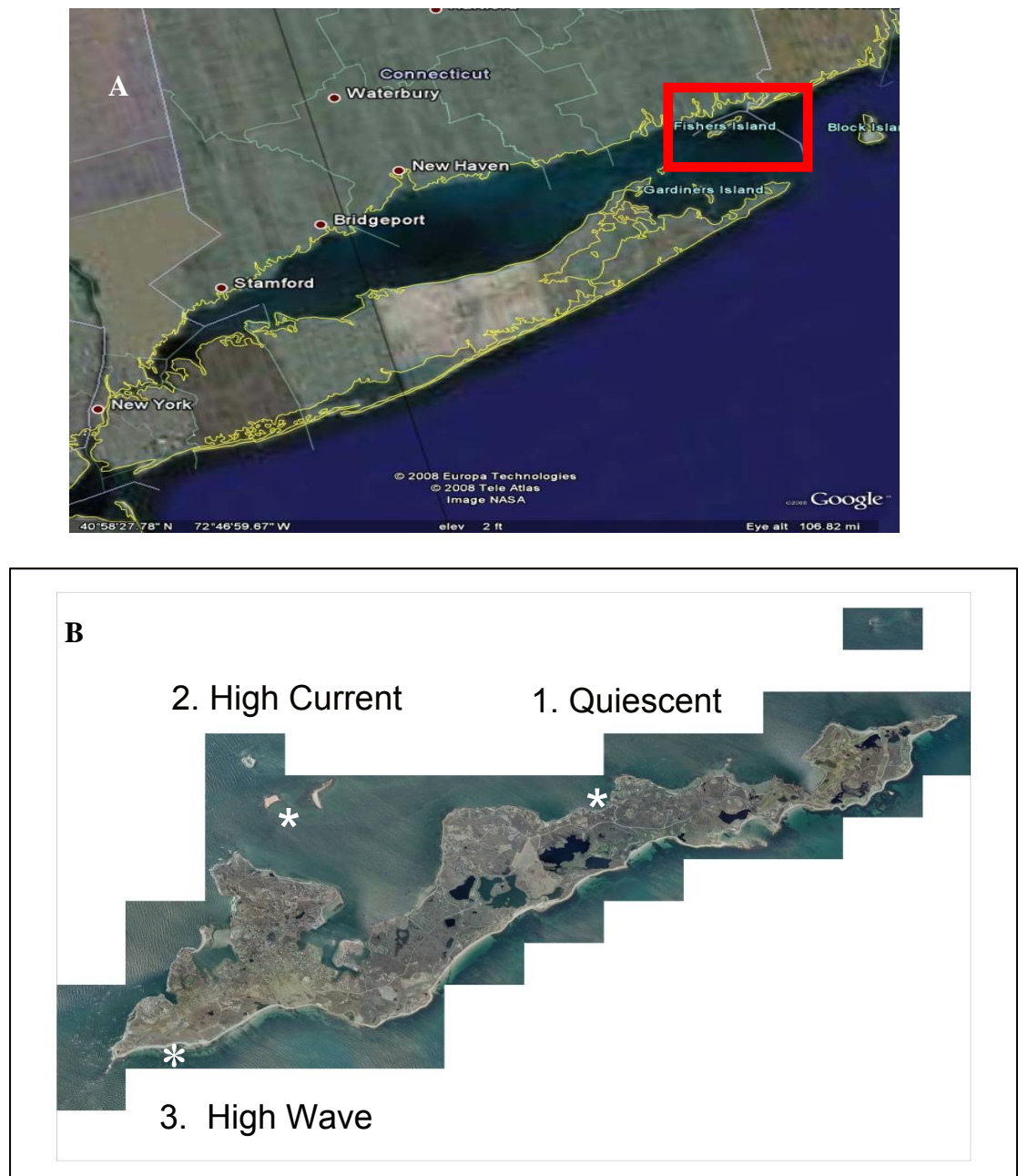


Figure 2.1. A) Location of Fisher's Island, NY within Long Island Sound; note the extremely long fetch in the SE direction, and B) location of the three field sites around Fisher's Island, NY: 1) quiescent site which is protected from currents and waves, 2) high current site as tidal currents are increased between the island and 3) high wave site with oceanic swell.

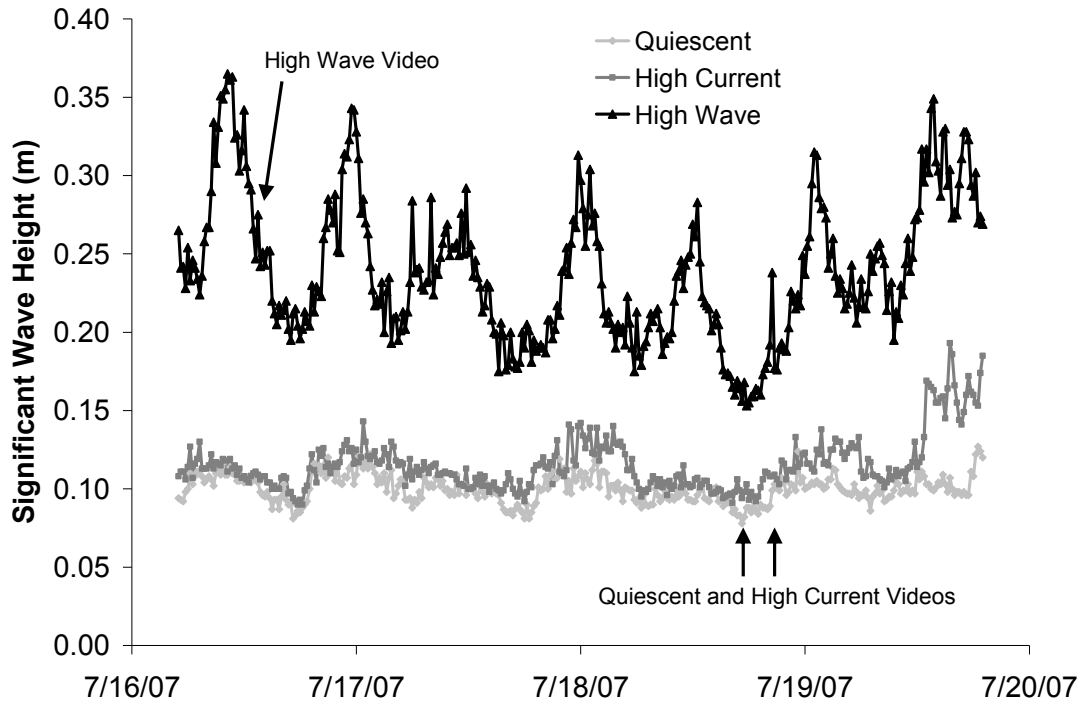


Figure 2.2. Significant wave height (m) at quiescent (light grey diamonds), high current (dark grey squares), and high wave (black triangles) sites off Fisher's Island, NY measured over a five day period in July, 2007. Arrows indicate when videos of seagrass in motion were taken. The tidal signal present at the high wave site was found to be significantly related to water depth ($p < 0.0001$) such that when the tide was low, significant wave height decreased, and when the tide was high, significant wave height increased.

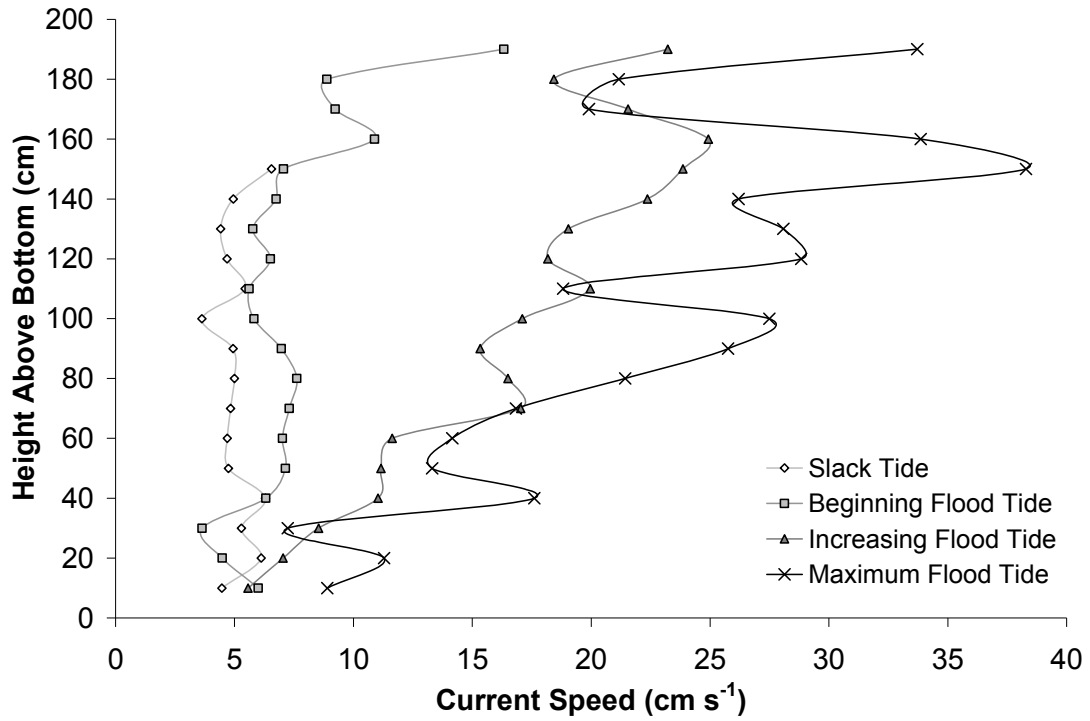


Figure 2.3. Average current profile (cm s^{-1}) throughout the water column at the high current site during slack (white circles), beginning (light grey squares), increasing (dark grey triangles), and maximum (black x) flood tide over a six-hour period in June, 2008 during a neap tide. Pictures were taken at each of these tidal phases to supplement the video analysis and to determine bending angle over an entire tidal cycle.

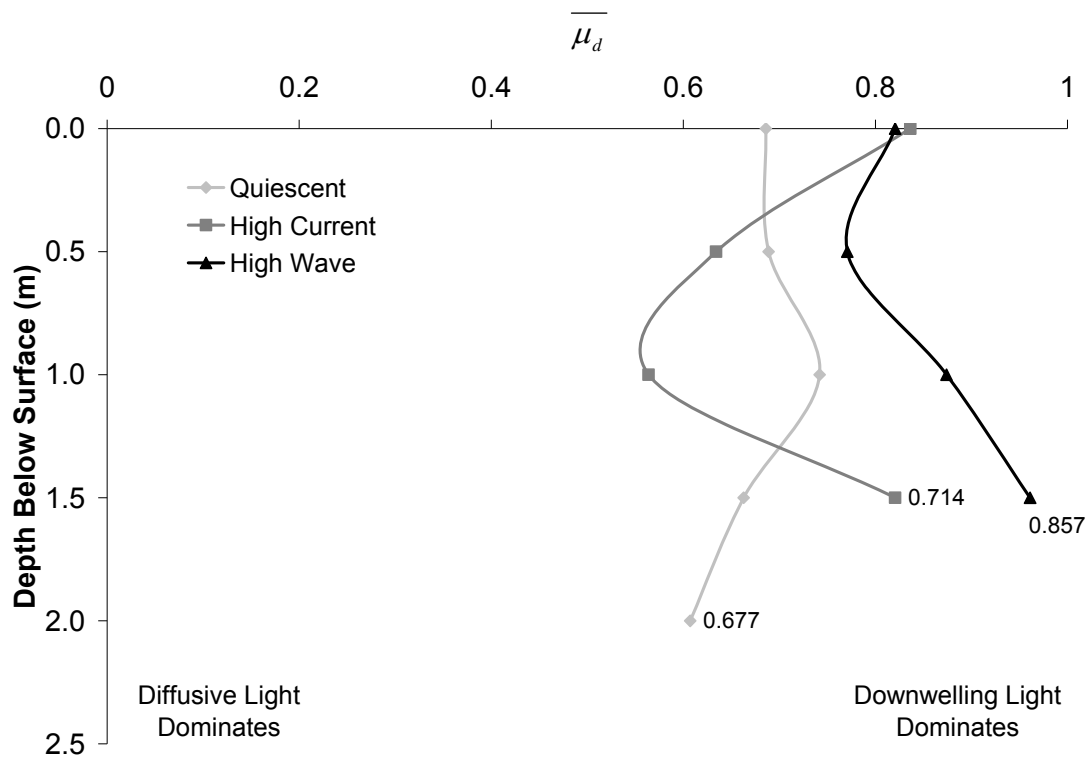


Figure 2.4. Average cosine for downwelling light ($\overline{\mu_d}$) calculated at the surface, 0.5, 1.0, 1.5 and 2.0 m (if available) below the surface at the quiescent (light grey diamonds), high current (dark grey squares), and high wave (black triangles) sites off Fisher's Island, NY. Numbers at the bottom of the profile are averages over depth.

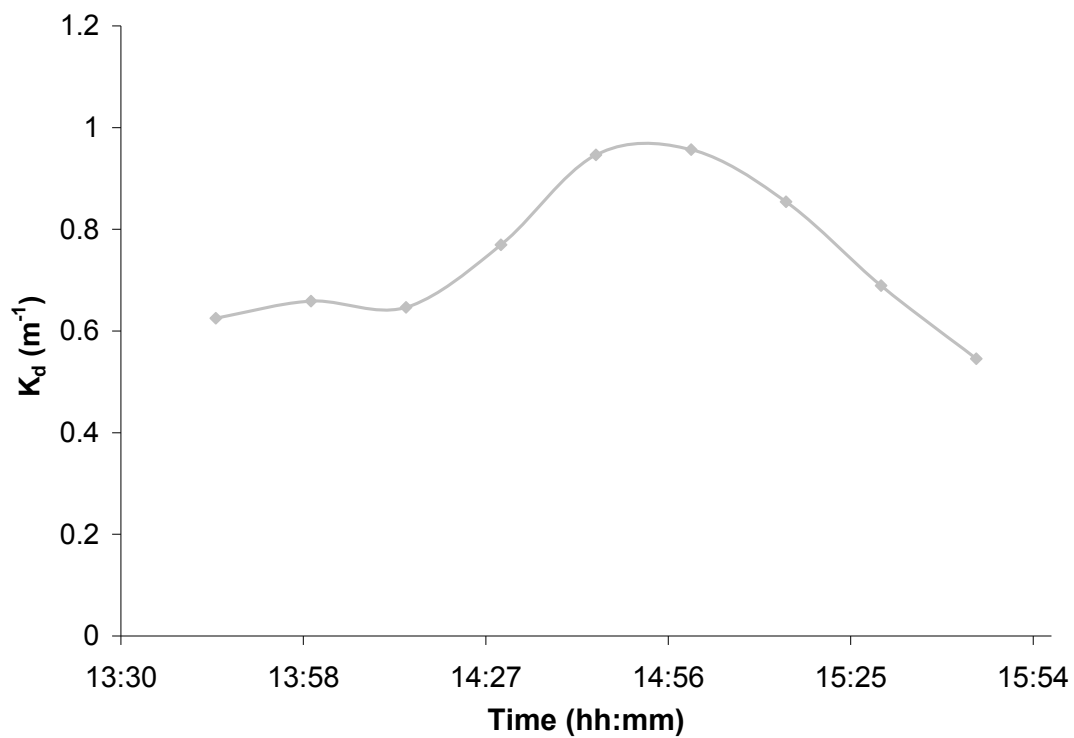


Figure 2.5. $K_d (\text{m}^{-1})$ over time at the quiescent site off Fisher's Island, NY measured in July 2008 between 13:30 and 16:00.

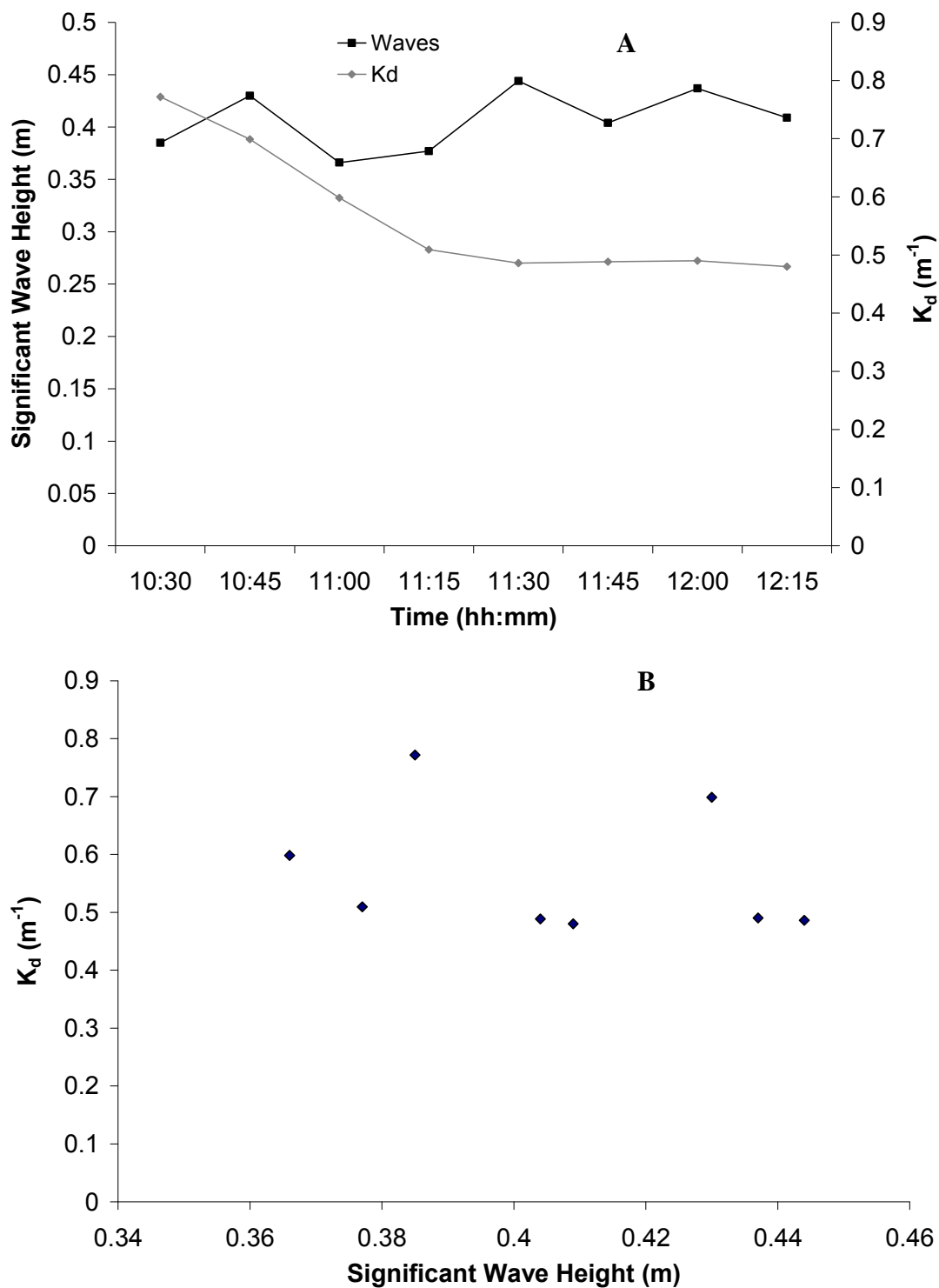


Figure 2.6. At the high wave site off Fisher's Island, NY: A) Significant wave height (m) and K_d (m^{-1}) measured between 10:30 and 12:30 in July 2008. B) Linear relationship between significant wave height and K_d was not significant ($p=0.5132$).

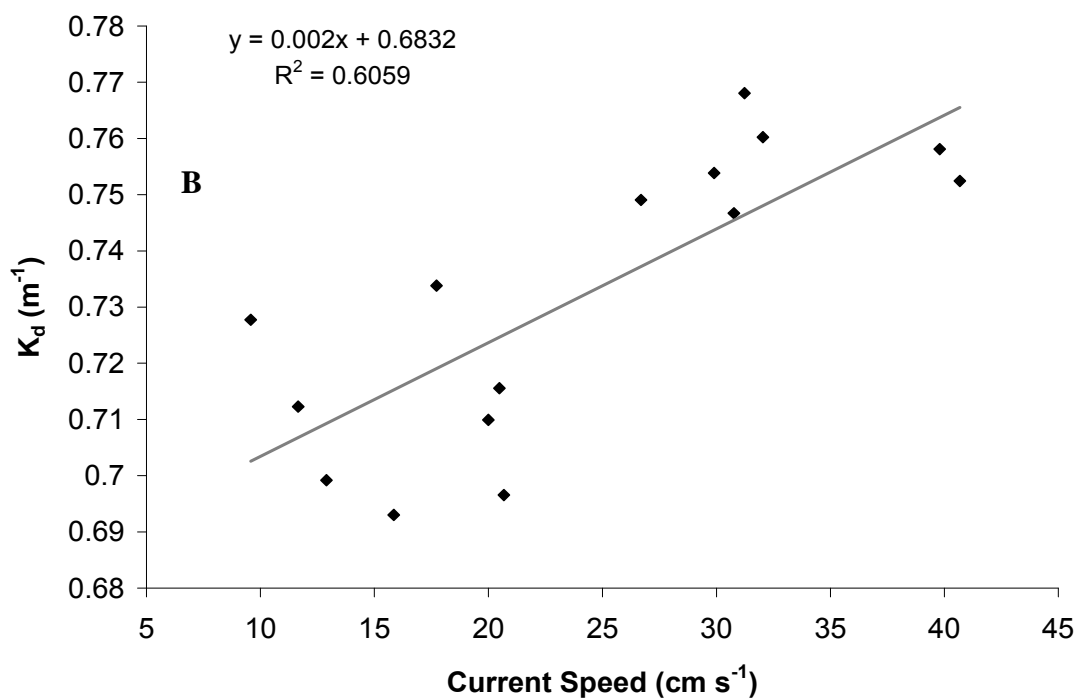
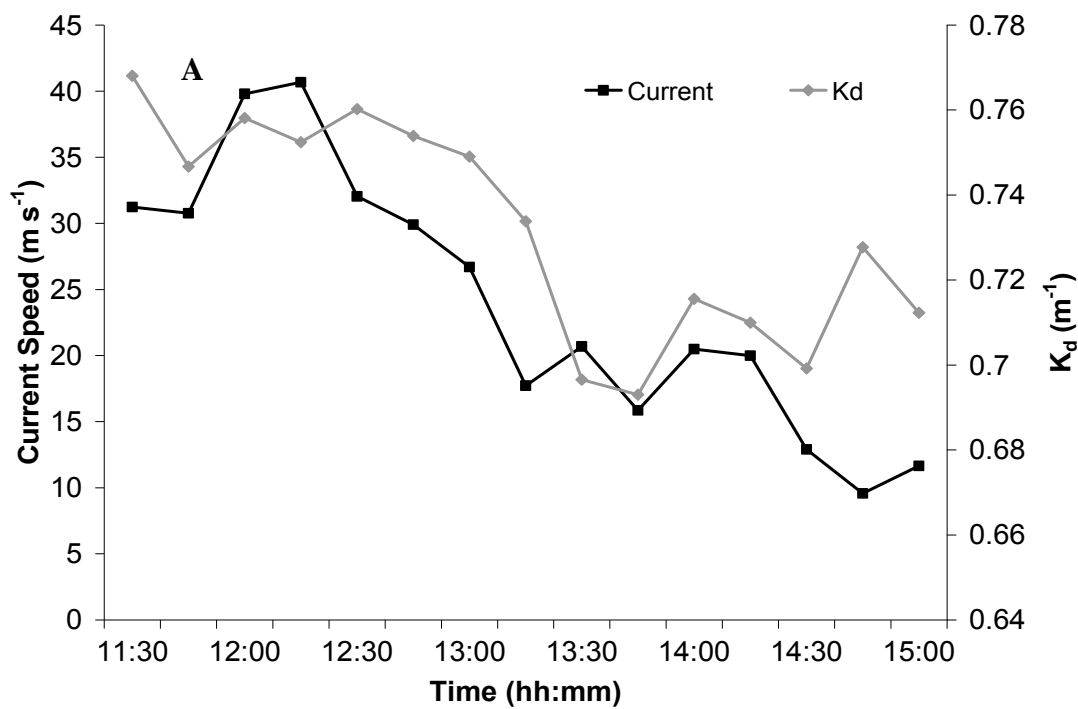


Figure 2.7. At the high current site off Fisher's Island, NY: A) Current speed (cm s⁻¹) and K_d (m⁻¹) measured between 11:30 and 15:00 in July 2008. B) Positive, linear relationship between current speed and K_d (p=0.0006) such that as current speed increases by 10 cm s⁻¹, K_d increases by 0.02.

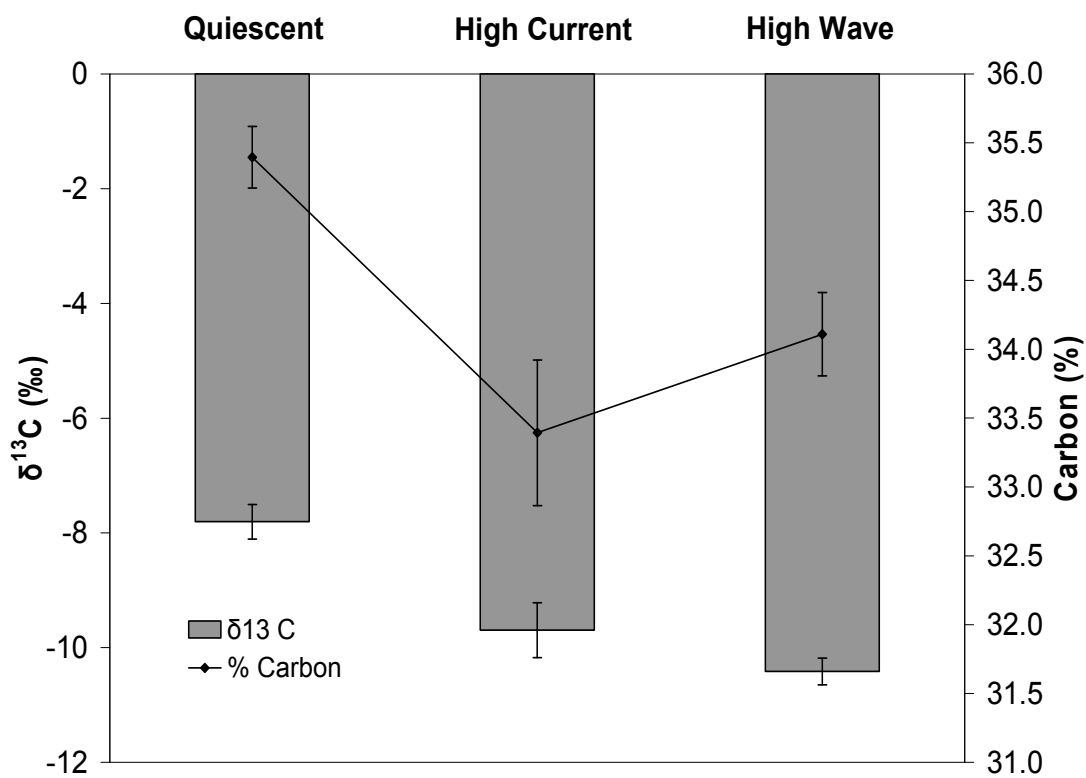


Figure 2.8. Average $\delta^{13}\text{C}$ (‰) (bars) and carbon content (%) (black diamonds) of *Z. marina* leaves collected from the quiescent, high current and high wave sites off Fisher's Island, NY. Error bars represent \pm S.E., $n = 4$.

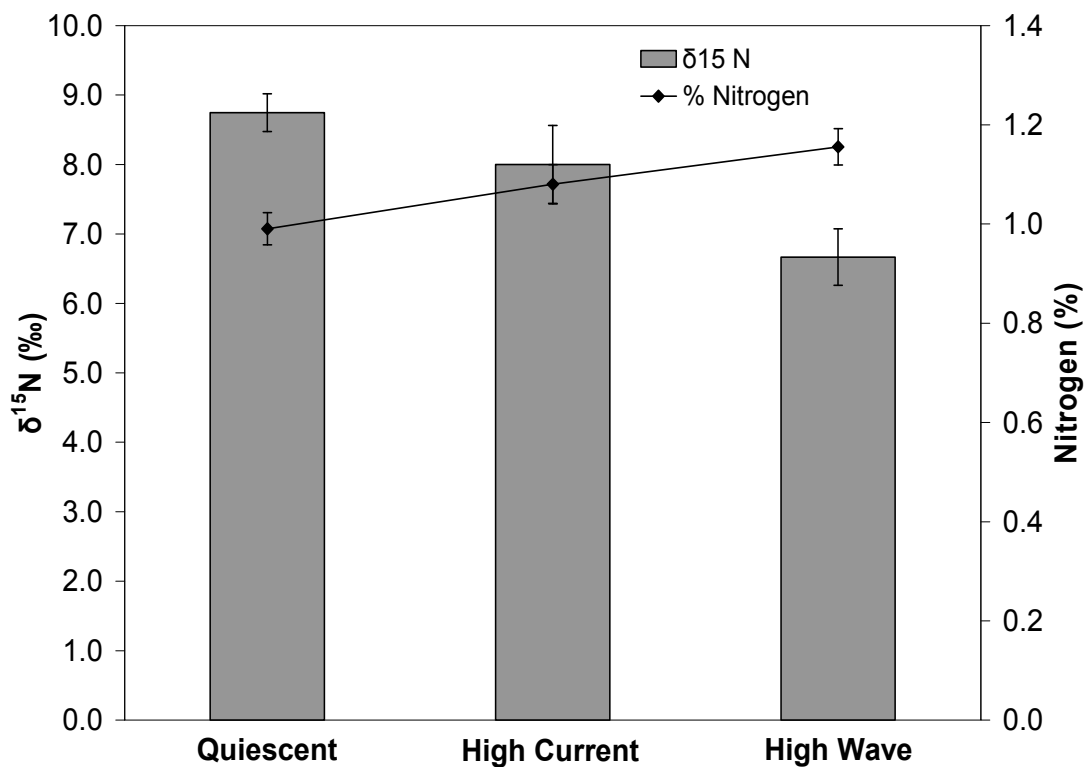


Figure 2.9. Average $\delta^{15}\text{N}$ (‰) (bars) and nitrogen content (%) (black diamonds) of *Z. marina* leaves collected from the quiescent, high current and high wave sites off of Fisher's Island, NY. Error bars represent \pm S.E., n = 4.

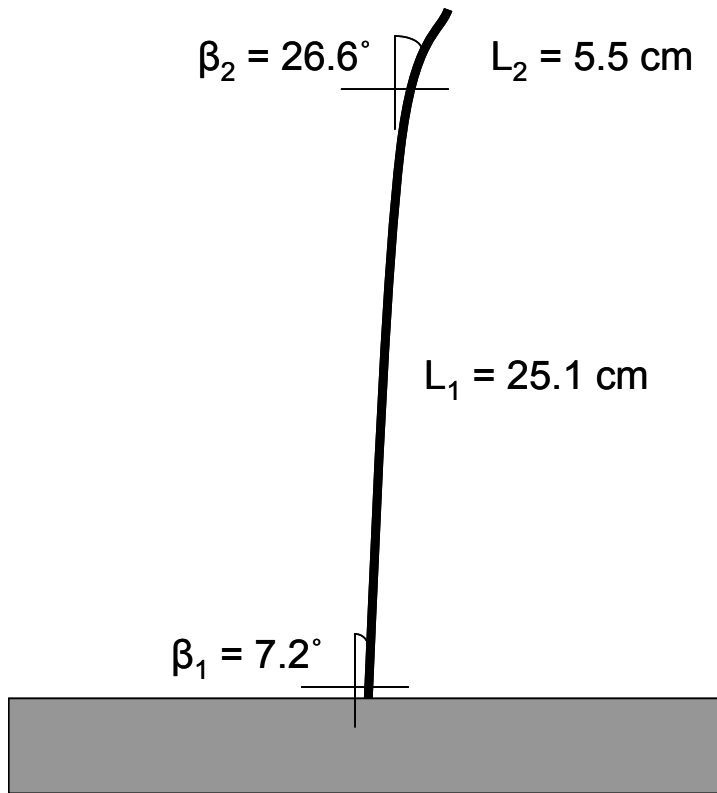


Figure 2.10. Schematic view of the average shape of a *Z. marina* leaf video taped at the quiescent site off Fisher's Island, NY where β_n = leaf bending angle and L_n = leaf length at β_n . Leaves stayed in this position at all times.

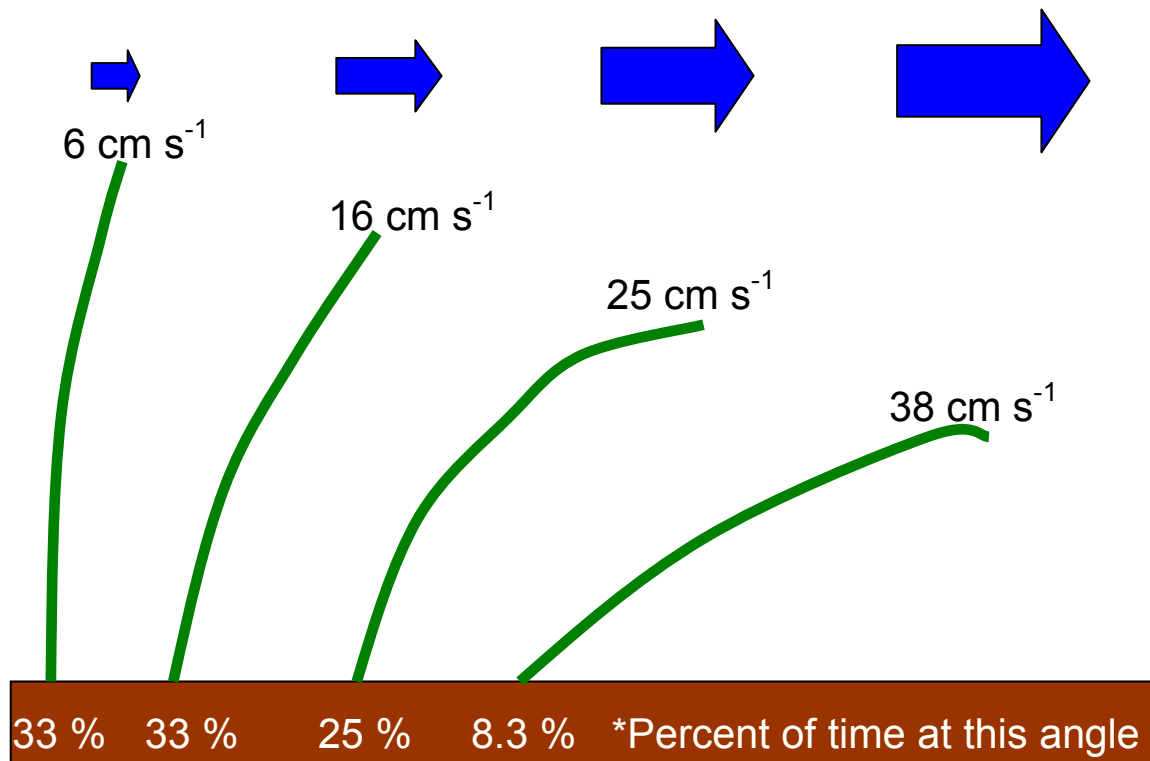


Figure 2.11. Schematic view of the average shapes of a *Z. marina* leaf video taped and photographed over a half tidal cycle at the high current site off Fisher's Island, NY. Tidal currents ranged from 3 to 41 cm s^{-1} during different phases of the tide. The percent of time a leaf spent bent at a certain angle for current velocities of 6, 16, 25, and 38 cm s^{-1} are shown below each shape.

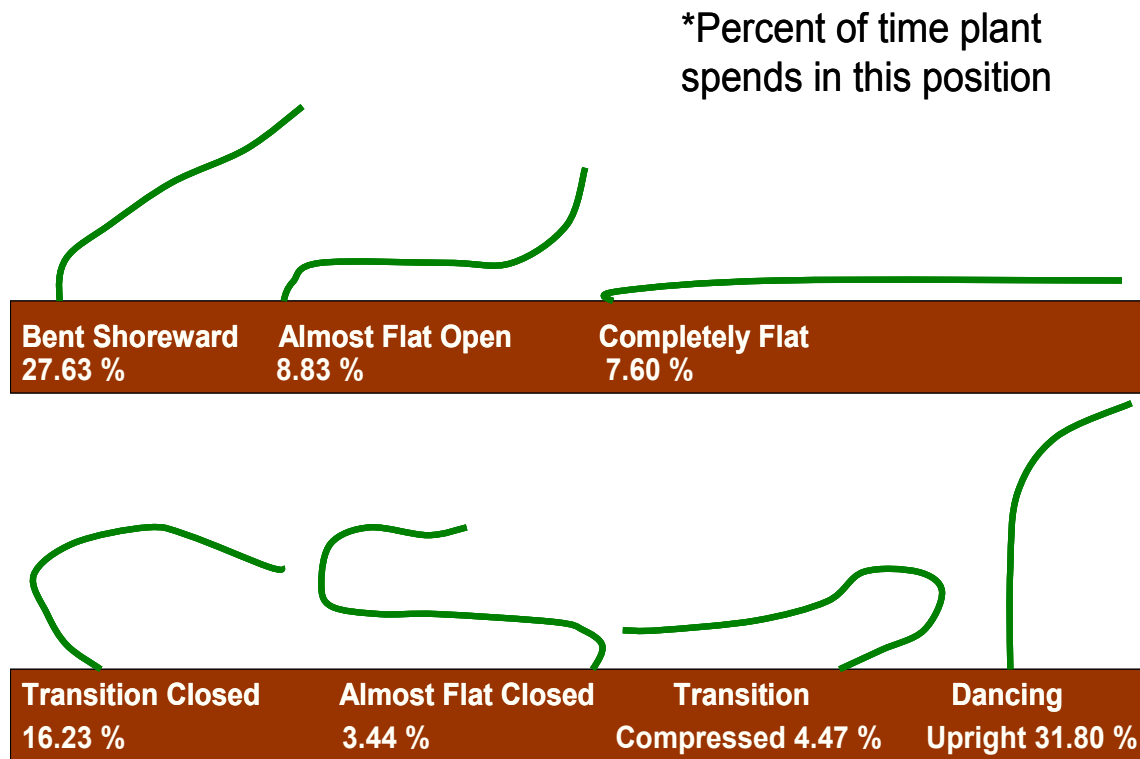


Figure 2.12. Schematic view of the average shapes a *Z. marina* leaf occupies during a passage of a wave at the high wave site off Fisher's Island, NY where significant wave height ranged from 0.15 to 0.37 m. The percent of time a leaf spent at a certain position for each of the 7 key phases of the plants motion are shown below each shape.

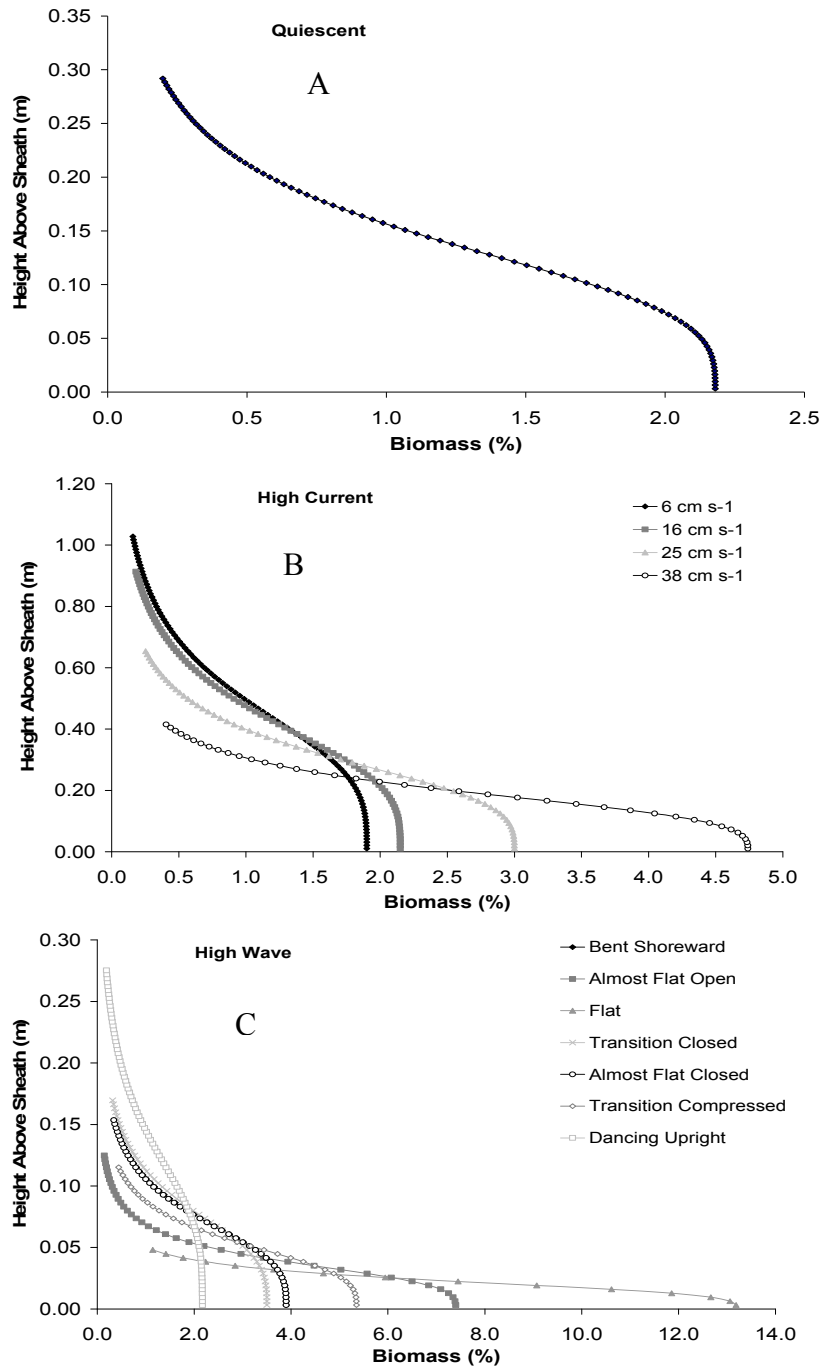


Figure 2.13. Vertical biomass (%) distribution for *Z. marina* at A) the quiescent site, B) the high current site for each of the 4 dominate shapes that the canopy occupied during different current velocities, and C) the high wave site for each of the 7 shapes that the seagrass canopy occupied under different wave phases. Note that the vertical biomass distribution in A does not change over time; biomass distribution fluctuated every few hours between curves in B and in a matter of seconds or fractions of a second in C.

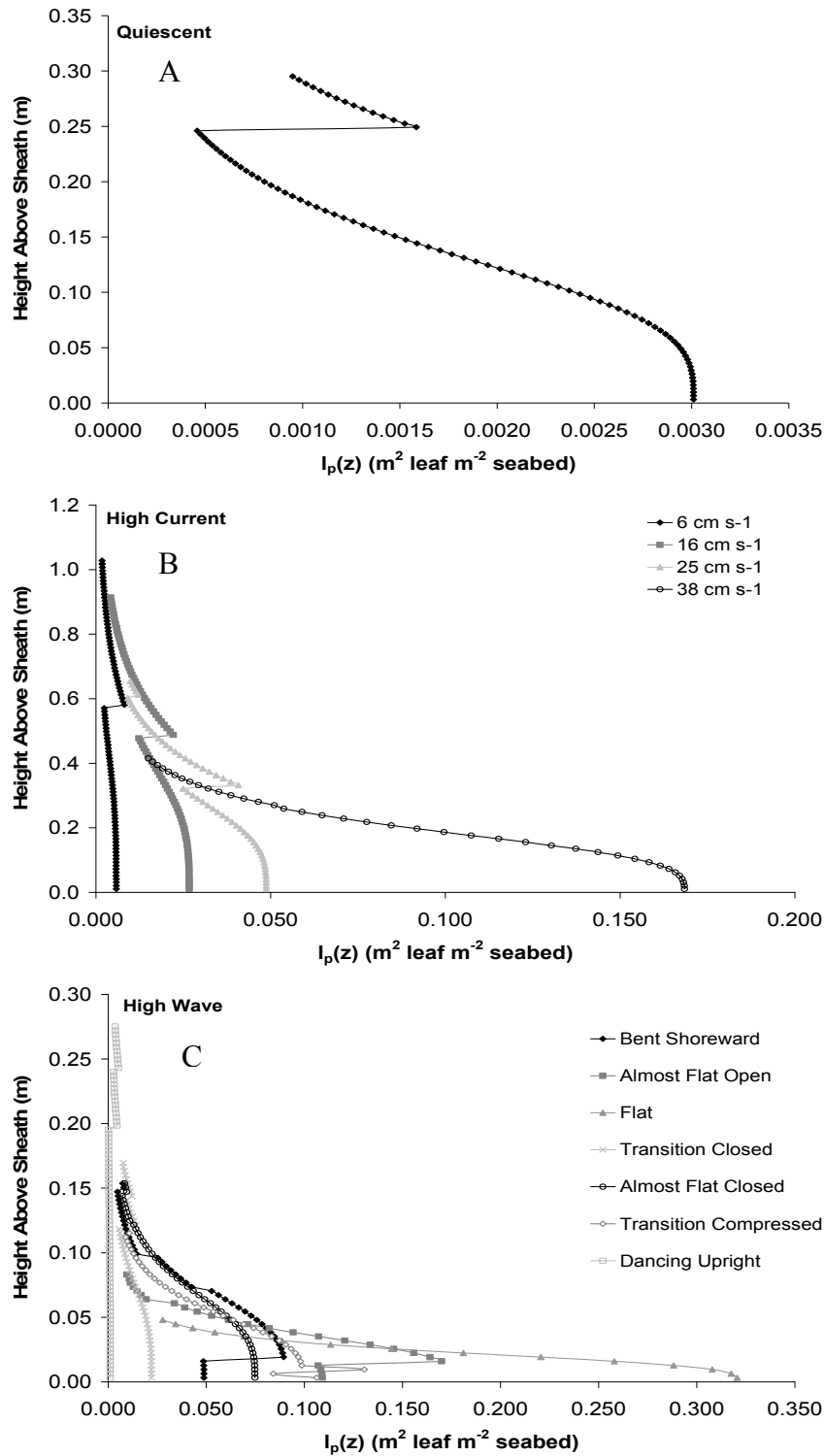


Figure 2.14. Horizontally projected leaf area [$l_p(z)$] ($\text{m}^2 \text{ leaf m}^{-2} \text{ seabed}$) for *Z. marina* at A) the quiescent site, B) the high current site for each of the 4 dominate shapes that the canopy occupied during different current velocities, and C) the high wave site for each of the 7 shapes that the seagrass canopy occupied under different wave phases.

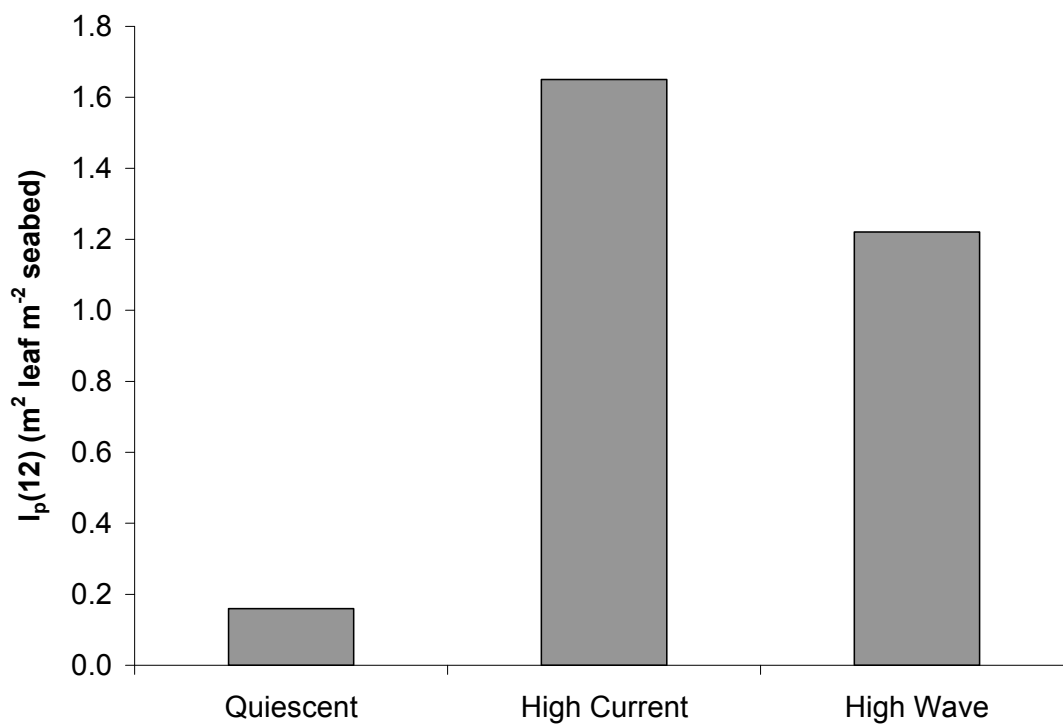


Figure 2.15. B) Vertically integrated horizontally projected leaf area [$I_p(12)$] for *Z. marina* leaves from the quiescent, high current, and high wave sites located off Fisher's Island, NY.

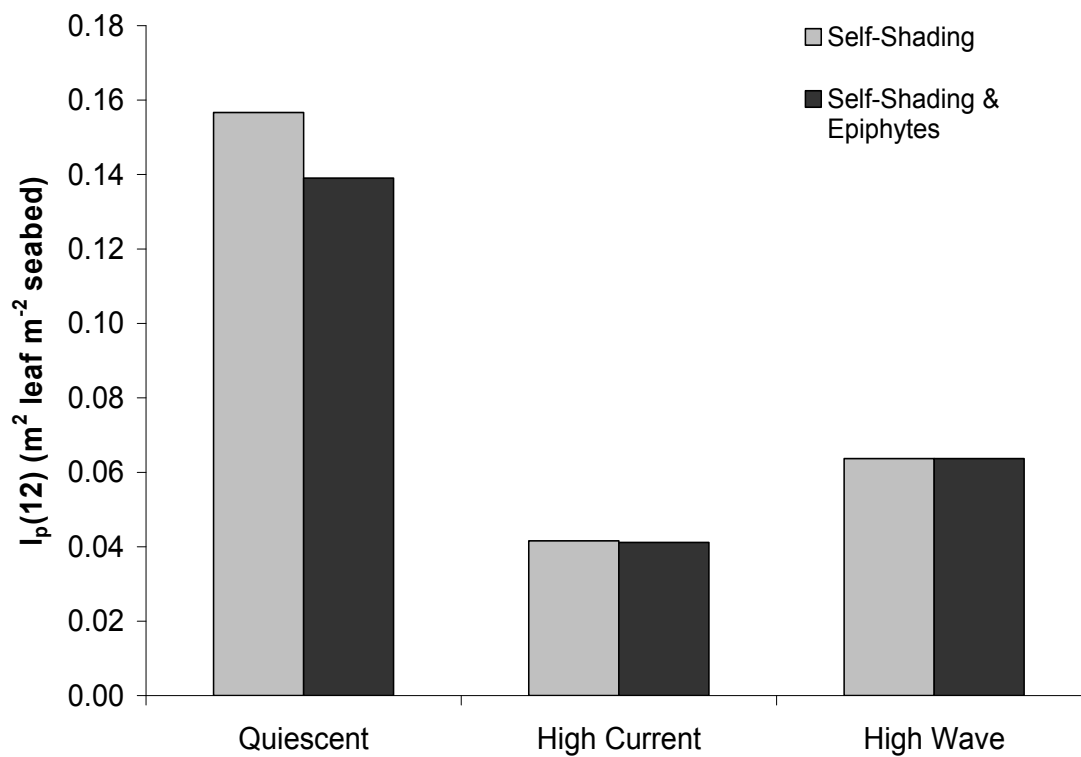


Figure 2.16. Vertically integrated horizontally projected leaf area [$I_p(12)$] adjusted for self-shading (gray) and self-shading plus epiphyte growth (black) for *Z. marina* leaves from the quiescent, high current, and high wave sites located off Fisher's Island, NY.

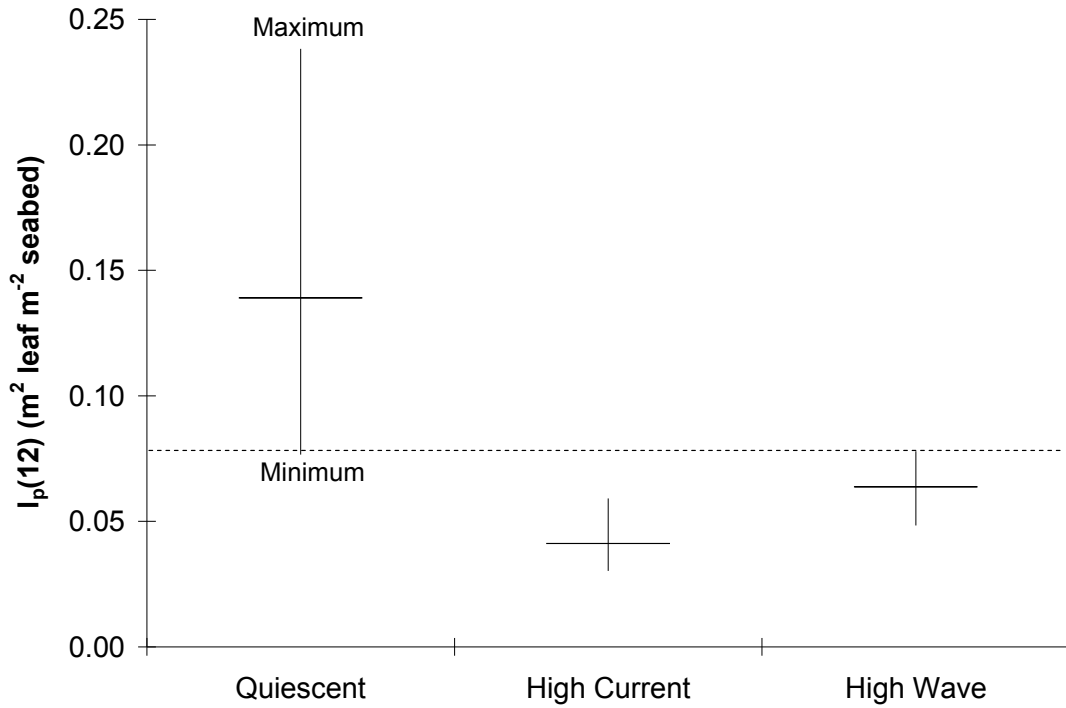


Figure 2.17. Range of vertically integrated horizontally projected leaf area [$I_p(12)$] (m^2 leaf m^{-2} seabed) adjusted for self-shading and epiphytic growth for *Z. marina* at the quiescent, high current, and high wave sites off Fisher's Island, NY. The horizontal line represents the average $I_p(12)$. The top of the vertical line is the maximum $I_p(12)$ and the bottom of the vertical line is the minimum $I_p(12)$. The horizontal dashed line is an extension of the minimum $I_p(12)$ possible for the quiescent site, which is greater than and equal to the high current and high wave maximums, respectively.

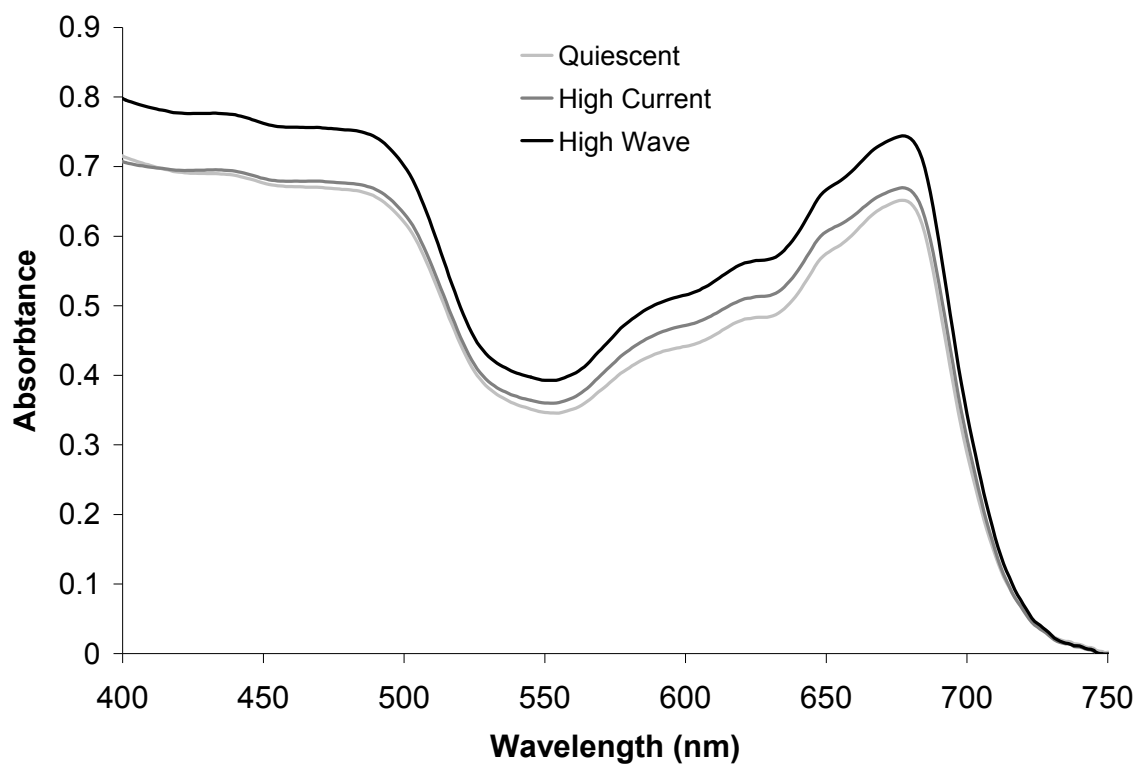


Figure 2.18. Average photosynthetic leaf absorbance of tertiary *Z. marina* leaves collected from the quiescent (light grey), high current (dark grey), and high wave (black) sites off Fisher's Island, NY in July, 2008.

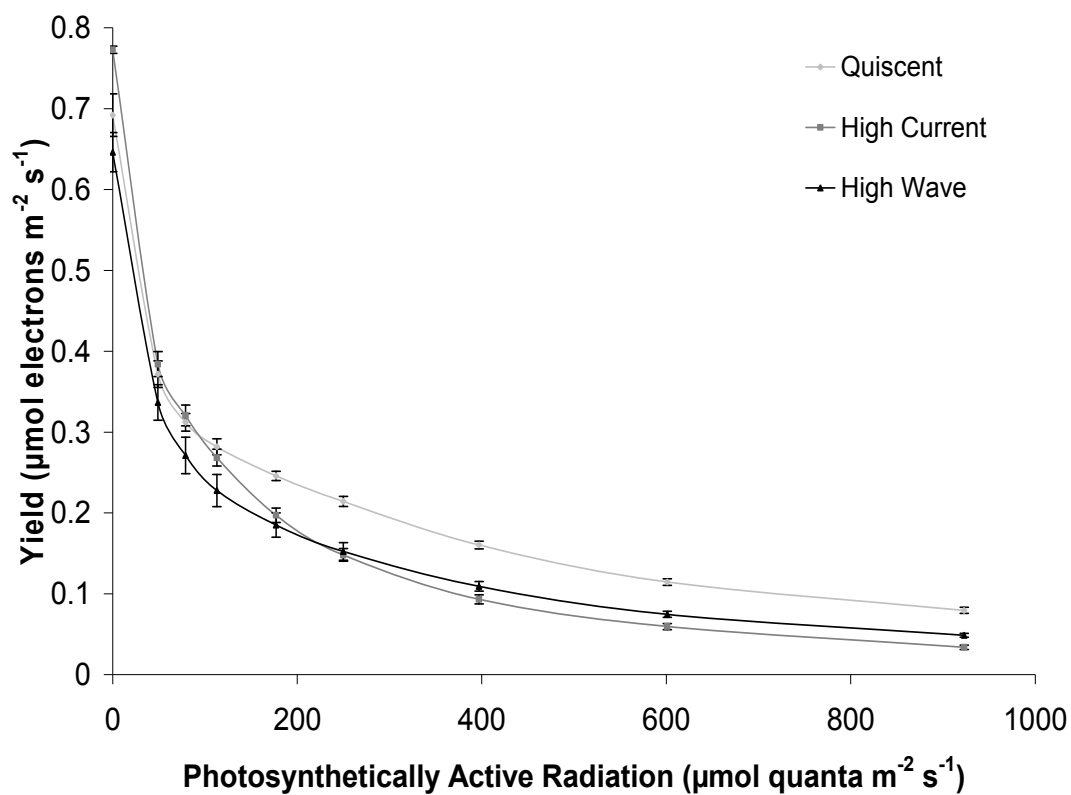


Figure 2.19. Average photosynthetic yield ($\mu\text{mol electrons m}^{-2} \text{s}^{-1}$) of tertiary *Z. marina* leaves from the quiescent (light grey diamonds), high current (dark grey squares), and high wave (black triangles) sites off Fisher's Island, NY measured in June, 2008. Error bars represent \pm S.E., n = 5.

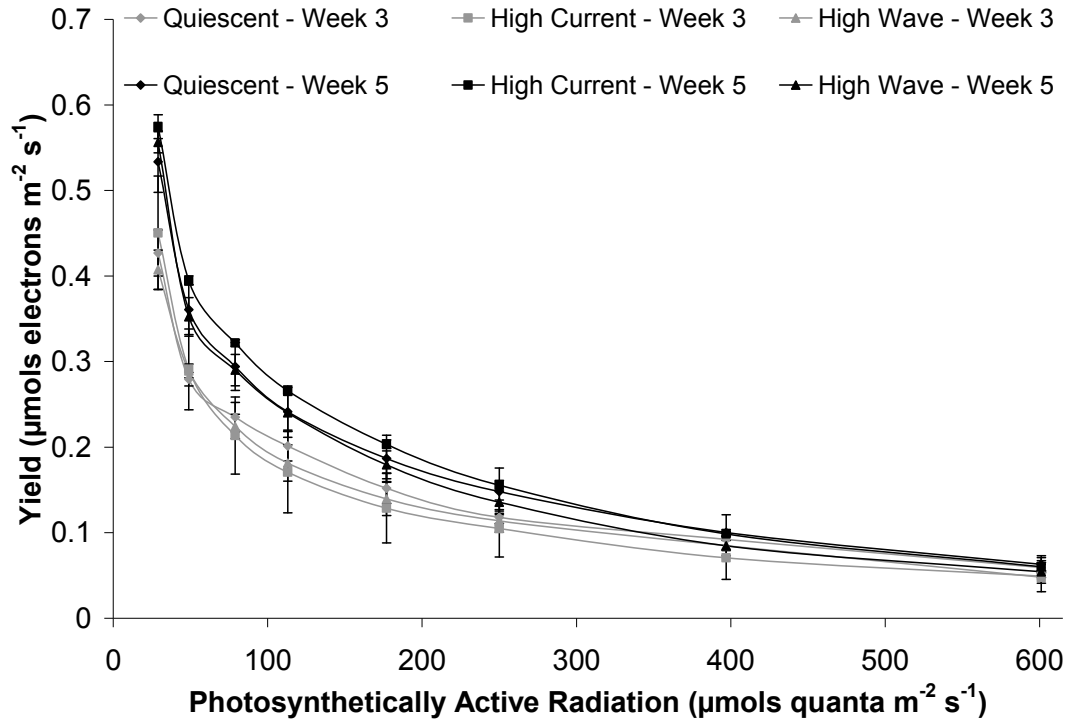


Figure 2.20. Average photosynthetic yield (μmols electrons m⁻² s⁻¹) of tertiary *Z. marina* leaves collected from quiescent (diamonds), high current (squares), and high wave (triangles) sites off Fisher's Island, NY and transplanted into outdoor flow tanks with similar currents (9 ± 2 cm s⁻¹) and sediment (fine sand, 0.52% organic content). Shown measurements were made at weeks 3 (grey) and 5 (black). Error bars represent +/- S.E., n = 4.

Illustrations

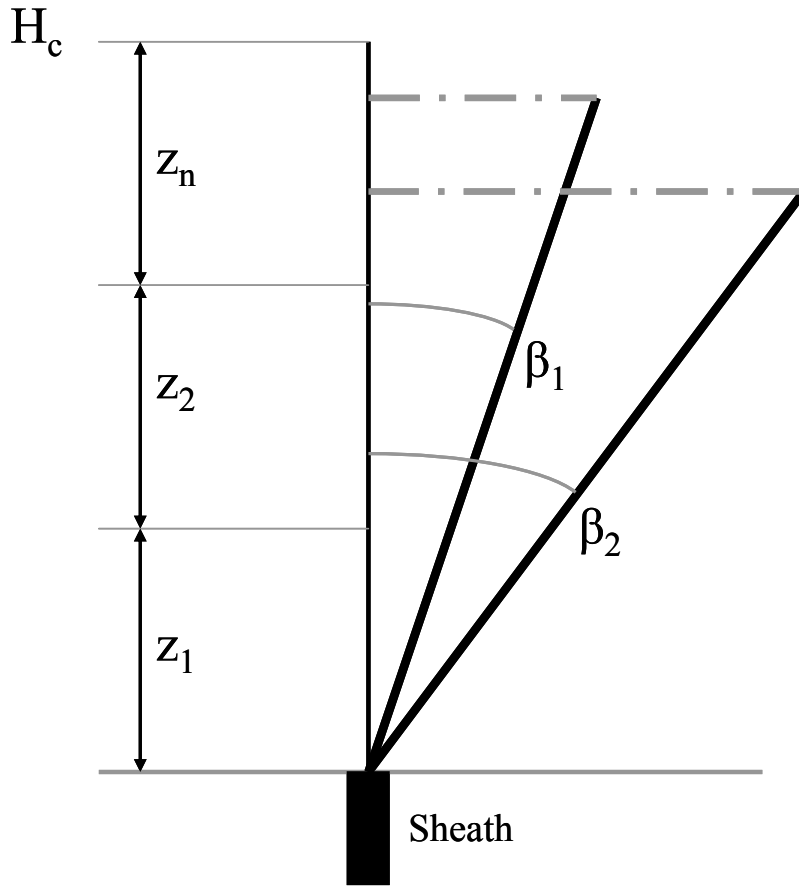


Illustration 2.1. Schematic of how a *Z. marina* shoot was treated in order to calculate horizontally projected leaf area (l_p). The maximum canopy height (H_c) was divided into 100 sections (z); only 3 are represented here (z_1, z_2, \dots, z_n). For each section (z), the amount of photosynthetic tissue that occupied that section of the water column (based on leaf length, width, and shoot density) was multiplied by the sine of the bending angle (β). l_p is denoted by the horizontal dashed line. As the leaf length is bent at a greater angle (β_2), the leaf occupies less of H_c , but l_p increases. This schematic does not take into account self-shading or epiphyte colonization, but visually demonstrates how a shoot, and the entire canopy, is manipulated in the calculations.

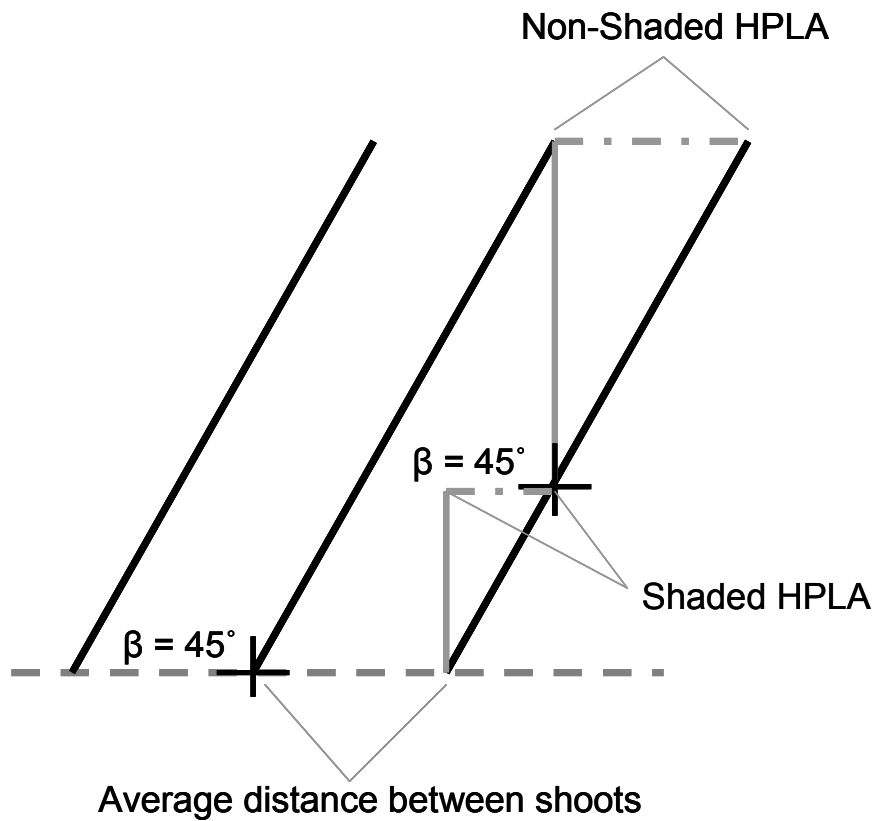
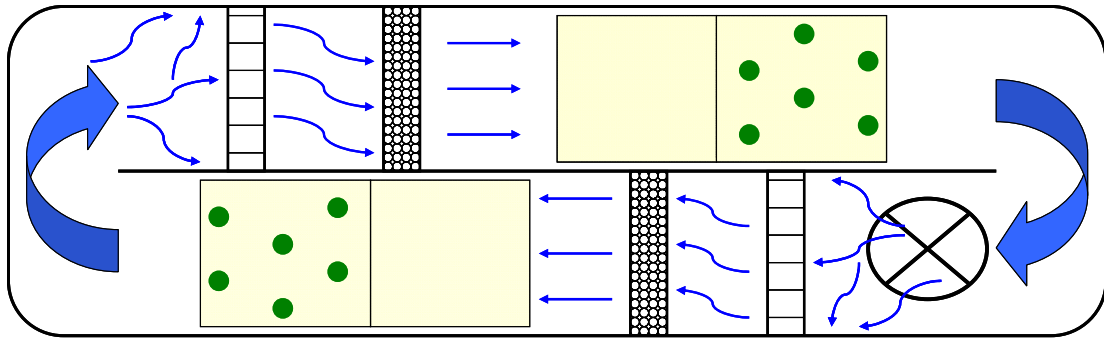


Illustration 2.2. Schematic of how the average distance between *Z. marina* shoots, bending angle, and leaf area were used to determine the shaded and non-shaded area of the leaf tissue, which was used in the EF calculation. In this example, $\beta = 45^\circ$ was used.



Legend:



Tray of sand with 6 *Z. marina* shoots



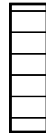
Tray of sand without plants



Trolling Motor



Collimator



Flow Straightener

Illustration 2.3. Schematic of flow tank set-up used for the common garden experiment. Current was generated with a trolling motor, which circulated water around the flow tank. Water flow was directed through a flow straightener and collimator before flowing over *Z. marina* shoots. There were 6 of these flow tanks, making a total of 12 trays with transplanted seagrass, which contained 6 *Z. marina* shoots each.

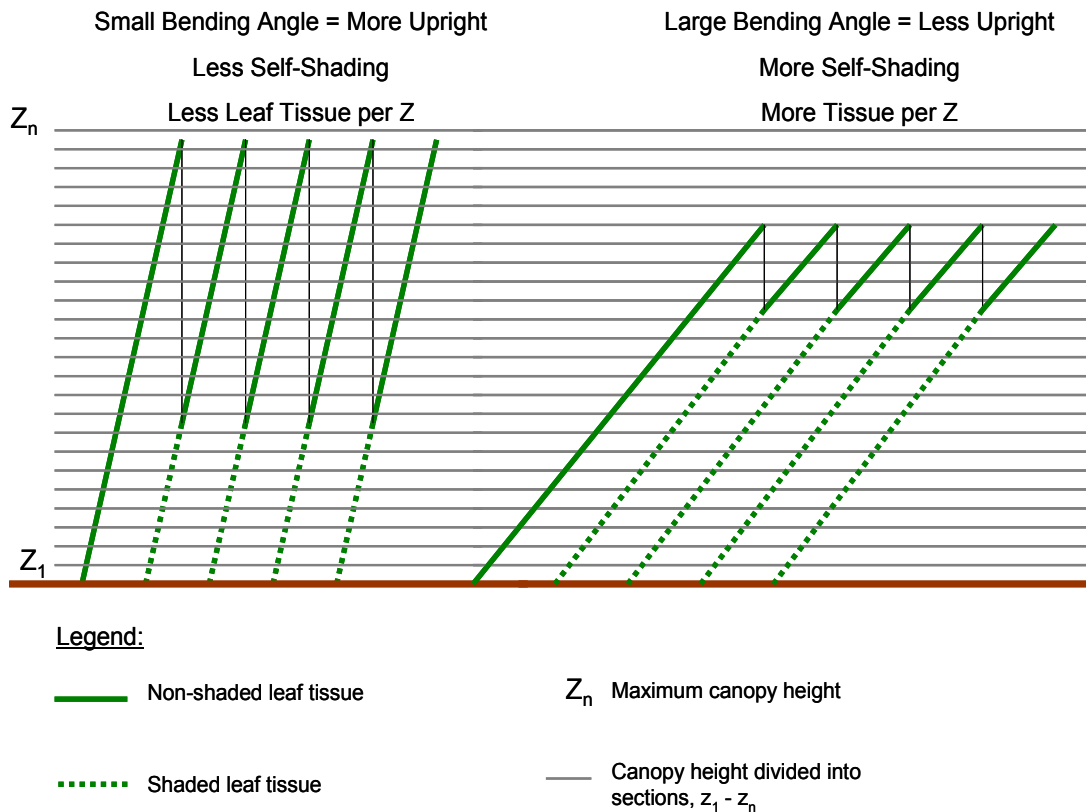


Illustration 2.4. Schematic view of how bending angle alters the amount of seagrass tissue occupying each canopy section (z), how much self-shading occurs, and how this affects horizontally projected leaf area [$l_p(z)$]. When a seagrass leaf is bent at a small angle and is in a more upright position, more z contain seagrass tissue, yet there is less tissue per z . Therefore, l_p per z is small but more z have l_p . Conversely, when a seagrass leaf is bent at a larger angle and is in a more horizontal position, fewer z contain seagrass tissue, yet there is more tissue per z . Therefore, l_p per z is large but fewer z have l_p . This schematic also demonstrates the self-shading factor (SSF), which is the percent of the leaf tissue that is potentially shaded by a neighboring leaf, which is bent over at some angle, as denoted by the dashed line. Bending leaves decrease the light incident on the tissue layer below the top layer of tissue, and the SSF increases with increasing bending angle.

Final Conclusions

Synthesis

The interaction between marine plants and their fluid environment has been shown to be quite complex (Gaylord and Denny 1997, Denny and Gaylord 2002) (Illustration FC.1). In order to understand how currents and waves affect seagrass morphology, leaf movement and orientation, and thus light availability, we studied *Zostera marina* under the extreme hydrodynamic conditions present around Fisher's Island, NY at the mouth of Long Island Sound.

In chapter 1, an analysis of *Zostera marina* morphology was conducted. It not only included a quantitative analysis of current speed, significant wave height, and sediment composition *in situ*, but also a quantitative analysis of the strength and flexibility of *Z. marina* leaves under different hydrodynamic conditions. The results of this chapter demonstrate that leaf length and width were not necessarily a mechanism to reduce drag. Instead, the inherent flexibility of seagrass leaves and their ability to sway in the waves or deflect with the current may be the main mechanism by which drag is reduced, while leaf strength may be an important acclimation when seagrass leaves are exposed to strong currents.

Chapter 1 also demonstrated the potential of sediment composition to alter seagrass morphology. Sediment composition, not local hydrodynamic conditions, directly affected *Zostera marina* root length; well sorted sand, presumably a low nutrient sediment, as was observed at the quiescent site, led to longer roots. Sediment composition could also potentially explain why leaves of *Z. marina* at the high current site were over 3 times longer than leaves of *Z. marina* from the quiescent and

high wave sites. We hypothesize that porewater nutrient turnover rate was potentially high at the high current site due to flow-induced particle entrainment into the sediment (sensu Huettel et al. 1996) and its decomposition by microbial processes, thereby continually replenishing nutrients to *Z. marina* shoots. Wave-induced particle intrusion into the sediments (sensu Precht and Huettel 2003) may also contribute to the high biomass at the high wave site but to a lesser extent as the sediment is finer and, therefore, less permeable.

In chapter 2, the quantitative analysis of waves and currents, or the lack thereof, was related to seagrass leaf movement via video analysis. This movement was described by leaf bending angles, and was used to calculate the amount of photosynthetic tissue available to capture downwelling light. The results were corrected for self-shading and colonization by epiphytes.

When *Zostera marina* was exposed to low water flow, the average distance between shoots minimized self-shading and optimized light availability. Leaf tissue carbon and nitrogen at the quiescent site were low possibly due to a thick diffusive boundary layer (DBL) on the leaves, less mixing between the water within and above the canopy, and a slower sediment nutrient turnover rate when compared to the high current site. Additionally, epiphyte colonization at the quiescent site was relatively high, which reduced light availability and potentially reduced water-column nutrient uptake, but still allowed the bed to be healthy and productive (Illustration FC.2). Therefore, life of seagrasses under quiescent and moving water involves trade-offs. Under quiescent conditions, light availability may be high (if epiphyte colonization is not excessive), but the flux of carbon and nutrients may be limiting. In contrast,

under moving water, light availability may be reduced due to self-shading but an ample availability of carbon and nutrients exists as a result of a thin leaf DBL.

Trade-offs also exist for seagrasses exposed to currents and waves. *Zostera marina* exposed to currents and waves experienced a high degree of self-shading when compared to *Z. marina* at the quiescent site. However, self-shading was found to be less for *Z. marina* exposed to waves than for *Z. marina* exposed to currents as leaves may have been benefiting from the “opening” and “closing” of the canopy as described by Koch and Gust (1999), where light available is high when the canopy is “open”.

Additionally, although *Z. marina* exposed to currents and waves had a higher availability of water-column carbon and nutrients over seagrass beds in quiescent waters, there were sedimentary differences between these two sites. Sediment grain size $> 500 \mu\text{m}$ was dominated by gravel, very coarse and coarse sand at the high current site, whereas it was dominated only by gravel at the high wave site but fine sand was deposited between the gravel. Huettel and Rusch (2000) demonstrated that particle entrainment into the sediment is more likely to occur in coarser sand than in finer-grained sand. This suggests that entrainment of a variety of grain sizes, including POM of all sizes, could be occurring at the high current site. The associated high nutrient turnover rate (Huettel et al. 2003) could potentially benefit the seagrasses and explain the extremely long leaves found at the high current site (Illustration FC.3). Particle entrainment into the sediment can also occur as a result of waves (Precht and Huettel 2003). Perhaps the high biomass of *Z. marina* at the high wave site could be a result of this process. In the water column, carbon appears

to be more readily available to *Z. marina* at the high wave site than at the high current site. This suggests that the constant motion of leaves exposed to waves more effectively reduces the leaf diffusive boundary layer. Alternatively, it could suggest that the reduced mixing that occurs when leaves are bent over in the current (“closed canopy”) is leading to carbon depletion within the canopy at the high current site (Illustration FC.4).

Although this thesis has answered many questions regarding the relationship between hydrodynamics, seagrass morphology and light availability, it has also raised new questions or has left questions unanswered. Whether these morphological variations are adaptations or acclimations to local hydrodynamics is still merely speculative. Our results suggest that some traits (strength, flexibility, root length and number) may be highly plastic, while others (leaf length and width) may be genetically fixed. However, the long and wide leaves could be a result of the Huettel effect described previously and further research is needed to understand the driving mechanism. Additionally, it is still unknown what structurally makes a seagrass leaf stronger or more flexible. Further studies that examine structural aspects of seagrasses exposed to varying hydrodynamic regimes are necessary to answer these questions.

This thesis indeed demonstrates that there are benefits and detriments to inhabiting varying hydrodynamic environments. Because of these advantages and disadvantages, some seagrasses may be more susceptible to light or nutrient availability than others. For example, seagrasses exposed to waves and currents may have a stronger need for good water quality than seagrasses in quiescent waters due to

the high degree of self-shading imposed by leaf bending and swaying. Hence, seagrasses exposed to currents and waves may be more sensitive to eutrophication than seagrasses that inhabit areas dominated by low water flow. On the other hand, seagrasses located in quiescent waters may be at higher risk of being negatively affected by epiphyte colonization, or carbon and nutrient limitation.

Beyond Long Island Sound

Seagrasses are among the most valuable ecosystems on the planet due to the ecosystem services and functions they provide (Costanza et al. 1997). The preservation of healthy seagrass beds does not only contribute to high species diversity, ample food availability and sediment stabilization, but also to local economies as many fisheries (e.g. blue crabs and scallops) use seagrass beds as a habitat and refuge from predators. Unfortunately, seagrasses have been declining worldwide (Green and Short 2003, Orth et al. 2006) for a variety of reasons including eutrophication (Burkholder et al. 2007, Cardoso et al. 2008), and sea level rise (Short and Neckles 1999), and more frequent and stronger storms may decimate even more beds along with the ecosystem services they provide. Increased storm activity has already been linked to the loss of seagrass beds in northeastern Brazil (Short et al. 2006). By understanding how seagrasses respond to hydrodynamic conditions associated with storms (strong currents and waves), we will be better prepared to predict their future and define mechanisms to protect them (if possible) from further losses. Their preservation is increasingly important since it has been hypothesized that, as global warming continues, seagrass productivity could increase (Beer and

Koch 1996, Zimmerman et al. 1997, Palacios and Zimmerman 2007), thus providing a sink for CO₂, as seagrasses, unlike the open oceans, are thought to be carbon limited (Beer 1989, Beer and Koch 1996, Zimmerman et al. 1997, Short and Neckles 1999, Invers et al. 2001, Palacios and Zimmerman 2007).

Seagrass restoration and transplantation has been used to accelerate the recovery of seagrass ecosystems. Turbidity of the water and amount of light reaching the seagrass canopy are usually the first parameters considered to limit seagrasses. However, currents, waves and sediment characteristics are receiving more attention as further limiting factors (Koch 2001). This work exemplifies the different sediment, above and belowground morphology, and hydrodynamic conditions necessary for a seagrass bed to survive, and must be considered as a package, instead of separate parameters acting in isolation, in order to achieve successful re-colonization. Hence, understanding how flexibility, strength, hydrodynamic conditions, and sediment characteristics interact and relate to morphology and self-shading could provide important insight as to the biophysical limitations imposed on *Zostera marina* beds. Therefore, the question is no longer whether an area has enough light for seagrasses to survive, but it becomes a question of whether the sediment that exists under certain hydrodynamic conditions can enable a seagrass of a certain morphology to survive based on the trade-offs present between nutrient uptake, epiphyte colonization, and self-shading. This illustrates the complexities of seagrasses in their fluid environment as previously mentioned by Gaylord and Denny (1997) and Denny and Gaylord (2002) for macroalgae.

Bibliography

- Beer, S. 1989. Photosynthesis and photorespiration of marine angiosperms. *Aquatic Botany* 34: 153 – 166.
- Beer, S., and E. Koch. 1996. Photosynthesis of marine macroalgae and seagrasses in globally changing CO₂ environments. *Marine Ecology Progress Series*: 199 – 204.
- Burkholder, J.M., D.A. Tomasko, and B.W. Touchette. 2007. Seagrass and eutrophication. *Journal of Experimental Marine Biology and Ecology* 350: 46 – 72.
- Cardoso, P.G., D. Raffaelli, A.I. Lillebo, T. Verdelhos, and M.A. Pardal. 2008. The impact of extreme flooding events and anthropogenic stressors on the macrobenthic communities' dynamics. *Estuarine Coastal and Shelf Science* 76: 553 – 565.
- Costanza, R., R. d'Arge, R. de Groot, S. Farberk, M. Grasso, B. Hannon, K. Limburg, S. Naeem, R.V. O'Neill, J. Paruelo, R.G. Raskin, P. Sutton, and M. van den Belt. 1997. The value of the world's ecosystem services and natural capital. *Nature* 387: 253 – 260.
- Denny, M., and B. Gaylord. 2002. The mechanics of wave-swept algae. *The Journal of Experimental Biology* 205: 1355 – 1362.
- Gaylord, B., and M.W. Denny. 1997. Flow and flexibility: Effects of size, shape and stiffness in determining waves forces on the stipitate kelps *Eisenia arborea* and *Pterygophora californica*. *The journal of Experimental Biology* 200: 3141 – 2164.
- Green, E.P. and F.T. Short. (eds.). 2003. *World Atlas of Seagrasses*. University of California Press, Berkeley, USA.
- Huettel, M., W. Ziebis, and S. Forster. 1996. Flow-induced uptake of particulate matter in permeable sediments. *Limnology and Oceanography* 41: 309 – 322.
- Huettel, M. and A. Rusch. 2000. Transport and degradation of phytoplankton in permeable sediment. *Limnology and Oceanography* 45: 534 – 549.
- Huettel, M., H. Roy, E. Precht, and S. Ehrenhauss. 2003. Hydrodynamical impact on biogeochemical processes in aquatic sediments. *Hydrobiologia* 494: 231 – 236.
- Invers, O., R.C. Zimmerman, R.S. Alberte, M. Perez, and J. Romero. 2001. Inorganic carbon sources for seagrass photosynthesis: an experimental evaluation of bicarbonate use in species inhabiting temperate waters. *Journal of Experimental Marine Biology and Ecology* 265: 203 – 217.
- Koch, E.W. 2001. Beyond Light: Physical, geological, and geochemical parameters as possible submersed aquatic vegetation habitat requirements. *Estuaries* 24: 1 – 17.
- Koch, E.W., and G. Gust. 1999. Water flow in tide- and wave-dominated beds of the seagrass *Thalassia testudinum*. *Marine Ecology Progress Series* 184: 63 – 72.
- Orth, R.J., T.J.B. Carruthers, W.C. Dennison, C.M. Duarte, J.W. Fourqurean, K.L. Heck Jr., A.R. Hughes, G.A. Kendrick, W.J. Kenworthy, S. Olyarnik, F.T. Short, M. Waycott, and S.L. Williams. 2006. A global crisis for seagrass ecosystems. *BioScience* 56: 987 – 996.

- Palacios, S.L. and R.C. Zimmerman. 2007. Response of eelgrass *Zostera marina* to CO₂ enrichment: possible impacts of climate change and potential for remediation of coastal habitats. *Marine Ecology Progress Series*: 344: 1 – 13.
- Precht, E., and M. Huettel. 2003. Advective pore-water exchange drive by surface gravity waves and its ecological implications. *Limnology and Oceanography* 48: 1674 – 1684.
- Short, F.T., and H.A. Neckles. 1999. The effects of global climate change on seagrasses. *Aquatic Botany* 63: 169 – 196.
- Short, F.T., E.W. Koch, J.C. Creed, K.M. Magalhães, E. Fernandez, and J.L. Gaeckle. 2006. SeagrassNet monitoring across the Americas: case studies of seagrass decline. *Marine Ecology* 27:277-289.
- Zimmerman, R.C. 2003. A biooptical model of irradiance distribution and photosynthesis in seagrass canopies. *Limnology and Oceanography* 48: 568 – 585.
- Zimmerman, R.C., D.G. Kohrs, D.L. Steller, and R.S. Alberte. 1997. Impacts of CO₂ enrichment of productivity and light requirements of eelgrass. *Plant Physiology* 115: 599 – 607.

Illustrations

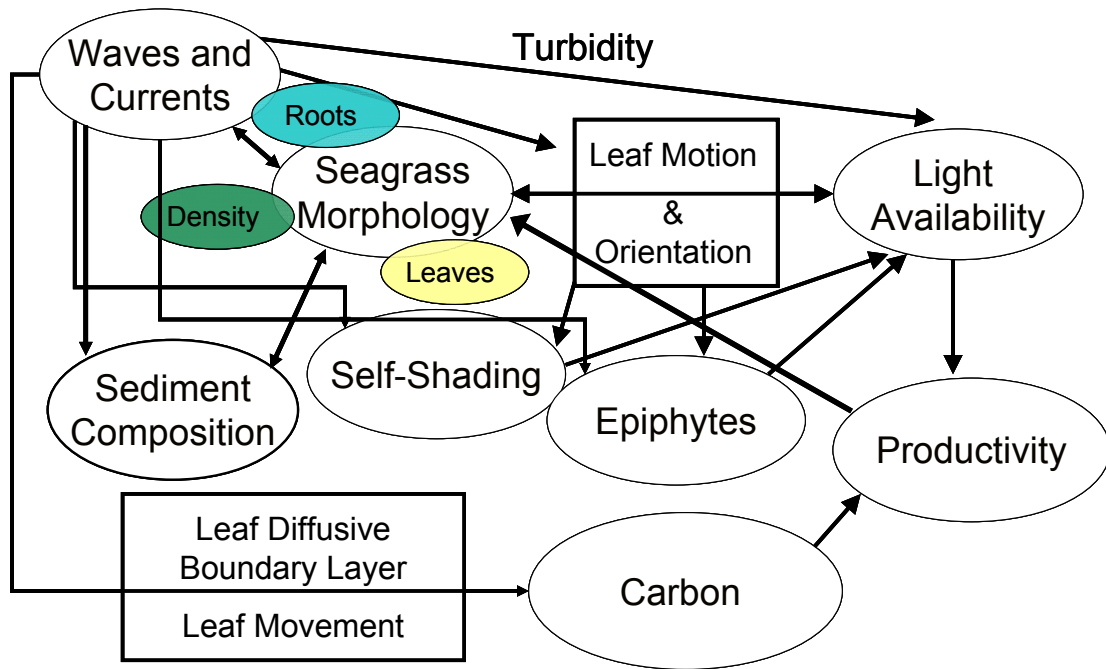


Illustration FC.1. Original schematic of how water flow and sediment affect seagrass morphology and light availability with the complexities presented in this thesis added. These complexities include self-shading, epiphyte colonization, hydrodynamically induced turbidity, leaf movement, and carbon availability, all of which contribute to the productivity of seagrass beds and are directly related to the local hydrodynamic climate.

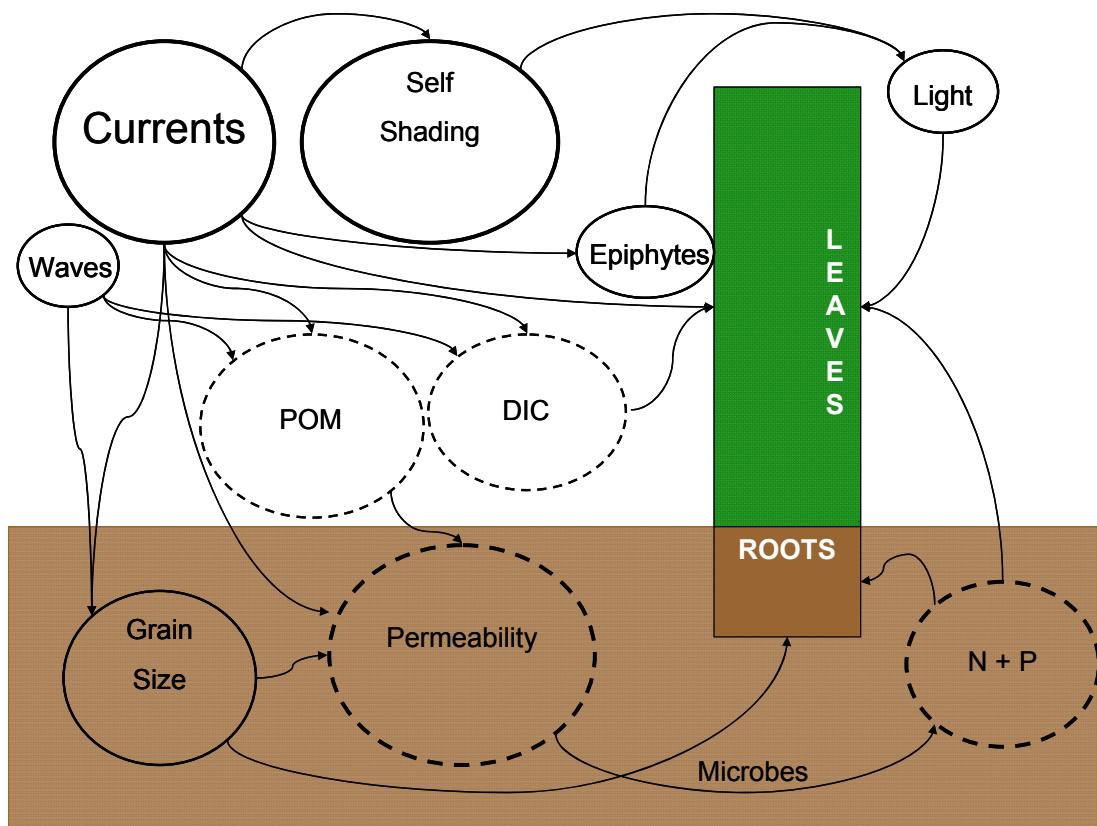


Illustration FC.3. Conceptual diagram of the advantages and disadvantages of occupying an environment dominated by strong currents, as was observed at our high current site. Solid lines represent variables that were quantified, whereas dashed lines represent hypotheses. Self-shading was high, and therefore light availability was low. Additionally, currents seemed to reduce the amount of epiphyte colonization, yet epiphytes were still present in a low abundance and therefore slightly reduced light availability to the seagrass leaves. However, we hypothesized that carbon and nitrogen availability were high due to a thin leaf diffusive boundary layer and high organic matter turnover rates in the sediment, respectively. This increase in nutrient availability in the sediment may account for the longer leaves present at this site.

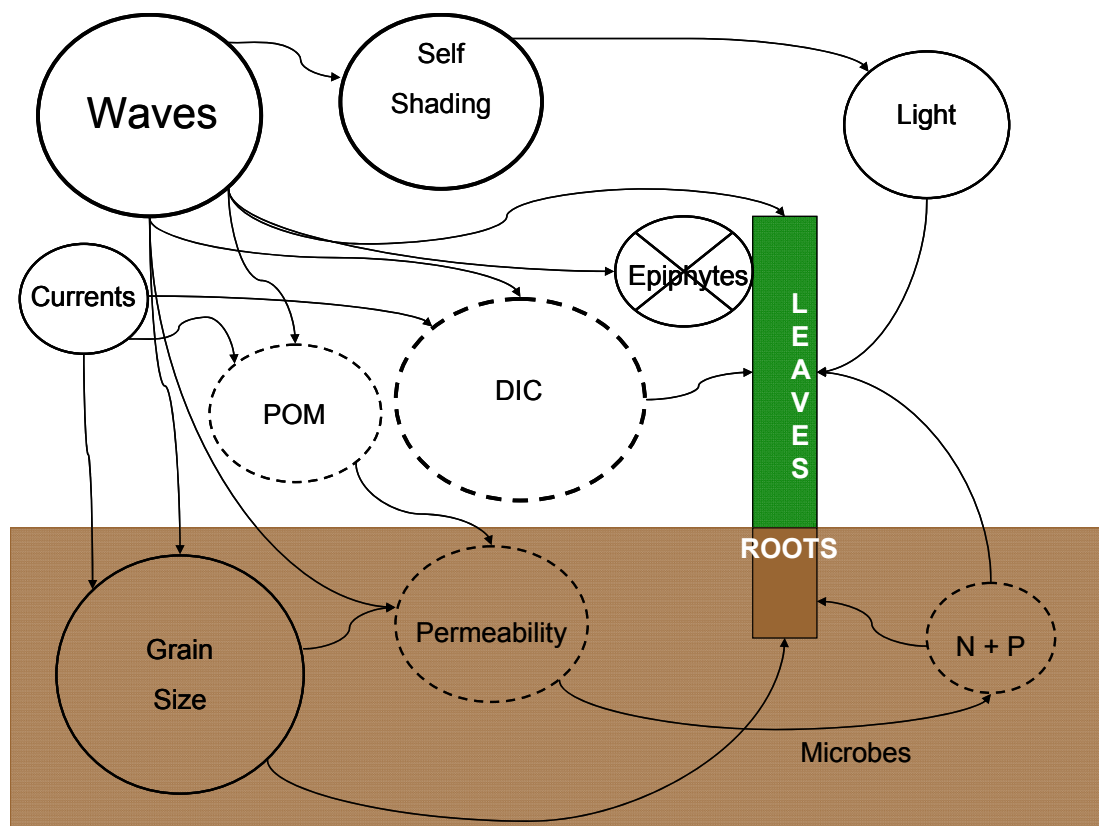


Illustration FC.4. Conceptual diagram of the advantages and disadvantages of occupying an environment dominated by waves, as was observed at our high wave site. Solid lines represent variables that were quantified, whereas dashed lines represent hypotheses. Self-shading was high, and therefore light availability to seagrass leaves was low, yet was not as low as the high current site, presumably because *Z. marina* was benefiting from the opening and closing of the canopy, which provides moments of high light availability (when the canopy is open). Additionally, wave action eliminated epiphyte colonization. We hypothesized that carbon and nitrogen availability were high due to a thin leaf diffusive boundary layer and high organic matter turnover rates in the sediment, respectively. However, at the high wave site sediment was a mixture of gravel and fine sand, which is less permeable than the sediment at the high wave site. On the other hand, *Z. marina* from the high wave site was the least carbon limited, which may account for the high shoot density present at this site.

Appendix 1: Spring versus summer morphology of the seagrass *Zostera marina*

We analyzed morphology of the seagrass *Zostera marina* in May, 2007 during preliminary data collection when plants, not patches, were used as replicates. Leaf length, width, and root length and number were quantified for 5 *Z. marina* shoots collected from the quiescent, high current, and high wave sites. Secondary leaves of *Z. marina* from the high wave site were significantly shorter than secondary leaves from the quiescent site ($p=0.0081$), whereas tertiary leaves of *Z. marina* from the high wave site were significantly shorter than tertiary leaves from the quiescent and high current sites ($p=0.0011$). Leaves of *Z. marina* from the quiescent and high current site had similar leaf lengths (Figure A1.1). These results are quite different than what we observed in July, 2007 (Chapter 1, Figure 1.7), when *Z. marina* leaves from the high current site were over 3 times longer than leaves from the quiescent and high wave site, which were found to have similar secondary and tertiary leaf lengths.

In May, secondary leaves of *Zostera marina* from the high wave site were significantly narrower ($p=0.0268$) than leaves from the quiescent and high current site, while tertiary leaves of *Z. marina* from the high wave site were significantly narrower than leaves from only the quiescent site ($p=0.0092$). *Zostera marina* leaves from the quiescent and high current site had similar leaf width when measured in May (Figure A1.2). This is similar to what we found in July in that *Z. marina* was narrower than *Z. marina* from the other two sites, yet is different as *Z. marina* from the high current site in July was wider than *Z. marina* from both the quiescent and high current sites (Chapter 1, Figure 1.8).

When root length was quantified in May, 2007, we found no significant differences between sites ($p=0.0730$) (Figure A1.3). These results differ from July, 2007 (Chapter 1, Figure 1.5), when *Z. marina* from the quiescent site was found to have significantly longer roots than *Z. marina* from the high current and high wave sites. Additionally, when root number was quantified in May, there were no significant differences between sites ($p=0.0897$) (Figure A1.4). This is also different from the root number results from July (Chapter 1, Figure 1.6), when it was found that *Z. marina* from the high current site had more roots per node than *Z. marina* from high wave site.

In regards to leaf morphology, due to the different results for root length and width of *Zostera marina* measured in May and June, our results demonstrate that *Z. marina* from the quiescent site may grow to its maximum leaf length early in the growing season, which minimizes self-shading, and then maintain this leaf length throughout the summer months. On the other hand, *Z. marina* from the high current and high wave sites may minimize self-shading in the beginning of the growing season (spring months) by having shorter leaves, and increase their leaf length (high current and high wave) and width (high current) throughout the summer as daylight hours become longer.

Root morphology of *Zostera marina* measured in May and July was also different. In Chapter 1 we concluded sediment composition, not local hydrodynamic conditions, determines root length, while local hydrodynamic conditions affect the number of roots that a *Z. marina* shoot contains, presumably in response to drag in order to aid in anchorage. The belowground biomass results from May do not

support these conclusions. However, it may be too early in the growing season for differences in belowground biomass to be observed, as young plants potentially have a greater demand to increase photosynthetic tissue that will facilitate further growth. As the growing season continues, and the plants have an increased nutrient demand, *Z. marina* from the quiescent site may produce longer roots in potentially nutrient poor, sandy sediment to meet this demand. On the other hand, *Z. marina* from the high current site, which has long and wide leaves later in the summer, may have to increase the number of roots per node in response to the potential drag that the long and wide leaves may experience.

Figures

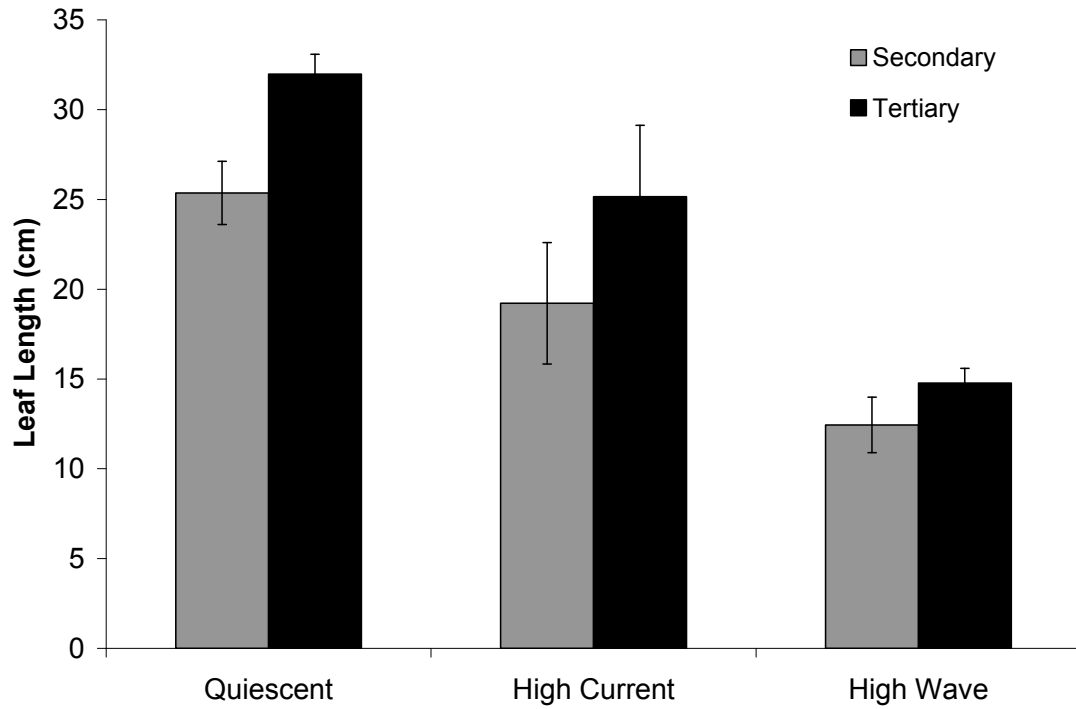


Figure A1.1. Average leaf length of the secondary (grey) and tertiary (black) leaves of *Z. marina* collected from the quiescent, high current, and high wave sites off Fisher's Island, NY in May, 2007. Error bars represent \pm S.E., n = 5.

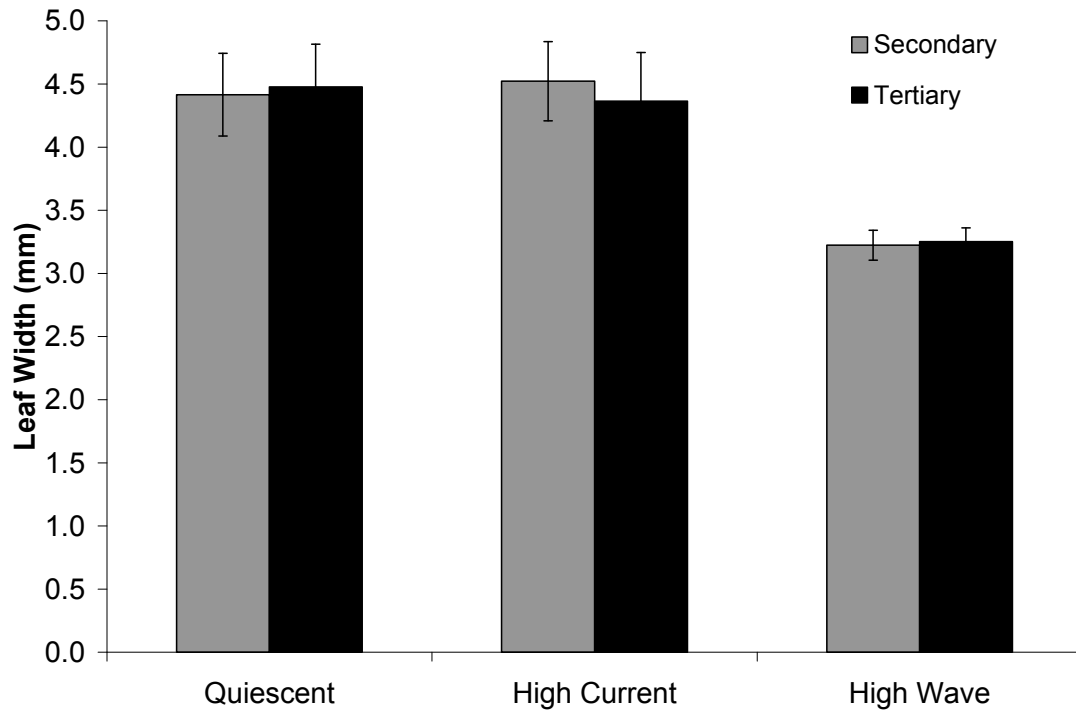


Figure A1.2. Average leaf width of the secondary (grey) and tertiary (black) leaves of *Z. marina* collected from the quiescent, high current, and high wave sites off Fisher's Island, NY in May, 2007. Error bars represent \pm S.E., n = 5.

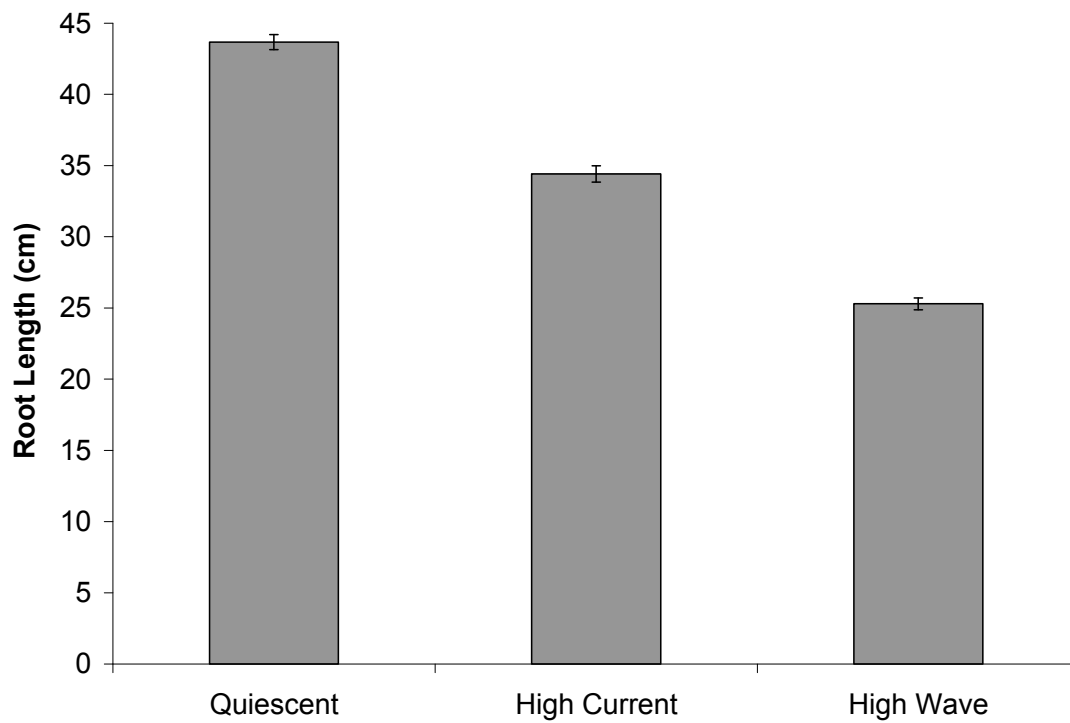


Figure A1.3. Average root length of *Z. marina* collected from the quiescent, high current, and high wave sites off Fisher's Island, NY in May, 2007. Error bars represent \pm S.E., $n = 5$.

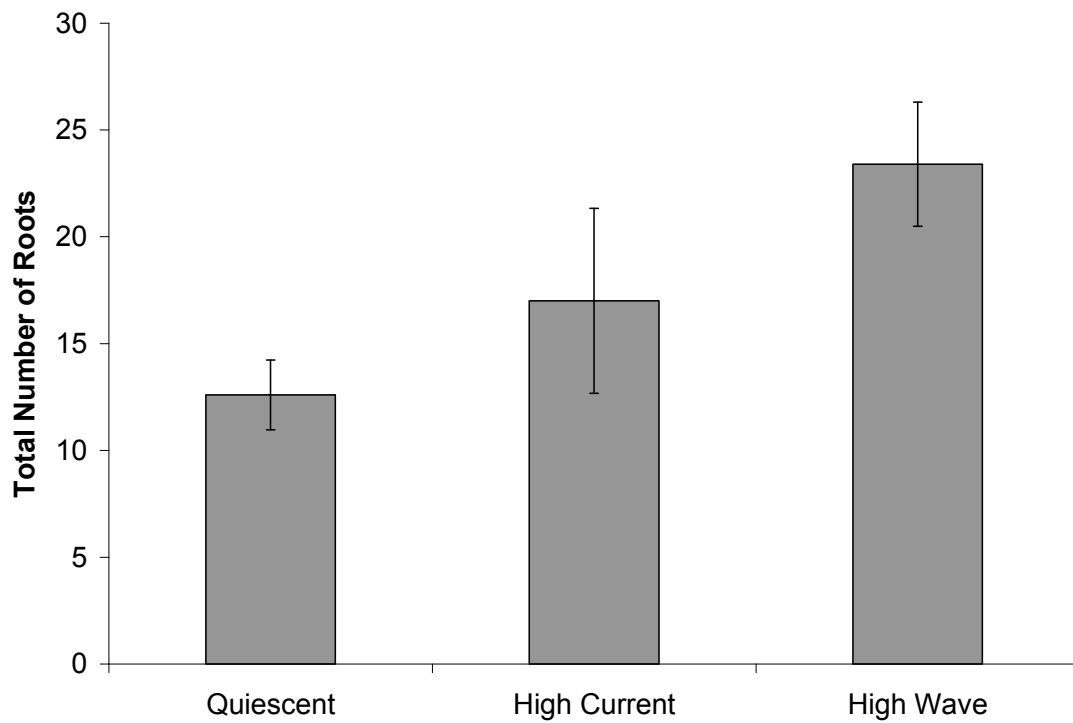


Figure A1.4. Average number of roots of *Z. marina* collected from the quiescent, high current, and high wave sites off Fisher's Island, NY in May, 2007. Error bars represent \pm S.E., $n = 5$.

Appendix 2: Linking carbon, chlorophyll, and water column nutrients (N & P) to *Zostera marina* productivity.

Parameters such as carbon content and chlorophyll concentration of *Zostera marina* leaves, and water column nutrient concentrations such as ammonia, nitrate-nitrite, and orthophosphate were quantified during field and laboratory experiments. Carbon, chlorophyll, and nutrients can all limit or enhance photosynthesis, growth, and productivity. The uptake of carbon and nutrients (nitrogen and phosphorous) has been linked to hydrodynamics conditions via the diffusive boundary layer (Koehl and Alberte 1988, Koch 1994, Koch and Beer 1996, Thomas et al. 2000, Thomas and Cornelisen 2003, Cornelisen and Thomas 2004, Morris et al. 2008), whereas chlorophyll concentration has been shown to increase with decreasing light levels, (Dennison and Alberte 1982, Cummings and Zimmerman 2003), which can result from self-shading due to local hydrodynamic conditions.

When leaf carbon content was measured in August, 2008, we found that *Zostera marina* from the high wave site had significantly higher percent carbon ($p=0.0123$) than *Z. marina* from the quiescent site (Figure A2.1). When *Z. marina* was collected in April, 2007 for the purpose of the flow tank experiment, a similar trend was found with *Z. marina* from the high wave site having significantly higher percent carbon than *Z. marina* from the high current site, which had significantly higher percent carbon than *Z. marina* from the quiescent site ($p=0.0002$) (Figure A2.2 A). After *Z. marina* had been grown under common garden conditions for 10 weeks, the trend reversed with *Z. marina* collected from the quiescent site having significantly higher percent carbon ($p=0.0010$) than *Z. marina* from the high wave site (Figure A2.2 B). These results support our $\delta^{13}\text{C}$ and percent carbon data (Chapter

2, Figure 2.10), and demonstrate that *Z. marina* from the quiescent site was more carbon limited than *Z. marina* from the high current and high wave site. Therefore, currents and waves do indeed effectively reduce the diffusive boundary layer promoting the uptake of carbon from the water column (Koehl and Alberte 1988, Koch 1994, Koch and Beer 1996) as demonstrated here and in Chapter 2.

Seagrasses have the ability to take up nutrients from both the sediment via their roots (Zimmerman et al. 1987, Hasegawa et al. 2005, Hasegawa et al. 2008) and the water column via their leaves (Zimmerman et al. 1987, Hasegawa et al. 2005, Cornelisen and Thomas 2004). Whether the uptake of nutrients is from the sediment or the water column depends upon the relative abundance of dissolved inorganic nitrogen (DIN) that each medium contains. It was observed that the uptake of DIN via seagrass leaves was high in the fall and winter when DIN concentrations in the water column were greater than those of the sediment; conversely, the uptake of DIN via seagrass roots was high in the spring and winter when DIN concentrations in the sediment exceeded those of the water column (Hasegawa et al. 2005). Therefore, water column nutrient concentrations can also effectively alter seagrass productivity.

When water column nutrients were examined at each field site in April, 2008, concentration of nitrate in the water column was found to be significantly lower ($p=0.0002$) at the high wave site when compared to the quiescent and high current sites (Figure A2.3 A). However, no significant differences between sites was found for water column ammonia (Figure A2.3 A, $p=0.3406$) or orthophosphate (Figure A2.3 B, $p=0.5322$) concentrations.

When *Zostera marina* was grown under common garden conditions, there was a significant interaction between time and tank ($p < 0.0001$) for ammonia, nitrate-nitrite, and orthophosphate concentrations, demonstrating that water-column nutrient concentrations were variable over time and that the variability was not tank specific as nutrient concentrations also varied between tanks. Therefore, none of the 6 tanks were found to have a nutrient advantage. Ammonia concentrations were variable over time, but *Z. marina* from each field site was not found to be exposed to significantly higher ammonia concentrations throughout the course of the experiment (Figure A2.4 A). Nitrate-nitrite concentrations were significantly higher during week 3, and then were consistently lower weeks 5 through 9. Despite changes in nitrate-nitrite concentrations over time, *Z. marina* leaves from each site were not exposed to significantly higher nitrate-nitrite concentrations over the course of the experiment (Figure A2.4 B). Lastly, orthophosphate concentrations were variable over time, but *Z. marina* leaves from each field site were not found to be exposed to significantly higher orthophosphate concentrations throughout the course of the experiment (Figure A2.5).

Since *Zostera marina* from the quiescent, high current, and high wave sites were not exposed to significantly different water column nutrients in both the field and laboratory, it can be concluded that differences in morphology such as leaf length, width, and density are not a result of higher nutrient concentrations being available to *Z. marina* from a particular field site or by being placed in a particular tank. The one exception is that *Z. marina* from the high wave site was exposed to significantly lower concentrations of nitrate-nitrite in the field, yet it was found that

Z. marina from the quiescent site was more nitrogen limited than *Z. marina* from the high wave site ($\delta^{15}\text{N}$ data, Chapter 2, Figure 2.11). Therefore, it does not seem probable that the lower water column nitrate-nitrite concentrations that *Z. marina* from the high wave site experienced limited its productivity. Additionally, nitrate-nitrite concentrations were greatly reduced after week 3 of the flow tank experiment, presumably due to an increase in phytoplankton communities in the Choptank River around that time of the year, which took up water column nutrients. Therefore, *Z. marina* shoots may have been slightly nutrient limited during the tank experiment after week 3. Despite being potentially nutrient limited, differences in leaf length and width were still present between sites, possibly demonstrating further that increased length and width of *Z. marina* from the high current site is an adaptation, not acclimation, to water flow.

Chlorophyll a concentration was examined for *Zostera marina* leaves collected from the quiescent, high current, and high wave sites in August, 2007. No significant differences were found between sites ($p=0.2810$) despite varying light availability to *Z. marina* leaves at each site (Figure A2.6).

When *Z. marina* was collected from the quiescent, high current, and high wave sites in April, 2008 for the flow tank experiment, there were no significant differences between sites in regards to chlorophyll a concentration initially or throughout the course of the experiment ($p=0.3262$) (Figure A2.7). However, chlorophyll a concentrations did vary over time, as chlorophyll a concentrations significantly decreased between the initial collection and week 2 ($p=0.0016$), but no significant differences were present between weeks 2, 5, and 10 (Figure A2.7).

Although it has been demonstrated that seagrasses photoacclimate to varying light environments via several mechanisms such as altering their pigment content or by changing the concentration of pigments such as chlorophyll a and b (Dennison and Alberte 1982, Cummings and Zimmerman 2003), we did not observe different concentrations of chlorophyll a between sites, suggesting that *Z. marina* from Long Island sound was optimizing light harvesting by a different mechanism. Additionally, it has been demonstrated that, since chloroplasts in seagrasses are located in the epidermis only, an increase in pigment content does not lead to a linear increase in light harvesting efficiency because of the package effect in which self-shading occurs on a chloroplast level (Cummings and Zimmerman 2003). Therefore, since water quality and light levels were high at our field sites, and low light availability was a result of self-shading on a canopy level, it may not be energetically efficient to increase chlorophyll a concentrations, as when light does reach a chloroplast, it is well above the saturating light level, and having a shaded chloroplast would be detrimental to light harvesting efficiency.

Carbon availability, water column nutrients, and chlorophyll a concentration all have the potential to alter the overall productivity of a seagrass bed, and can be altered by the local hydrodynamic environment. We did indeed observe that *Zostera marina* tissue from the quiescent site had reduced percent carbon when compared to *Z. marina* from the high current and high wave sites, which has been linked to a thick diffusive boundary layer that accompanies habitats characterized by low water flow (Koehl and Alberte 1988, Koch 1994, Koch and Beer 1996).

Although differences in carbon content were observed, *Zostera marina* from the quiescent, high current, and high wave sites were not found to experience different water column nutrient concentrations or have altered pigment content. Therefore, differences in leaf length and width, density, root length and number, and varying photosynthetic capacity present between sites was a result of varying hydrodynamic conditions, sediment composition, and the potential uptake and regeneration of carbon and nutrients as a result of these different habitat conditions.

Bibliography

- Cornelisen, C.D., and F.I.M. Thomas. 2004. Ammonium and nitrate uptake by leaves of the seagrass *Thalassia testudinum*: impact of hydrodynamic regime and epiphyte cover on uptake rate. *Journal of Marine Systems* 49: 177 – 194.
- Cummings, M.E. and Zimmerman, R.C. 2003. Light harvesting and the package effect in the seagrasses *Thalassia testudinum* Banks ex König and *Zostera marina* L.: optical constraints on photoacclimation. *Aquatic Botany* 75: 261 – 274.
- Dennison, W.C. and R.S. Alberte. 1982. Photosynthetic responses of *Zostera marina* L. (Eelgrass) to *in situ* manipulations of light intensity. *Oecologia (Berl)* 55: 137 – 144.
- Hasegawa, N., H. Iizumi, M. Mukai. 2005. Nitrogen dynamics of the surfgrass *Phyllospadix iwatensis*. *Marine Ecology Progress Series* 293: 59 – 68.
- Hasegawa N., M. Hori, H. Mukai. 2008. Seasonal changes in eelgrass functions: Current velocity reduction, prevention of sediment resuspension, and quiescent of sediment-water column nutrient flux in relation to eelgrass dynamics. *Hydrobiologia* 596: 387 – 399.
- Koch, E.W. 1994. Hydrodynamics, diffusion-boundary layers and photosynthesis of the seagrasses *Thalassia testudinum* and *Cymodocea nodosa*. *Marine Biology* 118: 767 – 776.
- Koch, E.W., and S. Beer. 1996. Tides, light and the distribution of *Zostera marina* in Long Island Sound, USA. *Aquatic Botany* 53: 97 – 107.
- Koehl, M.A.R., and R.S. Alberte. 1988. Flow, flapping, and photosynthesis of *Nereocystis luetkeana*: a functional comparison of undulate and flat blade morphologies. *Marine Biology* 99: 435 – 444.
- Morris, E.P., G. Peralta, F.G. Brun, L. van Duren, T.J. Bouma, and J.L. Perez-Llorens. 2008. Interaction between hydrodynamics and seagrass canopy structure: Spatially explicit effects on ammonium uptake rates. *Limnology and Oceanography* 53: 1531 – 1539.
- Thomas, F.I.M., C.D. Cornelisen, and J.M. Zande. 2000. Effects of water velocity and canopy morphology on ammonium uptake by seagrass communities. *Ecology* 81: 2704 – 2713.
- Thomas, F.I.M., and C.D. Cornelisen. 2003. Ammonium uptake by seagrass communities: effects of oscillatory versus unidirectional flow. *Marine Ecology Progress Series* 247: 51 – 57.
- Zimmerman, R.C., R.D. Smith, R.S. Alberte. 1987. Is growth of eelgrass nitrogen limited? A numerical simulation of the effects of light and nitrogen on the growth dynamics of *Zostera marina*. *Marine Ecology Progress Series* 41: 167 – 176.

Figures

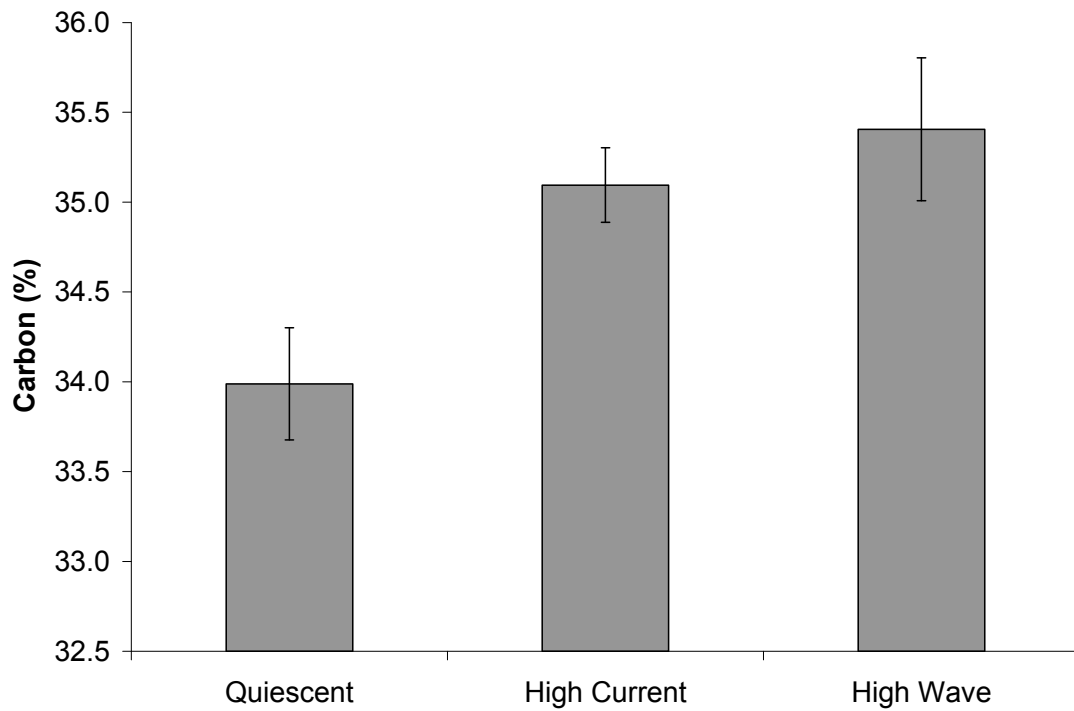


Figure A2.1. Average carbon (%) content of *Z. marina* leaves collected from the quiescent, high current, and high wave sites off Fisher's Island, NY in August, 2007. Error bars represent +/- S.E., n = 5.

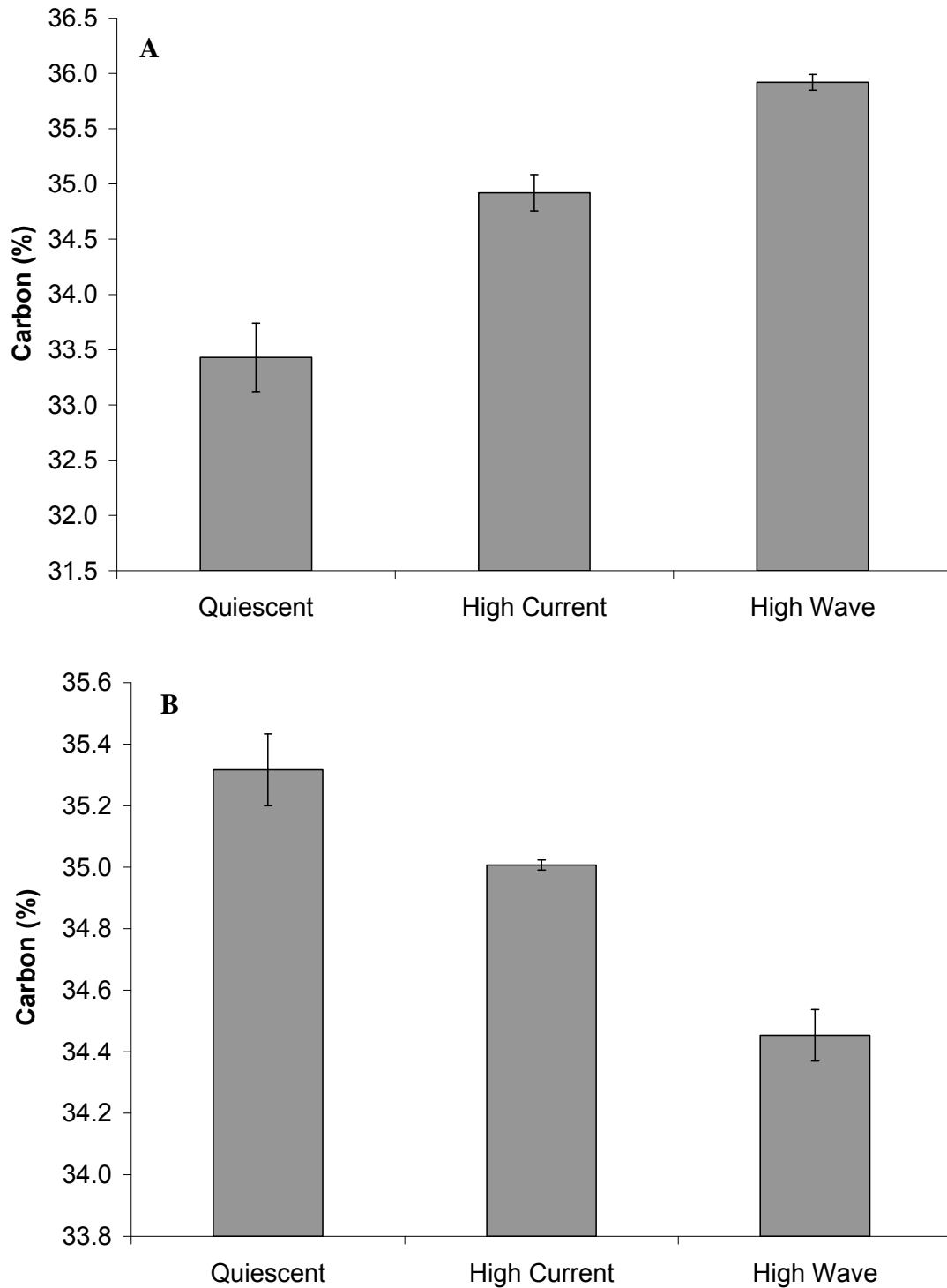


Figure A2.2. Average carbon (%) content of *Z. marina* collected at the quiescent, high current, and high wave sites off Fisher's Island, NY in April, 2008 for the purpose of the flow tank experiment A) initially and B) after 10 weeks of growing under common garden conditions. Error bars represent +/- S.E., n = 4.

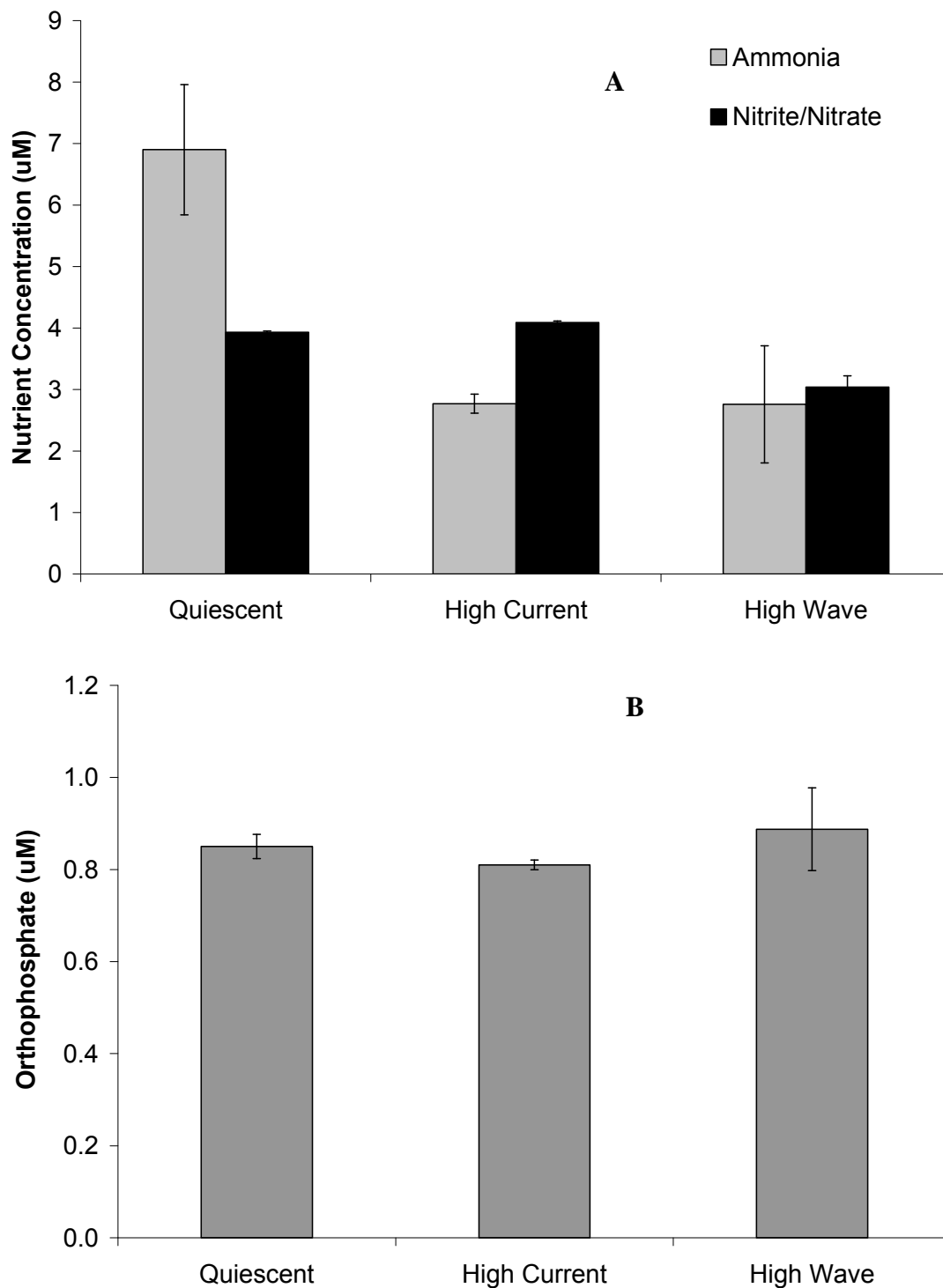


Figure A2.3. Average water column A) ammonia (μM), nitrate-nitrite (μM), and B) orthophosphate (μM) concentrations collected at the surface from the quiescent, high current, and high wave sites off Fisher's Island, NY in April, 2008. Error bars represent \pm S.E., $n = 4$.

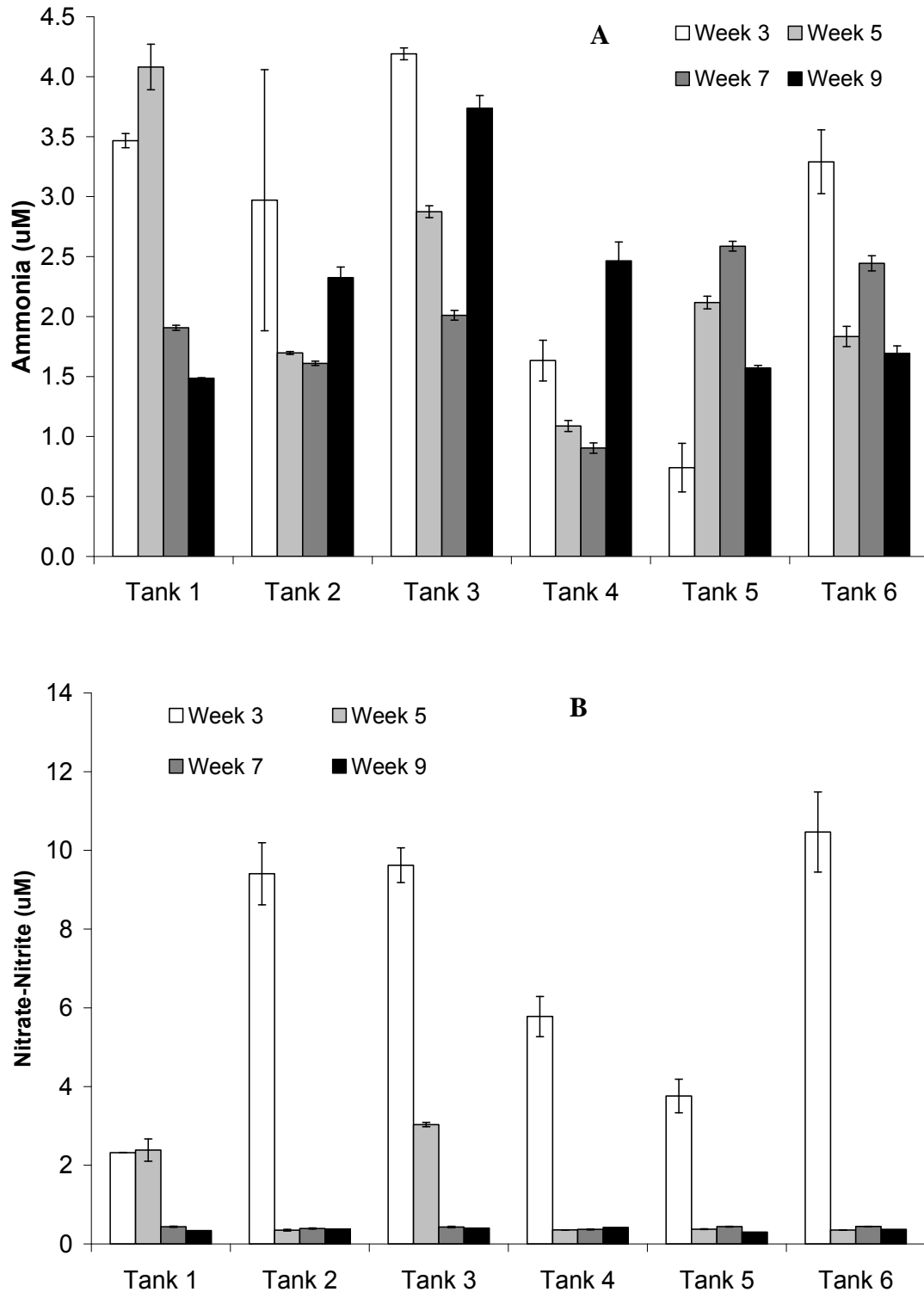


Figure A2.4. Average water column A) ammonia (μM) and B) nitrate-nitrite (μM) concentrations that *Z. marina* shoots experienced in each tank at weeks 3, 5, 7 and 9 of the flow tank experiment. Error bars represent \pm S.E., $n = 1 - 4$.

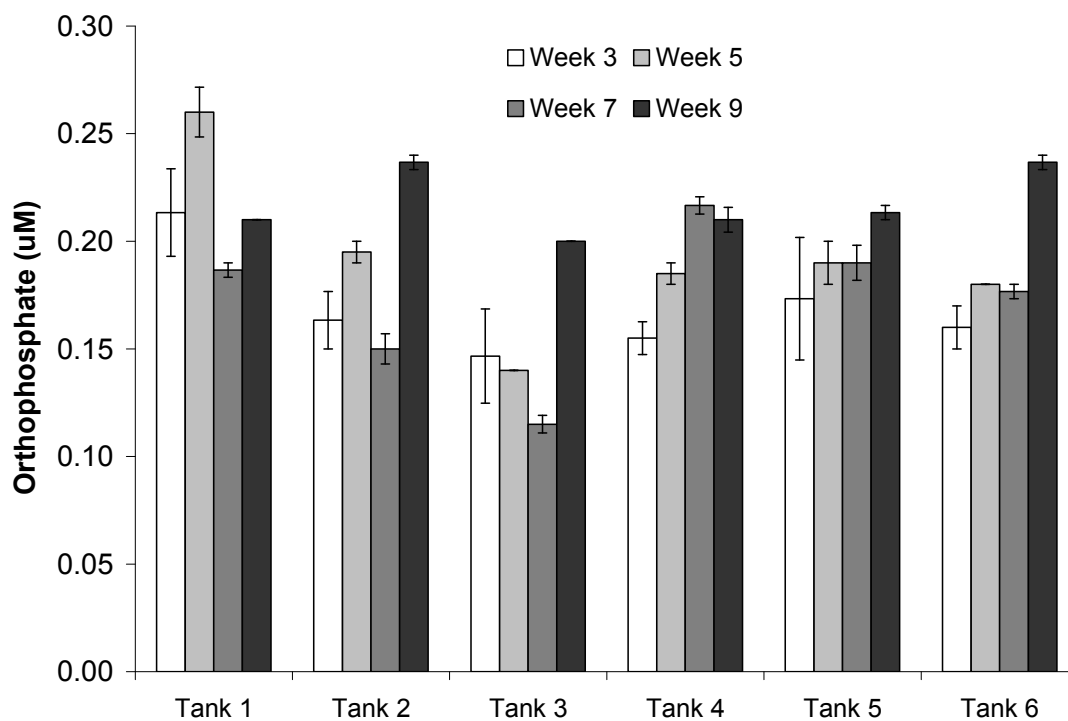


Figure A2.5. Average water column orthophosphate (μM) concentrations that *Z. marina* shoots experienced in each tank at weeks 3, 5, 7 and 9 of the flow tank experiment. Error bars represent \pm S.E., $n = 1 - 4$.

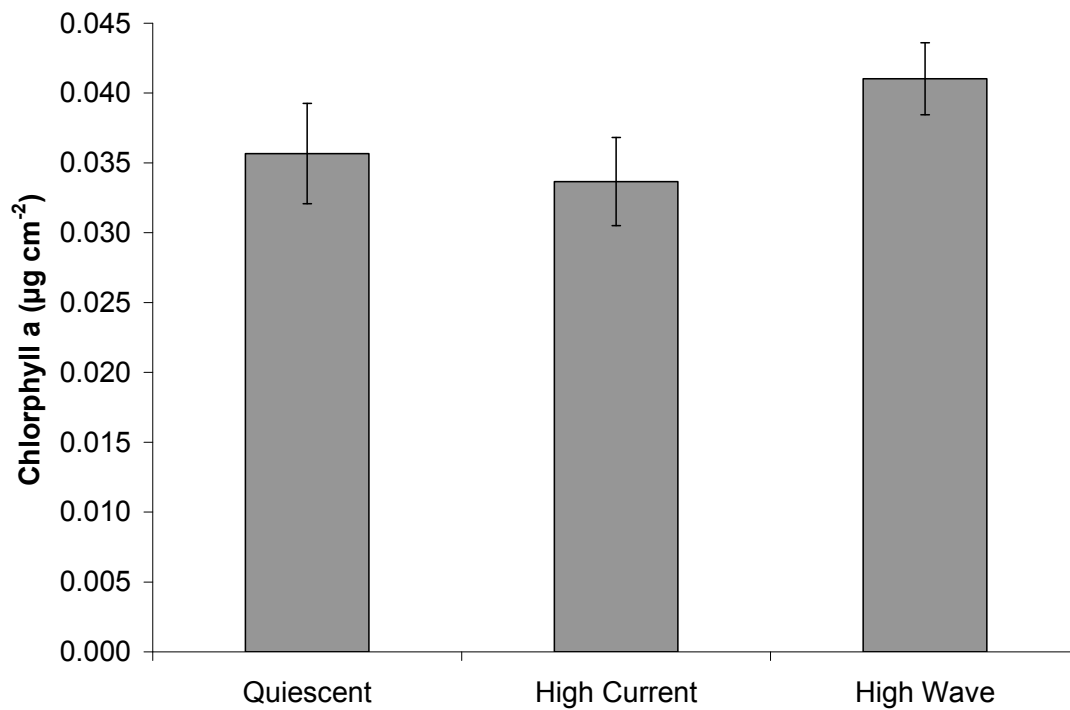


Figure A2.6. Average chlorophyll a concentration ($\mu\text{g cm}^{-2}$) of the tertiary leaf of *Z. marina* collected from the quiescent, high current, and high wave sites in August, 2007. Error bars represent \pm S.E., $n = 4$.

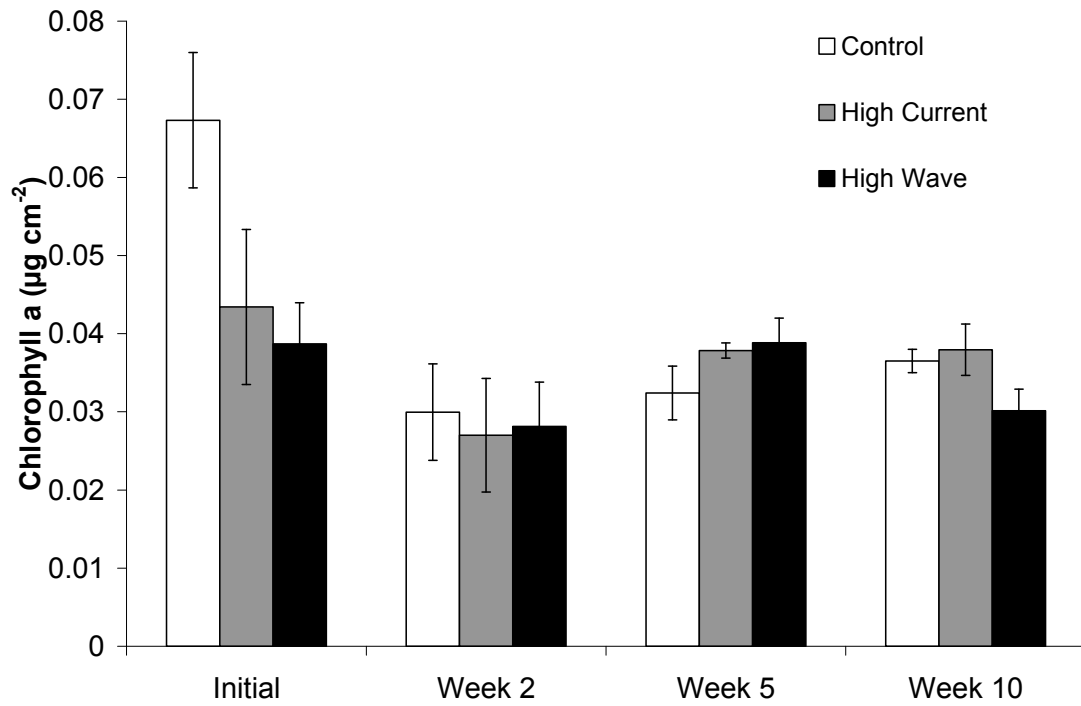


Figure A2.7. Average chlorophyll a concentration ($\mu\text{g cm}^{-2}$) of the tertiary leaf of *Z. marina* collected from the quiescent, high current, and high wave sites in April, 2008 and then planted in common garden conditions. Analysis of chlorophyll a was done initially and at weeks 2, 5 and 10. Error bars represent \pm S.E., $n = 4$.

Complete Bibliography

- Abdelrhman, M.A. 2007. Modeling coupling between eelgrass *Zostera marina* and water flow. Marine Ecology Progress Series 228: 81 – 96.
- Ackerman, J.D. 1986. Mechanistic implications for pollination in the marine angiosperm *Zostera marina*. Aquatic Botany 24: 343 – 353.
- Ackerman, J.D., and A. Okubo. 1993. Reduced mixing in a marine macrophyte canopy. Functional Ecology 7: 305 – 309.
- Barr, G.N., A. Kloeppel, T.A.V. Rees, C. Scherer, R.B. Taylor, and A. Wenzel. 2008. Wave surge increases rates of growth and nutrient uptake in the green seaweed *Ulva pertusa* maintained at low bulk flow velocities. Aquatic Biology 3: 179 – 186.
- Bell, E.C. and M.W. Denny. (1994) Quantifying "wave exposure": a simple device for recording maximum velocity and results of its use at several field sites. Journal of Experimental Biology and Ecology. 181: 9 – 29.
- Beer, S. 1989. Photosynthesis and photorespiration of marine angiosperms. Aquatic Botany 34: 153 – 166.
- Beer, S., and E. Koch. 1996. Photosynthesis of marine macroalgae and seagrasses in globally changing CO₂ environments. Marine Ecology Progress Series: 199 – 204.
- Binzer, T., and K. Sand-Jensen. 2002. Production in aquatic macrophyte communities: A theoretical and empirical study of the influence of spatial light distribution. Limnology and Oceanography 47: 1742 – 1750.
- Bouma, T.J., M.B De Vries, E. Low, G. Peralta, I.C. Tanczos, J. van de Koppel, and P.M.J. Herman. 2005. Trade-offs related to ecosystem engineering: A case study on stiffness of emerging macrophytes. Ecology 86: 2187 – 2199.
- Brown, E., A. Colling, D. Park, J. Phillips, D. Rothery, and J. Wright. 1999. Wave, Tides, and Shallow-Water Processes, 2nd Edition. Butterworth-Heinemann in association with The Open University, Oxford. Pp 11 – 49.
- Burkholder, J.M., D.A. Tomasko, and B.W. Touchette. 2007. Seagrass and eutrophication. Journal of Experimental Marine Biology and Ecology 350: 46 – 72.
- Cardoso, P.G., D. Raffaelli, A.I. Lillebo, T. Verdelhos, and M.A. Pardal. 2008. The impact of extreme flooding events and anthropogenic stressors on the macrobenthic communities' dynamics. Estuarine Coastal and Shelf Science 76: 553 – 565.
- Christiansen, C., H. Christoffersen, and S.E. Knud. 1981. Hydrography, sediments, and sedimentation in a low-energy embayment, Knebel Vig, Denmark. Geografiska Annaler Series A, Physical Geography 63: 95 – 103.
- Cooper, L.W., and C.P. McRoy. 1988. Anatomical adaptations to rocky substrates and surf exposure by the seagrass genus *Phyllospadix*. Aquatic Botany 32: 365 – 381.
- Cornelisen, C.D., and F.I.M. Thomas. 2004. Ammonium and nitrate uptake by leaves of the seagrass *Thalassia testudinum*: impact of hydrodynamic regime and epiphyte cover on uptake rate. Journal of Marine Systems 49: 177 – 194.

- Costanza, R., R. d'Arge, R. de Groot, S. Farberk, M. Grasso, B. Hannon, K. Limburg, S. Naeem, R.V. O'Neill, J. Paruelo, R.G. Raskin, P. Sutton, and M. van den Belt. 1997. The value of the world's ecosystem services and natural capital. *Nature* 387: 253 – 260.
- Cummings, M.E. and Zimmerman, R.C. 2003. Light harvesting and the package effect in the seagrasses *Thalassia testudinum* Banks ex König and *Zostera marina* L.: optical constraints on photoacclimation. *Aquatic Botany* 75: 261 – 274.
- Cunha, A.H., and C.M. Duarte. 2007. Biomass and leaf dynamics of *Cymodocea nodosa* in the Ria Formosa lagoon, South Portugal. *Botanica Marina* 50: 1 – 7.
- Den Hartog, C. 1970. *The Seagrasses of the World*. North-Holland Publishers, Amsterdam.
- Denman, K.L. 1975. *Spectral analysis: A summary of the theory and techniques*. Fisheries and Marine Service, Technical Report N. 539.
- Dennison, W.C. and R.S. Alberte. 1982. Photosynthetic responses of *Zostera marina* L. (Eelgrass) to *in situ* manipulations of light intensity. *Oecologia (Berl)* 55: 137 – 144.
- Denny, M., and B. Gaylord. 2002. The mechanics of wave-swept algae. *The Journal of Experimental Biology* 205: 1355 – 1362.
- Denny, M., and L. Roberson. 2002. Blade motion and nutrient flux to the kelp *Eisenia arborea*. *Biological Bulletin* 203: 1 – 13.
- Di Carlo, G., F. Badalamenti, A. Terlizzi. 2007. Recruitment of *Posidonia oceanica* on rubble mounds: Substratum effects on biomass partitioning and leaf morphology. *Aquatic Botany* 87: 97 – 103.
- Duarte, C.M. 1990. Seagrass nutrient content. *Marine Ecology Progress Series* 67: 201 – 207.
- Duarte, C.M. and H. Kirkman. 2003. Methods for the measurement of seagrass abundance and depth distribution. In: Short, F.T. and R.G. Coles (eds.), *Global Seagrass Research Methods*, Elsevier Science, Amsterdam. Pp 141 – 153.
- Erflemeijer, P.L.A. and Koch, E.W. 2003. Measurements of Physical Parameters in Seagrass Habitats. In: Short, F.T. and R.G. Coles (eds.), *Global Seagrass Research Methods*, Elsevier Science, Amsterdam. Pp 345 – 367.
- Fonseca, M.S., J.S. Fisher, J.C. Zieman, and G.W. Thayer. 1982. Influence of the seagrass, *Zostera marina* L., on current flow. *Coastal and Shelf Science* 15: 351 – 364.
- Fonseca, M.S., Zieman, J.C., G.W. Thayer, and J.S. Fisher. 1983. The role of current velocity in structuring eelgrass (*Zostera marina* L.) meadows. *Estuarine and Coastal Shelf Sciences* 17: 367 – 380.
- Fonseca, M.S., and W.J. Kenworthy. 1987. Effects of current on photosynthesis and distribution of seagrasses. *Aquatic Botany* 27: 59 – 78.
- Fonseca, M.S., M.A.R. Koehl, and B.S. Kopp. 2007. Biomechanical factors contributing to self-organization in seagrass landscapes. *Journal of Experimental Marine Biology and Ecology* 340: 227 – 246.

- Gambi, M.C., A.R.M. Nowell, and P.A. Jumars. 1990. Flume observations on flow dynamics in *Zostera marina* (eelgrass) beds. *Marine Ecology Progress Series* 61: 159 – 169.
- Gaylord, B., and M.W. Denny. 1997. Flow and flexibility: Effects of size, shape and stiffness in determining waves forces on the stipitate kelps *Eisenia arborea* and *Pterygophora californica*. *The journal of Experimental Biology* 200: 3141 – 2164.
- Gerard, V.A. 1982. *In situ* water motion and nutrient uptake by the giant kelp *Macrocystis pyrifera*. *Marine Biology* 69: 51 – 54.
- Gerard, V.A., and K.H. Mann. 1979. Growth and production of *Laminaria longicruris* (Phaeophyta) populations exposed to different intensities of water movement. *Journal of Phycology* 15: 33 – 41.
- Ghisalberti, M., and H.M. Nepf. 2002. Mixing layers and coherent structures in vegetated aquatic flows. *Journal of Geophysical Research* 107: C2, 3011.
- Green, E.P. and F.T. Short. (eds.). 2003. *World Atlas of Seagrasses*. University of California Press, Berkeley, USA.
- Grice, A.M., N.R. Loneragan, W.C. Dennison. 1996. Light intensity and the interactions between physiology, morphology and stable isotope ratios in five species of seagrass. *Journal of Experimental Marine Biology and Ecology* 195: 91 – 110.
- Grizzle, R.E., F.T. Short, C.R. Newell, H. Hoven, and L. Kindblom. 1996. Hydrodynamically induced synchronous waving of seagrasses: ‘monami’ and its possible effects on larval mussel settlement. *Journal of Experimental Marine Biology and Ecology* 206: 165 – 177.
- Harring, R.N. and R.C. Carpenter. 2007. Habitat-induced morphological variation influences photosynthesis and drag on the marine macroalga *Pachydictyon coriaceum*. *Marine Biology* 151: 243 – 255.
- Hasegawa, N., H. Iizumi, M. Mukai. 2005. Nitrogen dynamics of the surfgrass *Phyllospadix iwatensis*. *Marine Ecology Progress Series* 293: 59 – 68.
- Hasegawa N., M. Hori, H. Mukai. 2008. Seasonal changes in eelgrass functions: Current velocity reduction, prevention of sediment resuspension, and quiescent of sediment-water column nutrient flux in relation to eelgrass dynamics. *Hydrobiologia* 596: 387 – 399.
- Hendriks, I.E., T. Sintes, T.J. Bouma, C.M. Duarte. 2008. Experimental assessment and modeling evaluation of the effects of the seagrass *Posidonia oceanica* on flow and particle trapping. *Marine Ecology Progress Series* 356: 163 – 173.
- Højerslev, N. 1975. A spectral light absorption meter for measurement in the sea. *Limnology and Oceanography* 20: 1024 – 1034.
- Holbrook, N.M., and F.E. Putz. 1989. Influence of neighbors on tree form: effects of lateral shade and prevention of sway on the allometry of *Liquidambar styraciflua* (sweet gum). *American Journal of Botany* 76: 1740 – 1749.
- Huettel, M., W. Ziebis, and S. Forster. 1996. Flow-induced uptake of particulate matter in permeable sediments. *Limnology and Oceanography* 41: 309 – 322.
- Huettel, M. and A. Rusch. 2000. Transport and degradation of phytoplankton in permeable sediment. *Limnology and Oceanography* 45: 534 – 549.

- Huettel, M., H. Roy, E. Precht, and S. Ehrenhauss. 2003. Hydrodynamical impact on biogeochemical processes in aquatic sediments. *Hydrobiologia* 494: 231 – 236.
- Infantes, E., J. Terrados, A. Orfila, B. Canellas, and A. Alvarez-Ellacuria. 2009. Wave energy and the upper depth limit distribution of *Posidonia oceanica*. *Botanica Marina* 52: In Press.
- Invers, O., R.C. Zimmerman, R.S. Alberte, M. Perez, and J. Romero. 2001. Inorganic carbon sources for seagrass photosynthesis: an experimental evaluation of bicarbonate use in species inhabiting temperate waters. *Journal of Experimental Marine Biology and Ecology* 265: 203 – 217.
- Jordan, T. 2008. Acclimation of two marine macrophytes (*Saccharina latissima* and *Zostera marina*) to water flow. Masters of Science Thesis. University of Maryland, Center for Environmental Sciences, Horn Point Laboratory. Cambridge, MD.
- Kawamata, S. 2001. Adaptive mechanical tolerance and dislodgement velocity of the kelp *Laminaria japonica* in wave-induced water motion. *Marine Ecology Progress Series* 211: 89 – 104.
- Kirk, John T.O. 1983. Light and photosynthesis in aquatic ecosystems. Cambridge University Press, Cambridge, Great Britain.
- Koch, E.W. 1994. Hydrodynamics, diffusion-boundary layers and photosynthesis of the seagrasses *Thalassia testudinum* and *Cymodocea nodosa*. *Marine Biology* 118: 767 – 776.
- Koch, E.W. 1999. Preliminary evidence on the interdependent effect of currents and porewater geochemistry on *Thalassia testudinum* Banks ex König seedlings. *Aquatic Botany* 63: 95 – 102.
- Koch, E.W. 2001. Beyond Light: Physical, geological, and geochemical parameters as possible submersed aquatic vegetation habitat requirements. *Estuaries* 24: 1 – 17.
- Koch, E.W., and S. Beer. 1996. Tides, light and the distribution of *Zostera marina* in Long Island Sound, USA. *Aquatic Botany* 53: 97 – 107.
- Koch, E.W., and G. Gust. 1999. Water flow in tide- and wave-dominated beds of the seagrass *Thalassia testudinum*. *Marine Ecology Progress Series* 184: 63 – 72.
- Koch, E.W., and M. Huettel. 2000. The impact of single seagrass shoots on solute fluxes between the water column and permeable sediments. *Biologia Marina Mediterranea* 7: 235 – 239.
- Koch, E.W., E.B. Barbier, B.R. Silliman, D.J. Reed, G.M.E. Perillo, S.D. Hacker, E.F. Granek, J.H. Primavera, N. Muthiga, S. Polasky, B.S. Halpern, C.J. Kennedy, C. V. Kappel, and E. Wolanski. 2009. Non-linearity in ecosystem services: temporal and spatial variability in coastal protection. *Frontiers in Ecology and the Environment* 7: 29 – 37.
- Koehl, M.A.R. 1994. Biomechanics of microscopic appendages: Functional shifts caused by changes in speed. *Journal of Biomechanics* 37: 789 – 795.
- Koehl, M.A.R. 1996. When does morphology matter? *Annual Review of Ecology Systems* 27: 501 – 542.
- Koehl, M.A.R., and S.A. Wainwright. 1977. Adaptations of a giant kelp. *Limnology and Oceanography* 22: 1067 – 1071.

- Koehl, M.A.R., and R.S. Alberte. 1988. Flow, flapping, and photosynthesis of *Nereocystis luetkeana*: a functional comparison of undulate and flat blade morphologies. *Marine Biology* 99: 435 – 444.
- Lavery, P.S., T. Reid, G.A. Hyndes, and B.R. van Elven. 2007. Effect of leaf movement on epiphytic algal biomass of seagrass leaves. *Marine Ecology Progress Series* 338: 97 – 106.
- Marbà, N., and C.M. Duarte. 2003. Scaling of ramet size and spacing in seagrasses: implication for stand development. *Aquatic Botany* 77: 87 – 98.
- Milligan K.L.D. and R.E. DeWreede. 2004. Morphological variations do not effectively reduce drag forces at high wave-exposure for the macroalgal species, *Hedophyllum sessile* (Laminariales, Phaeophyta). *Phycologia* 43: 236 – 244.
- Molloy, F.J., and J.J. Bolton. 1996. The effects of wave exposure and depth on the morphology of inshore populations of the Namibian Kelp, *Laminaria schinzii* Foslie. *Botanica Marina* 39: 525 – 531.
- Morris, E.P., G. Peralta, F.G. Brun, L. van Duren, T.J. Bouma, and J.L. Perez-Llorens. 2008. Interaction between hydrodynamics and seagrass canopy structure: Spatially explicit effects on ammonium uptake rates. *Limnology and Oceanography* 53: 1531 – 1539.
- Nepf, H.M. and E.W. Koch. 1999. Vertical secondary flows in submersed plant-like arrays. *Limnology and Oceanography* 44: 1072 – 1080.
- Orth, R.J., T.J.B. Carruthers, W.C. Dennison, C.M. Duarte, J.W. Fourqurean, K.L. Heck Jr., A.R. Hughes, G.A. Kendrick, W.J. Kenworthy, S. Olyarnik, F.T. Short, M. Waycott, and S.L. Williams. 2006. A global crisis for seagrass ecosystems. *BioScience* 56: 987 – 996.
- Palacios, S.L. and R.C. Zimmerman. 2007. Response of eelgrass *Zostera marina* to CO₂ enrichment: possible impacts of climate change and potential for remediation of coastal habitats. *Marine Ecology Progress Series*: 344: 1 – 13.
- Patterson, M.P., M.C. Harwell, L.M. Orth, and R.J. Orth. 2001. Biomechanical properties of the reproductive shoots of eelgrass. *Aquatic Botany* 69: 27 – 40.
- Peralta, G., J.L. Perez-Llorens, I. Hernandez, F. Brun, J.J. Vergara A. Bartual, J.A. Galvez, J., and C.M. Garcia. 2000. Morphological and physiological differences between two morphotypes of *Zostera noltii* Hornem. From the south-western Iberian Peninsula. *Helgoland Marine Research* 54: 80 – 86.
- Peralta, G., F.G. Brun, I. Hernandez, J.J. Vergara, and J.L. Perez-Llorens. 2005. Morphometric variations as acclimation mechanisms in *Zostera noltii* beds. *Estuarine, Coastal and Shelf Science* 64: 347 – 356.
- Precht, E., and M. Huettel. 2003. Advective pore-water exchange drive by surface gravity waves and its ecological implications. *Limnology and Oceanography* 48: 1674 – 1684.
- Puijalon, S., J.-P. Lena, and G. Bornette. 2007. Interactive effects of nutrient and mechanical stresses on plant morphology. *Annals of Botany* 100: 1297 – 1305.
- Ramirez-Garcia P., A. Lot, C.M. Duarte, J. Terrados, and N.S.R. Agawin. 1998. Bathymetric distribution, biomass and growth dynamics of intertidal

- Phyllospadix scouleri* and *Phyllospadix torreyi* in Baja California (Mexico). Marine Ecology Progress Series 173: 13 – 23.
- Ramirez-Garcia, P., J. Terrados, F. Ramos, A. Lot, D. Ocana, and C.M. Duarte. 2002. Distribution and nutrient limitation of surfgrass *Phyllospadix scouleri* and *Phyllospadix torreyi*, along the Pacific coast of Baja California (Mexico). Aquatic Botany 74: 121 – 131.
- Roberson, L.M., and J.A. Coyer. 2004. Variation in blade morphology of the kelp *Eisenia arborea*: incipient speciation due to local water motion? Marine Ecology Progress Series 282: 115 – 128.
- Schanz, A., and H. Asmus. 2003. Impact of hydrodynamics on development and morphology of intertidal seagrasses in the Wadden Sea. Marine Ecology Progress Series 261: 123 – 134.
- Short, F.T. 1983. The seagrass, *Zostera marina* L: Plant morphology and bed structure in relation to sediment ammonium in Izembek Lagoon, Alaska. Aquatic Botany 16: 149 – 161.
- Short, F.T. 1987. Effects of sediment nutrients on seagrasses: Literature review and mesocosm experiment. Aquatic Botany 27: 41 – 57.
- Short, F.T., and H.A. Neckles. 1999. The effects of global climate change on seagrasses. Aquatic Botany 63: 169 – 196.
- Short, F.T., E.W. Koch, J.C. Creed, K.M. Magalhães, E. Fernandez, and J.L. Gaeckle. 2006. SeagrassNet monitoring across the Americas: case studies of seagrass decline. Marine Ecology 27:277-289.
- Sidik, J.B., M.Z. Harah, M.A. Pauzi, and S. Madhavan. 1999. *Halodule* species from Malaysia – distribution and morphological variation. Aquatic Botany 65: 33 – 45.
- Stewart, H.L. 2006. Morphological variation and phenotypic plasticity of buoyancy in the macroalga *Turbinaria ornata* across a barrier reef. Marine Biology 149: 721 – 730.
- Thomas, F.I.M., C.D. Cornelisen, and J.M. Zande. 2000. Effects of water velocity and canopy morphology on ammonium uptake by seagrass communities. Ecology 81: 2704 – 2713.
- Thomas, F.I.M., and C.D. Cornelisen. 2003. Ammonium uptake by seagrass communities: effects of oscillatory versus unidirectional flow. Marine Ecology Progress Series 247: 51 – 57.
- Vila-Gispert, A., M.G. Fox, L. Zamora, and R. Moreno-Amich. 2007. Morphological variation in pumpkinseed *Lepomis gibbosus* introduction into Iberian lakes and reservoirs; adaptation to habitat type and diet? Journal of Fish Biology 71: 163 – 181.
- Wargo, C.A., and R. Styles. 2007. Along channel flow and sediment dynamics at North Inlet, South Carolina. Estuarine, Coastal, and Shelf Science 71: 669 – 682.
- Widdows, J., N.D. Pope, M.D. Brinsley, H. Asmus, and R.M. Asmus. 2008. Effects of seagrass beds (*Zostera noltii* and *Z. marina*) on near-bed hydrodynamics and sediment resuspension. Marine Ecology Progress Series 358: 125 – 136.

- Wilson, A.M., M. Huettel, S. Klein. 2008. Grain size and depositional environment as predictors of permeability in coastal marine sands. *Estuarine, Coastal and Shelf Science* 80: 193 – 199.
- Zimmerman, R.C. 2003. A biooptical model of irradiance distribution and photosynthesis in seagrass canopies. *Limnology and Oceanography* 48: 568 – 585.
- Zimmerman, R.C., R.D. Smith, R.S. Alberte. 1987. Is growth of eelgrass nitrogen limited? A numerical simulation of the effects of light and nitrogen on the growth dynamics of *Zostera marina*. *Marine Ecology Progress Series* 41: 167 – 176.
- Zimmerman, R.C., D.G. Kohrs, D.L. Steller, and R.S. Alberte. 1997. Impacts of CO₂ enrichment of productivity and light requirements of eelgrass. *Plant Physiology* 115: 599 – 607.